

**Electrochemical methods optimization to study the function
of transient adenosine changes in brain slices**

Ashley E. Ross
Williamsburg, Virginia

Bachelor of Science in Chemistry, Christopher Newport University, 2009

A Dissertation presented to the Graduate Faculty
Of the University of Virginia in Candidacy for the Degree of
Doctor of Philosophy

Department of Chemistry

University of Virginia
May, 2014

Electrochemical methods optimization to study the function of transient adenosine changes in brain slices

Abstract:

Adenosine is found throughout the brain and is an important signaling molecule. Fast-scan cyclic voltammetry (FSCV) at carbon-fiber microelectrodes is an electrochemical technique which allows rapid detection of neurotransmitters *in vivo*, and has become increasingly popular for adenosine detection in the brain. Adenosine detection can be difficult because a few neurochemicals have similar electrochemical signatures as adenosine and it also requires a high oxidizing potential; so optimizing electrochemical methods for rapid detection of adenosine is beneficial. This thesis describes optimized methods for adenosine detection and uses FSCV to study adenosine signaling in the brain.

Adenosine is introduced in Chapter 1. This chapter goes into detail about adenosine signaling, function, and mechanisms of release. The chapter also reviews the latest literature on rapid adenosine detection in the brain and what is still unknown. FSCV is introduced and types of methods optimization are discussed. Chapters 2-4 go into detail about specific methods used for optimized adenosine detection. Chapter 2 focuses on comparing electrode modification techniques for dopamine, and Chapter 3 uses the Nafion-CNT modified electrodes, described in Chapter 2, for adenosine detection. In this chapter, Nafion-CNT modified electrodes show enhanced sensitivity and selectivity for adenosine over ATP both *in vitro* and *in situ*. Chapter 4 proposes a new waveform for adenosine detection which allows increased sensitivity for adenosine at lower switching potentials and enhanced analyte differentiation. Together, these new techniques provide tools in which optimal adenosine detection can be achieved, specifically when interferences are expected.

Chapters 5-6 describe the use of FSCV to study rapid changes in extracellular adenosine concentration in the brain. Chapter 5 explains a new method of evoking adenosine in the prefrontal cortex via mechanically stimulating the tissue using either the electrode or a pulled glass pipette. The mechanism of evoked adenosine is proven to be both activity-dependent and partially a downstream result of ATP metabolism. Chapter 6 studies the function of transient adenosine release. The Chapter demonstrates how transient adenosine release modulates stimulated dopamine release in the caudate putamen. This was the first characterized function of transient adenosine in the brain. Together, these findings provide new information on how adenosine can be stimulated and the function of these rapid changes in the brain.

Overall, this thesis optimizes methods for rapid adenosine detection in the brain and uses FSCV to characterize previously unknown adenosine phenomenon. New electrode and waveform modifications provide the field new methods for not only enhanced adenosine detection, but ideas for enhancing current tools for other analytes that are difficult to detect; while mechanically evoked adenosine, along with a function for transient adenosine release, provides the field new information of rapid adenosine signaling. The combination of new analytical tools for enhanced adenosine detection and the new methods to evoke and study adenosine in the brain will help piece together the intricate role of rapid adenosine release in the brain.

Table of Contents

Abstract	i
Table of Contents	iii
List of Figures	vii
List of Tables	ix
Acknowledgments	x

Chapter 1: Introduction **2****1.1 Overview of adenosine** **2**

1.1.1 Adenosine regulation in the central nervous system	2
1.1.1.1 Intra- and Extracellular Formation of Adenosine.	3
1.1.1.2 Adenosine Receptors.....	4
1.1.1.3 Adenosine Transporters.....	5
1.1.2 Function of adenosine in the central nervous system.....	6
1.1.2.1 Adenosine as a neuroprotector.....	6
1.1.2.2 Adenosine as a neuromodulator.	7

1.2 Electrochemical detection of adenosine in vivo **8**

1.2.1 Adenosine characterization using fast-scan cyclic voltammetry at carbon-fiber microelectrodes.....	9
1.2.1.1 Characterization of carbon-fiber microelectrodes for adenosine detection using FSCV.....	13
1.2.1.2 Characterization of diamond electrodes for adenosine detection using FSCV.	14
1.2.1.3 Adenosine modulates respiratory rhythmogenesis.	15
1.2.1.4 Short electrical stimulations elicit rapid adenosine changes.	15
1.2.1.5 Adenosine transiently regulates oxygen concentrations.....	16
1.2.1.6 A1 receptors self-regulate stimulated adenosine release.....	17
1.2.1.7 Stimulated adenosine release is activity dependent in multiple brain regions.....	17
1.2.1.8 FSCV to study adenosine deaminase kinetics.	19
1.2.1.9 Adenosine release during deep brain stimulation causes microthalamotomy effect.	20
1.2.1.10 AMP hydrolysis to adenosine inhibits pain-sensing response in spinal cord.	21
1.2.1.11 Spontaneous transient adenosine release.	23
1.2.1.12 Enhanced understanding of adenosine signaling using FSCV.....	24
1.2.2 Adenosine characterization using amperometric adenosine micro-biosensors	25
1.2.2.1 Activity-dependent adenosine release in the cerebellum is modulated by endogenous neurotransmitters.	26
1.2.2.2 Adenosine is released during hypoxia in the hippocampus.....	28
1.2.2.3 Adenosine is released during hypoxia in the nucleus tactus solitarii (NTS) of the brainstem.....	29
1.2.2.4 Adenosine is released during ischemia.	30
1.2.2.5 Adenosine modulates chemoreceptor responses.....	31

1.2.2.6 Adenosine is linked to modulating seizures induced by CO ₂	32
1.2.2.7 Increase in extracellular adenosine levels provides anticonvulsant behavior during epilepsy.	32
1.2.2.8 Adenosine is involved in the sleep-wake cycle.....	33
1.3 Contributions of electrochemical detection of adenosine to the field and remaining uncertainties.....	36
1.4 References.....	38
<i>Chapter 2: Comparison of Nafion- and overoxidized polypyrrole-carbon nanotube electrodes for neurotransmitter detection</i>	<i>46</i>
2.1 Introduction.....	47
2.2: Methods.....	49
2.2.1 Chemicals:	49
2.2.2: Carbon-fiber microelectrodes.....	49
2.2.3 Functionalization of CNTs:.....	50
2.2.5 Preparation of OPPY and OPPY-CNT modified electrodes:	50
2.2.6 Preparation of Nafion and Nafion-CNT modified electrodes:.....	51
2.2.7 Electrochemistry measurements:.....	52
2.2.8 In vivo experiments:	53
2.2.9 Scanning electron microscopy:	53
2.2.10 Statistics:	53
2.3 Results and Discussion.....	54
2.3.1 Introduction:	54
2.3.2 Comparison of Polymer and Polymer-CNT electrodes:.....	54
2.3.3 Optimizing CNT concentrations:	56
2.3.4 Electrode characterization:	59
2.3.5 In vivo use of polymer-CNT microelectrodes:.....	64
2.4 Conclusions	67
2.5 References	69
<i>Chapter 3: Nafion-CNT Coated Carbon-Fiber Microelectrodes for Enhanced Detection of Adenosine</i>	<i>72</i>
3.1 Introduction.....	73
3.2 Methods.....	75
3.2.1 Solutions and chemicals:	75
3.2.2 Preparation of microelectrodes:	75
3.2.3 Functionalization of CNTs:.....	76
3.2.4 Electrochemistry:.....	76
3.2.5 Scanning Electron Microscopy:.....	77
3.2.6 Brain slice experiments:	77
3.2.7 Statistics:.....	78
3.3 Results and Discussion.....	78
3.3.1 Surface structure characterization:	78

3.3.2 Nafion-CNT carbon-fiber microelectrodes increase sensitivity to adenosine:	80
3.3.3 Optimization of CNT concentration:	82
3.3.4 Time response of Nafion-CNT modified electrodes:	84
3.3.5 Investigation of other electroactive purines, purine derivatives, and neurotransmitters:	85
3.3.6 Selectivity of Nafion-CNT modified electrodes in brain slices:.....	90
3.4 Conclusions	92
3.5 References	93
<i>Chapter 4: Sawhorse waveform voltammetry for selective detection of adenosine, ATP, and hydrogen peroxide</i>	97
4.1 Introduction.....	98
4.2 Methods.....	100
4.2.1 Chemicals	100
4.2.2 Carbon-fiber microelectrodes.....	100
4.2.3 Electrochemistry measurements.....	101
4.2.4 Brain slice experiments	101
4.2.5 Principal component analysis	102
4.2.6 Statistics.....	103
4.3 Results and Discussion.....	103
4.3.1 Comparison of the triangle and sawhorse waveform.....	103
4.3.2 Sawhorse waveform optimization	109
4.3.3 Analyte differentiation using principal component analysis	112
4.3.4 Mechanically stimulated adenosine is predicted as adenosine in brain slices	115
4.3.5 Advantages of modified waveforms versus modified electrodes	117
4.4 Conclusions	119
4.5 References	120
<i>Chapter 5: Mechanical stimulation evokes rapid increases in adenosine concentration in the prefrontal cortex.....</i>	124
5.1 Introduction.....	125
5. 2 Methods.....	126
5.2.1 Chemicals:	126
5.2.2 Electrochemistry:.....	127
5.2.3 Brain slice preparation/experiments:.....	128
5.2.4 Pharmacology experimental details in slices:	128
5.2.5 Picospritzing method:.....	129
5.2.6 Staining Experiment.....	129
5.2.7 Enzyme biosensors:.....	130
5.2.8 In vivo experiments:	131
5.2.9 Statistics:.....	131
5.3 Results.....	131
5.3.1 Mechanically-stimulated adenosine in brain slices and in vivo:.....	131

5.3.2 Evaluation of other methods for mechanical stimulation:	136
5.3.3 Mechanism of mechanically-evoked adenosine:	139
5.4 Discussion.....	143
5.4.1 Mechanically evoked adenosine occurs via different methods:.....	144
5.4.2 Mechanical stimulation evokes large, transient adenosine changes:	145
5.4.3 Mechanism and function of mechanically evoked adenosine release:	146
5.5 Conclusion	148
5.6 References	149
<i>Chapter 6: Adenosine transiently modulates stimulated dopamine release in the caudate putamen via A₁ receptors.....</i>	153
6.1 Introduction.....	154
6.2 Methods	156
6.2.1 Chemicals	156
6.2.2 Electrochemistry.....	156
6.2.3 Brain slice experiments	157
6.2.4 Pharmacology experiments	158
6.2.5 Statistics.....	158
6.3 Results.....	159
6.3.1 Exogenously-applied, transient adenosine modulates dopamine on a rapid time scale	161
6.3.2 Bath application of adenosine does not modulate dopamine release	162
6.3.3 Mechanically stimulated (endogenous) adenosine modulates dopamine release	164
6.3.4 Adenosine modulation of dopamine is regulated by A ₁ receptors	166
6.4 Discussion.....	168
6.4.1 Adenosine transiently modulates phasic dopamine release.....	168
6.4.2 Rapid dopamine modulation is regulated by A ₁ receptors in the caudate putamen ...	169
6.4.3 Adenosine perfusion does not modulate stimulated dopamine release	170
6.4.4 Function of transient adenosine release	171
6.5 Conclusion	172
6.6 References	173
<i>Chapter 7: Conclusions and Future Directions</i>	177
7.1 Novel analytical tools for optimized adenosine detection	177
7.2 Adenosine rapid signaling in the brain	180
7.3 Final Conclusions	184
7.4 References	185
<i>Appendix: Brain Slice protocol</i>	187

List of Figures:

Figure 1.1: Adenosine mechanism of formation.....	5
Figure 1.2: Adenosine electrochemical reaction.....	10
Figure 1.3: Example FSCV adenosine waveform and data in vitro.....	12
Figure 1.4: Scanning electron microscopy (SEM) image of a carbon-fiber microelectrode.....	12
Figure 1.5: Stimulated release is adenosine and not histamine in the caudate putamen.....	16
Figure 1.6: Mechanism of stimulated adenosine release varies by brain region.....	19
Figure 1.7: Adenosine release occurs after high frequency stimulation (125 Hz, 200 μ A, for 5s, 100 μ s pulse width) in thalamic slices.....	21
Figure 1.8: AMP hydrolysis to adenosine is reduced in PAP and NT5E knockout mice.....	23
Figure 1.9: Schematic of biosensor.....	26
Figure 1.10: Increased adenosine after sleep deprivation is modulated by iNOs production.....	35
Figure 2.1: Example polymer and polymer-CNT coated electrode data for 1 μ M dopamine.....	56
Figure 2.2: Optimization of the amount of nanotubes in the coating solution.....	57
Figure 2.3: Scanning electron micrographs of electrode surfaces.....	60
Figure 2.4: Measuring different concentrations of dopamine.....	61
Figure 2.5: Response of polymer-CNT electrodes to other neurochemicals.....	63
Figure 2.6: In vivo detection of short trains of stimulated dopamine release.....	66
Figure 3.1: Scanning electron microscopy (SEM) images of Nafion and Nafion-CNT modified carbon-fiber microelectrodes at 100,000x resolution.....	79
Figure 3.2: Nafion-CNT coated electrodes improve sensitivity.....	80
Figure 3.3: The electrochemical reactions observed after Nafion-CNT coated are primarily adsorption controlled.....	81
Figure 3.4: Average peak oxidation current ratios for adenosine at microelectrodes modified with Nafion, 0.05 mg/mL CNT in Nafion, or 0.2 mg/mL CNT in Nafion.....	83
Figure 3.5: Current versus time profiles of A.) Nafion and B.) Nafion-CNT modified carbon-fiber microelectrodes for 5 μ M adenosine.....	85
Figure 3.6: Cyclic voltammograms of A.) 5 μ M histamine and B.) Basic pH shift of +0.2 pH units before and after Nafion-CNT coating.....	86
Figure 3.7: Cyclic voltammograms of each purine base and nucleoside Insets show structures for each analyte.....	87
Figure 3.8: Calibration curves for purines and associate nucleosides for both bare and coated electrodes.....	88
Figure 3.9: Brain slice data comparing bare and coated electrodes selectivity for adenosine.....	91
Figure 4.1: Cyclic voltammograms (CVs) for the A) triangle and B) sawhorse waveform.....	104
Figure 4.2: Background current for both waveforms.....	105

Figure 4.3: Scan rate experiments for both 5 μ M ATP and 100 μ M hydrogen peroxide.	107
Figure 4.4: Adenosine current decays significantly quicker than hydrogen peroxide. ...	108
Figure 4.5: Cyclic voltammogram of 5 μ M adenine	109
Figure 4.6: Optimization of the sawhorse waveform switching potential and plateau time	110
Figure 4.7: Comparison of current at both the triangle and sawhorse waveform at various switching potentials	111
Figure 4.8: Mechanically evoked adenosine using the sawhorse waveform	117
Figure 5.1: Adenosine after mechanical stimulation	133
Figure 5.2: Enzyme biosensor measurements of mechanosensitive release	134
Figure 5.3: Four consecutive stimulations in vivo	136
Figure 5.5: Adenosine is not mechanically evoked by small amounts of pressure ejected aCSF	139
Figure 5.6: Mechanically evoked adenosine is activity dependent but is not released by equilibrative nucleoside transporters	140
Figure 5.7: Concentration versus time profiles for EDTA, TTX, CNQX, and POM-1....	141
Figure 5.8: Current versus time plots comparing clearance kinetics before and after the transport inhibitor, NBTI, perfusion	141
Figure 5.9: Mechanically evoked adenosine is not dependent on AMPA receptors but is a downstream effect of ATP metabolism	143
Figure 6.1: Adenosine and dopamine can be co-detected using FSCV.....	159
Figure 6.2: Schematic for exogenous application of adenosine in brain slices.	160
Figure 6.3: Time between exogenous application and dopamine stimulation optimization	162
Figure 6.4: Constant perfusion of 5 μ M adenosine does not modulate stimulated dopamine release	164
Figure 6.5: Mechanically evoked adenosine transiently modulates dopamine.....	166
Figure 6.6: Dopamine modulation is regulated by the A1 receptor and not the A2A receptor in the caudate putamen	167

List of Tables:

Table 2.1: Average improvement in oxidative current for different neurochemicals.	64
Table 3.1 Average current improvement for common purines, purine derivatives, and neurotransmitters	86
Table 3.2. Average calibration slope improvement for purines and nucleosides.....	89
Table 4.1: Predicted values for triangle waveform	114
Table 4.2: Predicted values for sawhorse waveform	114
Table 4.3: Statistics comparing predicted values versus actual values.....	115
Table 5.1: Mechanically evoked adenosine.....	135

Acknowledgements

I would like to acknowledge my advisor, Dr. Jill Venton, for her help in shaping me into a scientist and her countless hours of editing my papers. I would also like to thank everyone in the lab for being supportive and always available whenever I just needed to talk to someone. Big thanks to Dr. Megan Pajski for being extremely patient in training me on brain slices. Thank you to Jennifer Peairs for collecting all the OPPy-CNT data (Chapter 2) and to Ning Xiao for the SEM images (Chapter 2 and 3), Eve Privman for completing the staining experiment and Michael Nguyen for collecting the *in vivo* data for Chapter 5. I would also like to thank Dr. Nirmal Mazumder at the Keck Imaging Center at the University of Virginia for assistance using the Zeiss multiphoton microscope and Dr. Sherin Rouhani for providing the staining reagents.

I want to also thank my parents, Chris and Rhonda Mertens, for always encouraging me and pushing me to do my best in all things and for teaching me how to set priorities in life. You have truly raised me to set high standards for myself and to work hard to achieve my goals. I want to thank my mother- and father- in law for also encouraging and supporting me throughout all of this.

Lastly, I would like to thank my husband, Ronnie, and beautiful daughter, Haylee. You have supported me since day one and have kept me sane throughout all of this. You are my number one priority, always have and always will be. Grad school is tough and it has been so nice to have such a strong support system at home. And Haylee, a lot of people questioned whether I could handle you and school at the same time and honestly you have made it easier! I work harder knowing that I need to live by example! I can't wait to witness all that you will accomplish in life.

Chapter 1

Introduction

The great tragedy of Science: the slaying of a beautiful hypothesis by an ugly fact

~Thomas H. Huxley

Chapter 1: Introduction

1.1 Overview of adenosine

Adenosine is an important neuromodulator¹ and neuroprotector² in the brain and is a breakdown product of ATP. Previous knowledge of adenosine was based on slow time resolution techniques^{3,4}, which could not provide information on rapid signaling. Development of real-time measurements of adenosine release over the past several years has provided a wealth of information on adenosine signaling in the brain. Fast-scan cyclic voltammetry (FSCV) at carbon-fiber microelectrodes^{5,6} and amperometric enzyme biosensors⁷ have been the primary techniques for real-time, *in vivo* detection of adenosine. Adenosine is now viewed not only as a slow acting neuromodulator, but as a rapidly released signaling molecule in the brain which may be important for neuromodulation or protection on a much faster time scale. Real-time measurements have led to a better understanding of how quickly adenosine can be released^{6,7}, the mechanisms of release in different brain regions⁸, and how adenosine release regulates the response to acute brain injuries or non-physiological conditions such as hypoxia⁹, ischemia¹⁰, hypercapnia¹¹, and epileptic seizures¹⁰.

1.1.1 Adenosine regulation in the central nervous system

Adenosine is a nucleoside byproduct of adenosine triphosphate (ATP) metabolism and is specifically involved in neuromodulation^{12,13}, neuroprotection^{2,12,14,15}, and regulation of cerebral blood flow in the brain¹⁶. Adenosine is also important in many other organs of the body such as the heart^{17,18} and lung¹⁹. Regulation of adenosine in the brain is not fully understood; however, many studies have examined the function of adenosine receptors, transporters, and metabolic

pathways. Adenosine targeted treatments for diseases such as Parkinson's^{20,21} and Huntington's²² have become increasingly popular. Neuroprotective effects of adenosine can be exploited using adenosine receptor antagonists and agonists.^{20,23} Adenosine is involved in several brain disorders and diseases but little is still known about the immediate response of adenosine to acute disruptions in brain function or signaling in a diseased patient.

1.1.1.1 Intra- and Extracellular Formation of Adenosine.

Intra- and extracellular adenosine formation occurs by a variety of complicated mechanisms (Figure 1.1). In general, intracellular formation of adenosine is attributed to the catabolism of cytosolic ATP to adenosine monophosphate (AMP) due to metabolic stress²⁴ as shown in Figure 1.1. Cytosolic-5'-nucleotidase is responsible for converting AMP to adenosine. This intracellular mechanism of adenosine formation is linked to maintaining an energy balance within the cell.²⁴ ATP exists in much higher concentrations than AMP, therefore small changes in ATP concentration leads to significant changes in the amount of AMP available for adenosine production. Another method of intracellular adenosine formation proposed in Figure 1.1 is from the hydrolysis of s-adenosylhomocysteine; (however, this pathway is not connected to energy balance in the cell and therefore is not the main contributor to intracellular adenosine formation.²⁴

Extracellular formation of adenosine is primarily linked to extracellular ATP metabolism (Figure 1.1). ATP is released by exocytosis as a co-transmitter and broken down to adenosine by ecto-ATPase and ecto-5'-nucleotidase. Directly released cyclic AMP can also be extracellularly metabolized to adenosine, but this mode of formation has only been linked to slow changes in extracellular formation

(not shown in Figure 1.1).²⁴ Recently, activity dependent release of adenosine in the extracellular space was discovered^{6,25,26}; however, adenosine has not been identified in vesicles. More research is needed to determine the real-time mechanisms of adenosine release, whether it is directly released by exocytosis and how the mechanism affects the time course of adenosine signaling.

1.1.1.2 Adenosine Receptors.

Adenosine is regulated by four known G-protein-coupled receptors in the CNS^{27,28}: A₁, A_{2A}, A_{2B}, and A₃. A₁ is the most abundant adenosine receptor in the brain and inhibits neurotransmission by blocking adenylyl cyclase activity. A_{2A} is the second most abundant adenosine receptor expressed in the brain and activates adenylyl cyclase activity. Both of these receptors have low nanomolar affinities for adenosine, and are, therefore, the most important receptors in the brain for adenosine signaling.^{24,29} The excitatory receptor, A_{2B}, and the inhibitory receptor, A₃, are less abundant in the brain and are activated by micromolar concentrations of adenosine.²⁴

A₁ receptors are widely expressed and can be found presynaptically, postsynaptically, and nonsynaptically, whereas A_{2A} receptors are primarily in synapses.^{28,30} However, inhibitory actions are mostly a result of presynaptic A₁ receptors because they are primarily found on excitatory synapses.³⁰⁻³² Adenosine receptors are also located on astrocytes and they may serve as a modulator of non-neuronal brain functions.^{30,33,34}

1.1.1.3 Adenosine Transporters.

Extracellular adenosine is regulated by bi-directional nucleoside transporters in the brain as shown in Figure 1.1.^{24,35} Nucleoside transporters are classified into two main categories: equilibrative nucleoside transporters (ENTs) and concentrative nucleoside transporters.^{24,35} ENTs follow a concentration gradient and can transport both purines and pyrimidines, whereas concentrative transporters are driven by a sodium gradient. ENTs are the primary transporter responsible for regulation of extracellular adenosine in the brain.^{24,36} Equilibrative transporters, which are sensitive to the selective transport inhibitor nitrobenzylthioinosine (NBTI), are called equilibrative-sensitive, es, whereas equilibrative-insensitive, ei, transporters are not sensitive to NBTI. Most research studies on adenosine transport examine es transporters because of the selective inhibitor NBTI.

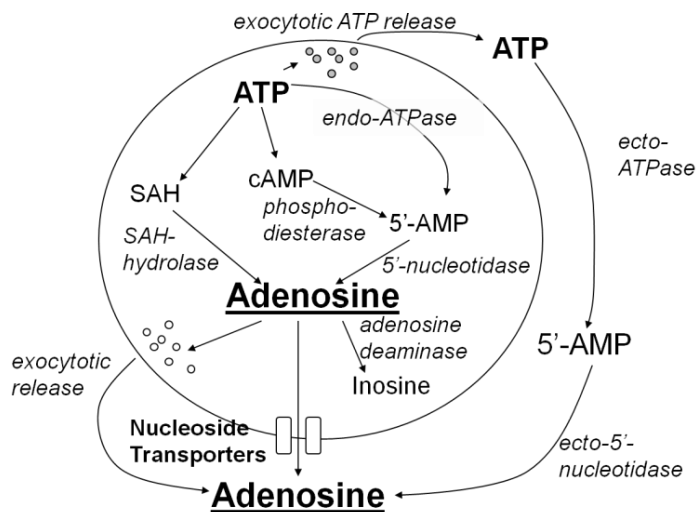


Figure 1.1: Adenosine mechanism of formation. Adenosine is formed intra- and extracellularly. Intracellularly, adenosine derives from ATP either from cAMP or SAH enzymes. Adenosine can then be transported out of the cell either by nucleoside transporters or by exocytosis or through connexin hemichannels (not shown). Extracellularly, adenosine can be formed by exocytotic release of ATP which is

broken down to adenosine or by direct release of adenosine from inside the cell. Modified from Pajski et al⁶.

1.1.2 Function of adenosine in the central nervous system

Adenosine is an important neuromodulator in the brain and can regulate cerebral blood flow, the sleep-wake cycle, and excitatory neurotransmission. Modulating adenosine may help treat diseases and disorders such as stroke, ischemia, Huntington's disease, Parkinson's disease, epilepsy, and Alzheimer's disease to name a few. Due to its widespread involvement in the brain and complicated regulatory system, more information is needed to improve therapeutics involving adenosine regulation.

1.1.2.1 Adenosine as a neuroprotector.

Neuroprotection by adenosine has been linked to the activation of A₁ receptors, due to their inhibitory nature.^{2,28} A₁ receptors provide neuroprotection during ischemic attack^{37,38}, neuroinflammation^{30,34}, excitotoxicity²², and epileptic episodes.^{10,28} Neuroprotection can occur presynaptically by inhibiting excitatory responses or postsynaptically by hyperpolarization of cells.^{15,28,39} Activation or deactivation of adenosine receptors has sparked a new avenue of pharmacological agents to be studied for therapeutics. Much is known about the long term effects of adenosine receptor manipulation; however, the rapid response of adenosine receptor manipulation specifically during injury and acute insults is not as well understood.

The changes on extracellular adenosine levels during brain injury and acute insults have primarily been studied using slow temporal resolution techniques such as microdialysis coupled to HPLC^{4,40,41} or histopathological scoring of fixed tissue collected up to months after injury⁴². Adenosine was shown to be released after

controlled cortical impact, a method often used to study traumatic brain injury, using microdialysis with HPLC⁴. A peak in adenosine was observed within 20 minutes of sampling and sampling was taken every 10 minutes. Information on amount of adenosine released and how long it was elevated was determined, but the sampling time is still too long to study mechanism of release. In another study, adenosine concentrations were measured during ischemia using HPLC⁴¹. Again, information such as ischemic markers was studied, but detailed information on time course and mechanisms of release were unattainable. These studies reveal the effects of adenosine during injury on a slow time scale; however, to understand what occurs immediately following injury or during conditions such as ischemia, advances in temporal resolution were required. The recent developments of adenosine detection using fast-scan cyclic voltammetry (FSCV) and amperometry have led to further advances of adenosine characterization in the brain which will be discussed later in the chapter.

1.1.2.2 Adenosine as a neuromodulator.

Distinct from its neuroprotective role, adenosine is classically recognized as a homeostatic neuromodulator in the brain and as a synaptic neuromodulator.¹ Like neuroprotection, neuromodulation occurs when adenosine binds to its receptor in the brain and either causes an inhibitory or excitatory response. The term “retaliatory metabolite” was given to adenosine, primarily because of its significant role in regulating cell metabolism.^{1,43} In short, adenosine release from the cell occurs because of a concentration gradient produced when ATP is used intracellularly. Small concentration shifts in ATP produce large changes in adenosine concentration because ATP exists in much higher concentrations in the

cell. When intracellular adenosine levels rise, adenosine is released by bi-directional ENTs.

In addition to modulating cell metabolism, adenosine modulates neurotransmission at the synaptic level. Adenosine can modulate dopamine⁴⁴⁻⁴⁷, serotonin⁴⁸, glutamate⁴⁹, and GABA⁴⁴. Typically, adenosine acts to suppress neurotransmission, particularly in response to insults such as traumatic brain injury^{4,34} and stroke⁵⁰. Glutamate regulation by adenosine leads to reduction in excitotoxicity and can reduce damage during ischemia.⁴⁹ Thus, the roles of neuromodulation and neuroprotection often overlap.

Neurotransmitter modulation by adenosine is traditionally thought of as a slow process where adenosine concentration builds up over minutes to hours after injury. High temporal resolution techniques have not been traditionally used to study adenosine modulation, so little is known about the extent to which adenosine modulates neurotransmission on the millisecond timescale. Over the last few years, real-time adenosine has been explored using electrochemistry.^{5,6,8,10,26,51,52} These new techniques for adenosine detection have led to the understanding that adenosine is not just a slow acting neuromodulator, but also operates on the millisecond timescale. This chapter will discuss electrochemical technique based adenosine discoveries and major contributions to the field.

1.2 Electrochemical detection of adenosine *in vivo*

Recently, electrochemical detection of adenosine *in vivo* has become increasingly popular to monitor adenosine changes in real time. There are three major electrochemistry techniques used for detection of adenosine *in vivo*. Fast-scan cyclic voltammetry (FSCV) at carbon-fiber microelectrodes is popular for

studying the mechanism of stimulated adenosine release^{6,53,54}, comparing adenosine release in different brain regions⁸, and understanding enzymes involved in extracellular breakdown of AMP in spinal nociceptive circuits^{51,55}. FSCV at diamond microelectrodes has been used to study respiratory rhythmogenesis.⁵⁶⁻⁵⁸ Amperometric enzyme biosensors have been used for studying the involvement of adenosine in hypercapnia¹¹, ischemia¹⁰, the sleep-wake cycle⁵⁹, and epilepsy¹⁰. Major advancements in the field have been made using electrochemical techniques; however, much is still unknown about cellular sources of adenosine in the brain in addition to if and how adenosine modulates neurotransmission on the fast time scale.

1.2.1 Adenosine characterization using fast-scan cyclic voltammetry at carbon-fiber microelectrodes

Fast-scan cyclic voltammetry is an electrochemical technique where a triangular waveform is rapidly applied to the working electrode and current monitored from electroactive species undergoing redox reactions at the electrode surface. Carbon-fiber microelectrodes were developed for dopamine detection and are also typically used for adenosine detection.^{5,6,60-62} The traditional triangle waveform for dopamine detection begins at -0.4 V and linearly ramps to 1.30 V and back down to the holding potential until the next scan. Adenosine oxidizes at a higher potential^{5,63}, so 1.45 V or 1.50 V is used as the switching potential for adenosine detection (adenosine waveform shown in Figure 1.3A). The frequency of data collection for FSCV is 10 Hz, so that scans are repeated every 100 milliseconds. Fast repetition rates are beneficial for studying neurotransmitters *in vivo*. Scan rates ranging from a hundred to a thousand V/s are used for neurotransmitter detection; however, 400 V/s is the typical scan rate used for most

compounds.^{5,64} High scan rates are beneficial for enhancing sensitivity but they can produce relatively large nonfaradaic background currents. The background current arises from the movement of ions in solution and oxidation of functional groups on the surface of the electrode and is larger than the typical Faradaic current. However, background currents are stable at carbon-fiber microelectrodes which enables background subtraction, leading to a background subtracted cyclic voltammogram (CV). CVs provide a fingerprint for the analyte of interest, allowing for some selectivity between analytes.

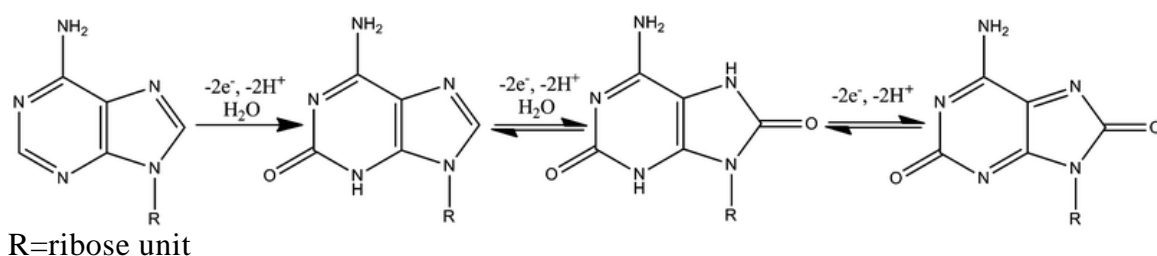


Figure 1.2: Adenosine electrochemical reaction. Adenosine has three oxidation reactions, but only two are typically detected at carbon-fiber microelectrodes. Each oxidation results in a loss of two electrons. The second and third oxidation reaction is reversible; however, the reduction peaks are harder to quantitate with FSCV for adenosine.

Adenosine is an electroactive molecule making it ideal for electrochemical detection⁶³. Adenosine undergoes a series of three oxidation reactions (Figure 1.2), only two of which are typically seen at carbon-fiber microelectrodes.⁵ The primary oxidation is at around 1.40 V and shows up on the cathodic scan due to slow kinetics. The secondary oxidation peak appears at 1.0 V. The primary oxidation for adenosine is irreversible so no reduction peak is observed. An example of a background-subtracted adenosine CV is shown in the inset of Figure 1.3B. The primary and secondary peaks for adenosine are marked. Figure 1.3B also shows a three dimensional color plot for adenosine. The plot displays voltage on the y-axis, time on the x-axis and current in false color. The green color represents oxidation of

adenosine and two oxidation peaks are visible. A current versus time trace is often used in FSCV to monitor changes in adenosine *in vivo*. (Figure 1.3, above the color plot). Current versus time traces are useful for studying clearance rates *in vivo* and adsorption properties *in vitro*. The trace can also be converted to a concentration vs time plot by using a calibration factor obtained either before or after the *in vivo* experiment.

Modifications to the traditional triangle shaped waveform have been shown in the past to increase sensitivity to specific analytes of interest⁶⁵ and to reduce fouling at the electrode⁶⁶. Optimized serotonin⁶⁶ and tyramine⁶⁷ waveforms have shown reduced fouling, while an extended dopamine waveform has shown increases in dopamine oxidative current⁶⁵. The holding potential, switching potential, and shape of the waveform can all be manipulated easily to maximize sensitivity and selectivity to a particular analyte. Traditionally, waveform modifications are for sensitivity enhancements and fouling diminishing only, but in this thesis I will discuss in chapter 4 how a waveform modification can be used to discriminate adenosine amongst some of its common interferents in the brain using principal component analysis (PCA).

Carbon-fiber microelectrodes are advantageous for rapid electrochemical measurements due to their ease of fabrication, affordability, and stability *in vivo*. They are advantageous for fast voltammetric measurements in small sample volumes because they have small diameters and a high surface area to volume ratio. Carbon-fiber microelectrodes are made by inserting a carbon-fiber into an empty glass capillary tube, pulling the capillary into two tapered electrodes via a capillary puller, and then cutting the fiber at the glass-fiber interface and polishing for a disk shaped electrode, or cutting the fiber approximately 50 μm from the glass

end to have a cylindrical electrode (SEM Figure 1.4). The opening between the glass and fiber is then sealed using an epoxy resin and hardener combination. Disk shaped electrodes are beneficial for spatially resolved measurements; however, cylindrically shaped electrodes are what is typically used *in vivo* because of larger surface area.

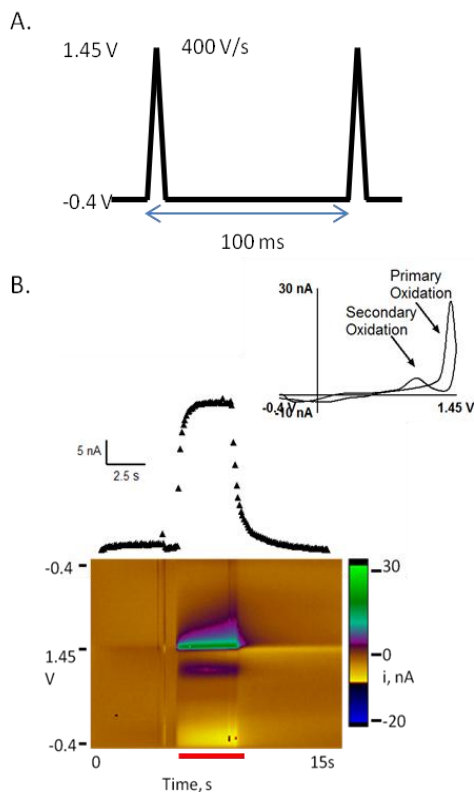
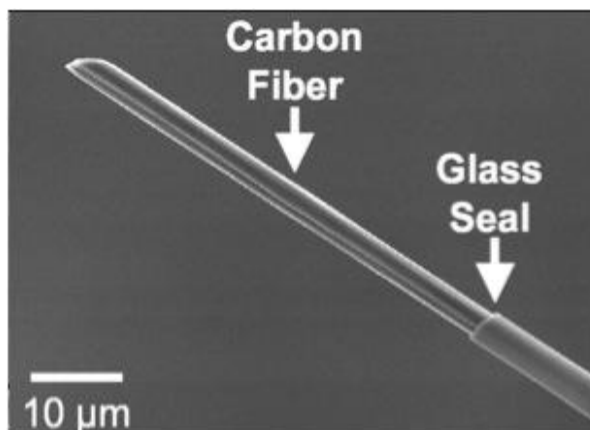


Figure 1.3: Example FSCV adenosine waveform and data *in vitro*. A) The adenosine waveform used is a triangle waveform starting at a -0.4 V holding potential and linearly ramping to 1.45 V and linearly ramping back down to the holding. The waveform is applied at a rate of 400 V/s and it repeated every 100 ms. B) A 3-D color plot for an *in vitro* calibration of 5 μ M adenosine is shown. The y-axis is voltage, x-axis is time, and the current is shown in false color. Green represents oxidative current. At 4 s, adenosine is injected into the flow cell and at 8 s the analyte is removed, shown by the red bar. An increase in current is observed at the switching potential (1.45 V) and at 1.0 V in subsequent scans. The current versus time plot, at the primary oxidation peak for adenosine, is shown directly above the color plot. The CV for adenosine in the inset. Distinct primary and secondary oxidation peaks characteristic of adenosine electrochemistry at carbon-fiber microelectrodes are marked.

Figure 1.4: Scanning electron microscopy (SEM) image of a carbon-fiber microelectrode. The carbon-fiber was vacuum aspirated into a glass capillary and pulled into two tapered electrodes (one shown). The fiber was cut ~ 50 μ m from the end of the glass for a cylinder electrode.



Modifications to carbon-fiber microelectrodes are often explored to further enhance sensitivity for analytes of interest and to increase electron transfer kinetics of the oxidation and reduction reaction. Carbon-fiber microelectrodes can be easily modified using polymers^{52,66}, enzymes⁶⁸, electrochemistry⁶⁵, and carbon nanotubes⁶⁹ or combination of techniques^{52,70}. Modification with polymers can be beneficial for selectivity enhancements based on charge; however, they also can be attributed to slowing the temporal response of the electrode. Electrochemical enhancement by applying a high potential to the electrode prior to use has shown an increase in sensitivity for dopamine.⁶⁵ The increases observed for dopamine are because of the renewable surface from breaking carbon-carbon bonds and oxygen functionalization.⁶⁵ Carbon nanotube modification is highly beneficial because of increases in electron transfer kinetics and surface area.⁷¹ Combinations of polymers and carbon nanotubes are not as well characterized in the literature. In Chapter 2 and 3 of this thesis, I will describe for the first time Nafion and carbon nanotube modified electrodes for enhanced detection of both dopamine and adenosine respectively.

1.2.1.1 Characterization of carbon-fiber microelectrodes for adenosine detection using FSCV.

Adenosine detection using FSCV was first reported by Brajter-Toth's group in 2000⁷². Nanostructured carbon-fiber microelectrodes were fabricated for enhanced detection of adenosine. The applied waveform was from -1.0 V to 1.50 V at a scan rate of 500 V/s. Electrochemical pretreatment of electrodes further enhanced the detection of adenosine *in vitro*. Several different methods of electrochemical treatments and buffer compositions for adenosine detection were explored, and

adenosine was best detected in phosphate buffer^{72,73} with a limit of detection (LOD) *in vitro* of 5 μM .

In 2007, our lab further characterized carbon-fiber microelectrodes for adenosine detection using FSCV⁵. The electrochemical reaction was analyzed and the two oxidation peaks in the adenosine CV were identified. By maximizing adsorption and minimizing noise, the LOD was 15 nM⁵, two orders of magnitude smaller than previously reported⁷³. Several other biologically relevant molecules chemically similar to adenosine were examined. Purines such as guanine and hypoxanthine have similar structures, however their oxidation peaks are at different potentials than adenosine. AMP and ATP have similar CVs to adenosine but carbon-fiber microelectrodes are not as sensitive to them.

1.2.1.2 Characterization of diamond electrodes for adenosine detection using FSCV.

Boron-doped diamond microelectrodes have also been explored for adenosine detection with FSCV⁵⁶. Diamond is electrically insulating, so it is essential to introduce impurities into the sp^3 -hybridized tetrahedral matrix of diamond, like boron, to make a conductive electrode. A thick film of boron-doped diamond is deposited onto a substrate, like metal, by chemical vapor deposition (CVD)⁵⁸. Low nanomolar limits of detection were obtained with diamond microelectrodes, which is beneficial for studying adenosine levels *in vivo*. Diamond microelectrodes are advantageous compared to carbon-fiber microelectrodes due to their increased sensitivity and resistance to fouling⁵⁸. Signal-to-background ratios are improved compared to carbon-fibers because of lack of functional group oxidation reactions and increased

capacitance. However, despite the increase in sensitivity, they are much larger than carbon-fiber microelectrodes (80 μm) and are difficult to reproducibly insulate⁵⁸.

1.2.1.3 Adenosine modulates respiratory rhythmogenesis.

Diamond microelectrodes were used to study the modulation of respiratory rhythmogenesis by adenosine in the PreBötzing complex of the rat brain stem⁵⁶. This region contains many adenosine releasing neurons responsible for regulation of respiration in the rat. After activation of adenosine A_{2A} receptors by CGS 21680, a large increase in current was observed and confirmed to be adenosine by its fingerprint CV. This was the first study to use FSCV in an animal model to study adenosine and showed that adenosine may have a role in respiration regulation⁵⁶.

1.2.1.4 Short electrical stimulations elicit rapid adenosine changes.

By applying pulse trains at a bipolar stimulating electrode to elicit release, stimulated release has been characterized using FSCV at carbon-fiber microelectrodes^{6,8,53}. Electrical stimulation mimics fast neuronal activation due to a discrete stimulus and causes rapid neurochemical changes in the brain. Our lab was the first to study electrically-stimulated adenosine in the caudate putamen *in vivo* using FSCV⁵³. Stimulated adenosine release was verified by administering an ENT inhibitor, a histamine synthetic precursor, and an adenosine kinase inhibitor. The ENT inhibitor, propentofylline, significantly decreased stimulated adenosine release, which demonstrated that short high frequency stimulations caused release of adenosine from inside the cell. ABT-702, the adenosine kinase inhibitor, significantly increased stimulated adenosine release which is expected since this drug blocks adenosine metabolism. No effect was observed after the addition of L-

histidine, a histamine synthetic precursor, which verified that the stimulated release was adenosine and not histamine since their CVs are fairly similar (Figure 1.5).

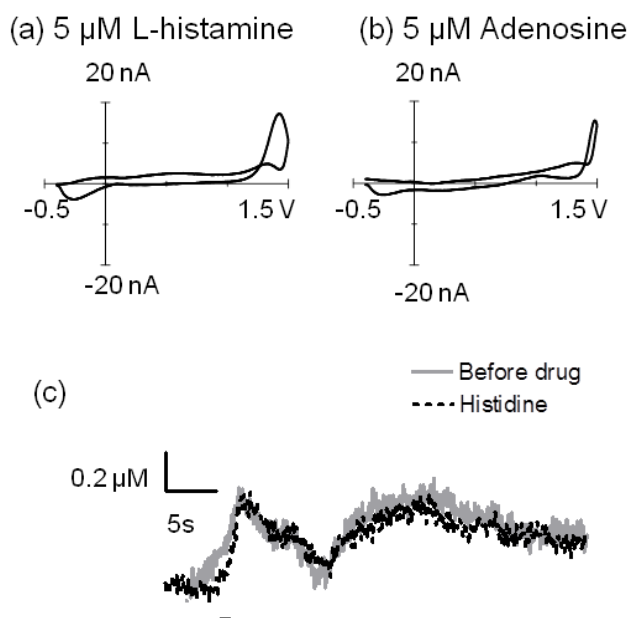


Figure 1.5: Stimulated release is adenosine and not histamine in the caudate putamen. Five μM L-histidine, a histamine precursor, was administered to verify the stimulated release signal was adenosine. A) *in vitro* signal of 5 μM L-histidine and B) adenosine. C) Current versus time trace of stimulated release *in vivo*. The signal did not change after L-histidine administration so histamine release is not being electrically stimulated in the caudate putamen. Reproduced from Cechova et al⁵³.

1.2.1.5 Adenosine transiently regulates oxygen concentrations.

The effect of adenosine on oxygen levels in the brain have also been studied *in vivo* using FSCV⁵³. Adenosine is a vasodilator and regulates cerebral blood flow so it was expected that stimulating adenosine release would affect oxygen levels in the brain¹⁶. To measure oxygen changes, a waveform was used that scanned to lower potential sufficient to reduce oxygen^{53,74}. Blocking intracellular release of adenosine with propentofylline caused a decrease in the amount of oxygen detected. From this study, the effects of adenosine as a vasodilator were confirmed to occur on the millisecond timescale.

1.2.1.6 A₁ receptors self-regulate stimulated adenosine release.

The A₁ receptor has been demonstrated to have some autoreceptor characteristics *in vivo* using FSCV⁵⁴. Cechova et al. showed that adenosine A₁ receptors modulate adenosine release in the caudate putamen, which means that they self regulate adenosine release⁵⁴. A₁ receptor agonists decreased both stimulated dopamine and adenosine release. A₁ agonists and antagonists had an immediate effect on stimulated adenosine release, whereas the effect on dopamine release was delayed, as previously reported^{54,75}. This study also examined how A₁ interactions with dopamine D₁ receptors modulated adenosine release. Administration of the A₁ receptor agonist, CPA, and the D₁ receptor antagonist SCH23390 showed that the A₁-D₁ interaction modulates adenosine and dopamine release *in vivo*⁵⁴.

1.2.1.7 Stimulated adenosine release is activity dependent in multiple brain regions.

The mechanism of stimulated adenosine release was first characterized using FSCV in brain slices from the rat caudate putamen⁶. Our lab showed that stimulated adenosine release is primarily activity-dependent and compared the mechanism of release using low frequency (10 Hz) and high frequency (60 Hz) stimulation⁶. Blocking equilibrative nucleoside transporters significantly increased both low and high frequency stimulated adenosine release, implying that intracellular formation of adenosine is not responsible for release. Low frequency stimulated adenosine release was dependent on extracellular ATP metabolism, whereas high frequency stimulated release was not. Adenosine release was dependent on calcium influx, as

perfusing with either EDTA or EGTA to chelate calcium decreased the signal for both low frequency and high frequency stimulations.

Activity-dependent adenosine release can be due to (1) direct vesicular release of ATP from neurons or glia, which gets metabolized to adenosine, (2) downstream release of adenosine after exocytosis of another neurotransmitter, or (3) direct release of adenosine from the cell by exocytosis^{25,76,77}. To determine the mechanism of activity-dependent adenosine release, case 1 and case 2 were tested using FSCV⁶. ATP metabolism (case 1) was blocked with a combination of an NTPDase inhibitor and an ecto-5'-nucleotidase inhibitor⁶. Blocking ATP metabolism did not affect high frequency stimulated adenosine release; but significantly reduced low frequency stimulated release. Thus, different stimulation frequencies produced different mechanisms of adenosine release. For example, high frequency stimulation occurs during stressful events, so adenosine release in response to a stressful environment is not dependent on extracellular ATP metabolism.

Case 2 was tested by decreasing dopamine release using a VMAT inhibitor and blocking downstream action of the ionotropic glutamate receptors, AMPA and NMDA⁶. Dopamine did not affect adenosine whereas blocking ionotropic glutamate receptors significantly reduced stimulated adenosine release for both low and high frequency stimulations in the caudate putamen⁶. Thus, adenosine release may be a downstream action of exocytotic glutamate release.

The mechanism of high frequency stimulated release was then compared in multiple brain regions: the dorsal caudate putamen, nucleus accumbens shell, CA1 region of the hippocampus, and the prefrontal cortex. Adenosine release in all regions was activity-dependent but the mechanism of release varied. In the caudate

putamen and nucleus accumbens, stimulated release was dependent on ionotropic glutamate receptors whereas in the hippocampus and prefrontal cortex, adenosine release was dependent on extracellular ATP metabolism⁸ (Fig. 6). This study demonstrates the complexity of adenosine release in the brain. Although adenosine release was activity-dependent in all regions, dependence on either glutamate or ATP changed based on the brain region.

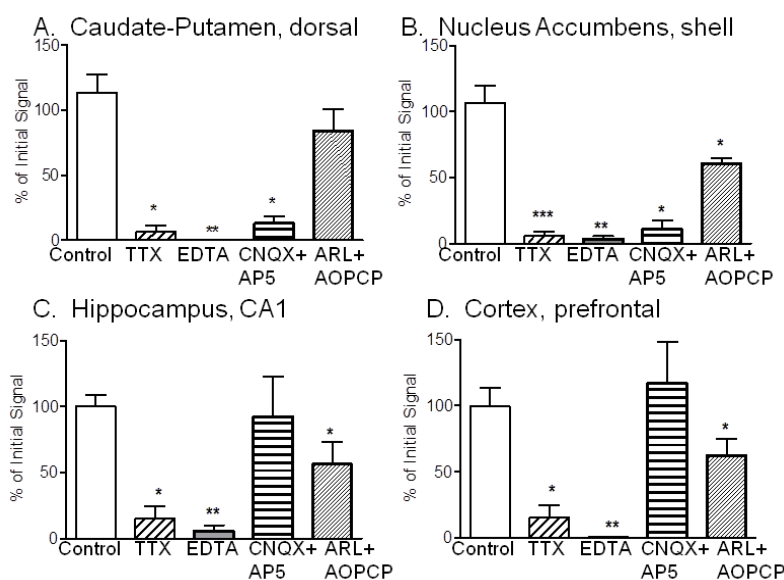


Figure 1.6: Mechanism of stimulated adenosine release varies by brain region: (A) Caudate putamen, (B) Nucleus accumbens shell, (C) CA1 region of the hippocampus and (D) Prefrontal cortex.

Stimulated adenosine release was dependent on both voltage-gated Na⁺ channels by 0.5 μ M tetrodotoxin (TTX) and Ca²⁺ by chelating calcium with 1 mM EDTA in all brain regions.

Adenosine release was dependent on ionotropic

glutamate receptors (10 μ M 6-cyano-7-nitroquinoxaline-2,3-dione, CNQX) in the dorsal caudate putamen (A) and nucleus accumbens shell (B). Adenosine release was dependent on ATP release (50 μ M ARL 67156 + 100 μ M α,β -methylene adenosine diphosphate, AOPCP) in the nucleus accumbens shell (B), hippocampus (C), and the prefrontal cortex (D). Reproduced from Pajski et al⁸.

1.2.1.8 FSCV to study adenosine deaminase kinetics.

Xu et al. showed how FSCV at carbon-fiber microelectrodes can be used to monitor enzyme kinetics⁷⁸. We examined the kinetics of adenosine deaminase, the major enzyme responsible for metabolic breakdown of adenosine to inosine. Salt concentrations dramatically changed enzyme activity, and inhibitors of adenosine deaminase were not competitive in the presence of divalent cations⁷⁸. Caffeine, an

adenosine receptor antagonist, increased enzyme activity. This provides a fast and easy way to screen drug effects on enzyme kinetics *in vivo*.

1.2.1.9 Adenosine release during deep brain stimulation causes microthalamotomy effect.

Essential tremor patients and Parkinson's disease patients often see an immediate relief from tremors immediately following electrode implantation during deep brain stimulation (DBS) procedures⁷⁹. This is referred to as the microthalamotomy effect. Kendall Lee's group discovered that adenosine was elevated immediately after electrode implantation, preceding the microthalamotomy effect in the ferret thalamus⁸⁰. In 2012, Lee et al. implanted a DBS probe into 7 human patients, and also saw the microthalamotomy effect along with release of adenosine in all patients⁷⁹. Future studies could probe whether adenosine is a cause or effect of the microthalamotomy effect during implantation in deep brain stimulation.

The Lee group also discovered that high frequency stimulation (HFS) in ferret thalamic slices causes non-activity dependent (TTX-resistant) adenosine release, indicating a non-neuronal source such as astrocytes⁸⁰. The waveform used for adenosine detection was scanning from -0.4 to 1.5 V at a scan rate of 400 V/s (Figure 1.7a). Figure 1.7b shows adenosine is released within 10-15s after HFS. A clear primary and secondary peak is observed, indicating the release is from adenosine. The primary and secondary peaks have similar current versus time profiles (Figure 1.7c), but the secondary peak did not last as long. Figure 1.7d shows the background current before and after stimulation, and a small change is indicated. The CV confirming adenosine release is shown in Figure 1.7e, and the

primary and secondary peaks are marked. No adenosine pharmacology experiments were performed, but they would help verify adenosine release in the future.

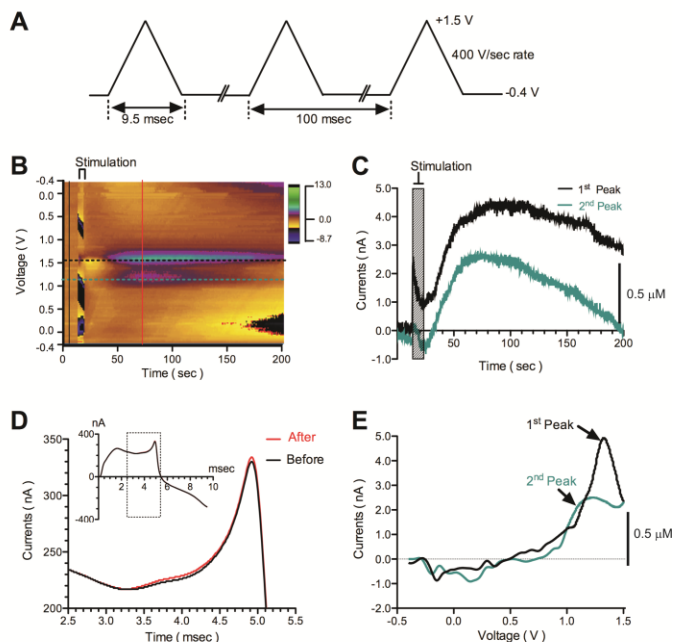


Figure 1.7: Adenosine release occurs after high frequency stimulation (125 Hz, 200 μ A, for 5s, 100 μ s pulse width) in thalamic slices. A) FSCV waveform for adenosine detection involved scanning from -0.4 to 1.5 V at 400 V/s. B) Color plot for adenosine shows adenosine release immediately following stimulation, as indicated by the black box at top of color plot. Release lasted for two minutes after stimulation. C) Current versus time trace of the primary and secondary peak of adenosine after stimulation. D) Background current changes over time before and after stimulation. E) CV for adenosine where primary and secondary peaks are denoted by the black arrows. Reproduced from Tawfik et al.⁸⁰

1.2.1.10 AMP hydrolysis to adenosine inhibits pain-sensing response in spinal cord.

AMP hydrolyzes to adenosine in spinal lamina II neurons responsible for nociceptive (pain-sensing) responses^{51,55}. Three enzymes were found to hydrolyze AMP to adenosine in these neurons: prostatic acid phosphatase (PAP), ecto-5'-nucleotidase (NT5E), and tissue-nonspecific alkaline phosphatase (TNAP). Figure 1.8 shows example data for adenosine release in spinal lamina II neurons. AMP was

applied to the slices and subsequent adenosine formation was measured at carbon-fiber microelectrodes (Figure 1.8a)⁵¹. CVs for adenosine in brain slices were compared to *in vitro* (Figure 1.8b), and both exhibit clear primary and secondary oxidation products. Color plots for all mouse types are shown in Figure 1.8c-f. Knockouts of PAP, NT5E, and dKO were all compared. Adenosine release was significantly reduced in both NT5E and dKO at pH 7.4 (Figure 1.8h) and was significantly reduced in all knockouts at pH 5.6 (Figure 1.8j). An acidic pH was used to test whether the enzymes had a pH preference since pH fluctuations are not uncommon under normal physiological conditions. For example, excitatory synapses become transiently acidified following glutamate release. The data also suggested that the third enzyme involved was not an acid phosphatase due to adenosine reduction in dKO mice; and this was later confirmed.

Street et al. also discovered spontaneous adenosine transients which occurred in spinal lamina II slices⁵¹. Double knockout mice of PAP and NT5E had reduced adenosine transient frequency, likely due because of limited AMP hydrolysis. This was the first time spontaneous transient adenosine release had been observed in the CNS. Together, these studies provide useful information on how adenosine is produced from pain-sensing neurons and may provide important therapeutic targets for adenosine manipulation.

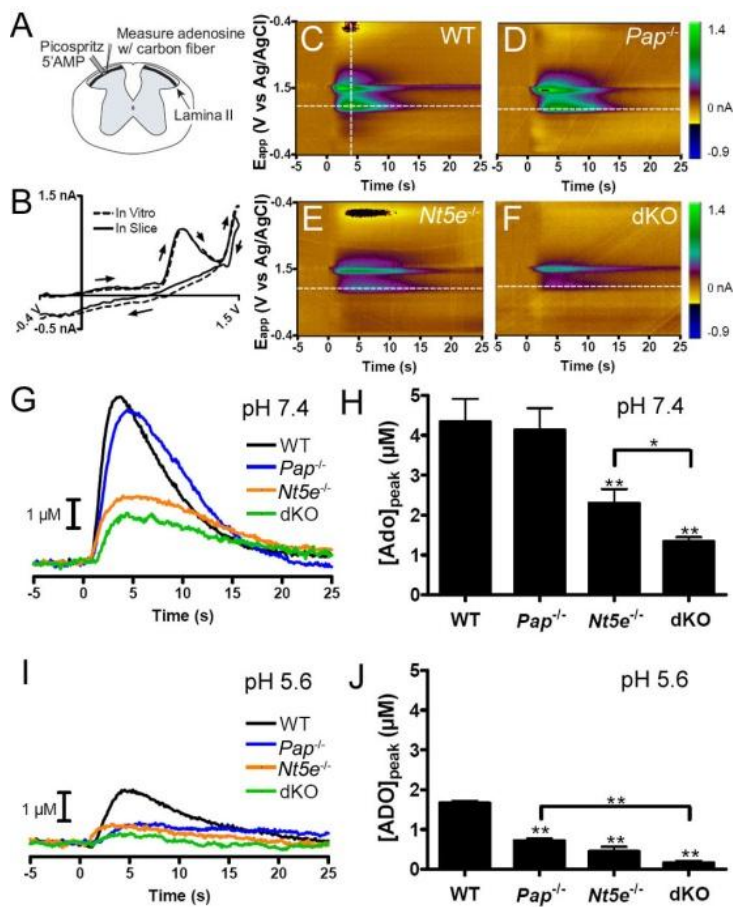


Figure 1.8: AMP hydrolysis to adenosine is reduced in PAP and NT5E knockout mice. Wild type (WT), *Pap*^{-/-}, *Nt5e*^{-/-}, and double knockout (dKO) mice were compared. A) Schematic of experimental set up. 5'-AMP was picospritzed onto spinal lamina II neurons and degradation to adenosine was detected at carbon-fiber microelectrodes with FSCV. B) Example CV of adenosine for both in vitro and in slice data. Two oxidation peaks characteristic for adenosine is observed. Color plot for WT (C), *Pap*^{-/-} (D), *Nt5e*^{-/-} (E), and dKO (F) show differences in concentration of adenosine released. Differences in pH were tested and pH 7.4 (G) produced more current for all mouse types compared to pH 5.6 (I). Average adenosine concentrations for each

mouse type in pH 7.4 (H) and pH 5.6 (J) show less adenosine in more acidic pH. Adenosine was significantly reduced in *Nt5e*^{-/-} and dKO (H & J) and in *Pap*^{-/-} (J). Figure was reproduced from Street et al⁵¹.

1.2.1.11 Spontaneous transient adenosine release.

Most recently, spontaneous transient adenosine release was detected using FSCV at carbon-fiber microelectrodes *in vivo*.⁸¹ In this study, adenosine release was detected both in the caudate putamen and the prefrontal cortex upon eliciting no stimulation. The release events only lasted a few seconds and were on average $0.17 \pm 0.01 \mu\text{M}$ in the caudate and $0.19 \pm 0.01 \mu\text{M}$ in the prefrontal cortex. Spontaneous adenosine release was more frequently detected in the prefrontal cortex. In both the caudate and the prefrontal cortex, transient adenosine release was regulated by inhibitory A₁ receptors. This is the first time spontaneous

adenosine release had ever been characterized and may provide useful information in the future on rapid adenosine signaling in the brain. Further characterization will provide information on how the transients are regulated in multiple brain regions, the mechanisms of release, and the importance of them in the brain.

1.2.1.12 Enhanced understanding of adenosine signaling using FSCV.

FSCV detection of adenosine with carbon-fiber microelectrodes has led to a wealth of information on the timescale of adenosine signaling and mechanisms of release. FSCV has shown that the mechanism of transient adenosine release is always activity dependent⁶, although the specific dependence on glutamate signaling or ATP breakdown can vary by region⁸. This is different than slower signaling which is primarily due to reverse transport^{24,82}. Rapid neuromodulation by adenosine during deep brain stimulation implantation for Parkinson's disease patients was also discovered using FSCV suggesting that adenosine is the important signaling molecule during the microthalatotomy effect⁷⁹. Parkinson's disease is a dopamine dysregulation disease so treatments have focused on dopamine therapies⁸³⁻⁸⁶; FSCV has also been used to study the mechanism of adenosine formation during pain-sensing regulation⁵¹. A new enzyme was discovered in spinal cord neurons which is responsible for adenosine formation from AMP. The most attractive attributes of FSCV with carbon-fiber microelectrodes are rapid detection and low limits of detection. Previously, adenosine was monitored on the minute to hour time scale using microdialysis coupled to HPLC, so fast changes in neuronal activity went undetected^{3,87}. The ability to measure adenosine changes in real time has led to a better understanding of the complex mechanism of stimulated adenosine release in different brain regions⁸. Real-time measurements after mimicking neuronal firing with stimulated release is beneficial to fully understand

adenosine rapid signaling. Utilization of fast sensing techniques such as FSCV has changed our understanding of adenosine signaling in the brain. Not only is it a neuromodulator, but it is important on the millisecond timescale in biological functions such as respiration⁵⁶. Understanding adenosine modulation on a rapid timescale will be beneficial for further developing adenosine therapeutics for disease treatments. In this thesis, in Chapters 5-6, I will show how FSCV at carbon-fiber microelectrodes have been used to study adenosine function in the brain.

1.2.2 Adenosine characterization using amperometric adenosine micro-biosensors

The development of small amperometric adenosine sensors in the early 2000s⁸⁸ has facilitated many studies on the release mechanisms of adenosine⁸⁹ and its roles in brain diseases^{10,11}. Adenosine selective enzyme sensors are made by entrapping xanthine oxidase, purine nucleoside phosphorylase and adenosine deaminase on a platinum microelectrode using a derivatized pyrrole polymer⁸⁸. This enzyme cascade causes adenosine to break down to inosine then hypoxanthine and then to uric acid and hydrogen peroxide⁹⁰. The hydrogen peroxide concentration is proportional to purine concentration and hydrogen peroxide is detected at the electrode using amperometry. Amperometry measurements do not provide a fingerprint CV for the analyte studied, so the confidence in detection is lowered.

The diameter of the biosensors ranges from 7 μm to 50 μm and the linear concentration range is similar to carbon-fiber microelectrodes (50 nM to 20 μM)⁹¹. A null sensor which contains no enzymes is often used in parallel with the adenosine sensor so that background subtraction of non-adenosine activity can be achieved. With FSCV and carbon-fiber microelectrodes, no additional electrode is required. A

sensor which lacks the first enzyme to break down adenosine to inosine can also be used to verify adenosine is detected, and not one of its metabolites⁹¹. With FSCV, a null sensor control is not needed. The enzyme sensors are typically held at 500 mV using a potentiostat so that hydrogen peroxide can be oxidized^{88,90}; however, many other chemicals in the brain oxidize at similar potentials so careful controls are needed to ensure other chemicals are not detected. Despite their drawbacks, adenosine biosensors have provided a wealth of information on adenosine biological function. Enzyme biosensors are also commercially available from Sarissa-biomedical.

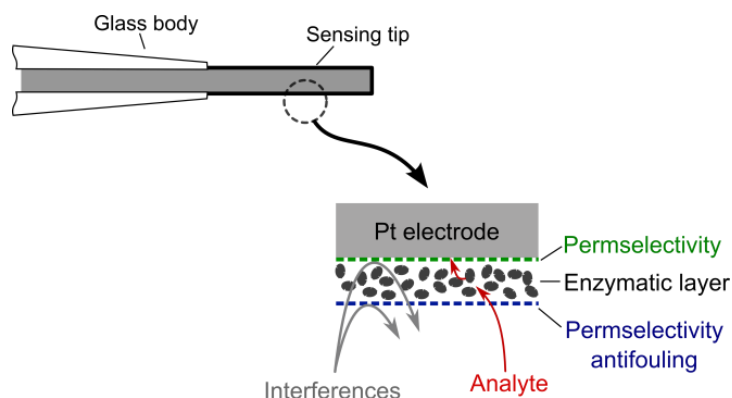


Figure 1.9: Schematic of biosensor. The enzyme layer is coated between two permselective layers which enhance biocompatibility and block interferences. For adenosine, the enzymatic layer consists of xanthine oxidase, purine nucleoside phosphorylase and adenosine deaminase in a derivatized pyrrole polymer. The sensing tip is insulated, is between 7-50 μm in diameter, and protrudes 0.5 to 2 mm in length. Reproduced from Dale et al.⁹¹

1.2.2.1 Activity-dependent adenosine release in the cerebellum is modulated by endogenous neurotransmitters.

Stimulated release has been characterized using amperometric adenosine biosensors. Activity-dependent adenosine release occurred after electrically stimulating cerebellar slices⁷⁶. Because the release was modulated by receptors which act on parallel fiber-Purkinje cell synapses, parallel fibers were considered

the most likely release sites⁷⁶. Parallel fiber-Purkinje cells are inhibited by both GABA_B and mGlu4 receptors^{92,93}. Administration of either a GABA_B receptor agonist, baclofen, or a mGluR receptor agonists, L-AP4, inactivated parallel fiber-Purkinje cell transmission and decreased adenosine release; therefore, adenosine release requires activation of parallel fiber-Purkinje cells and is modulated by GABA and glutamate in this region⁷⁶.

Blocking K⁺ channels with 4-aminopyridine (4-AP) increased adenosine release in the cerebellum²⁶. After applying 60 μM 4-AP, a single pulse stimulus could be used to evoke adenosine release²⁶. The adenosine metabolism blocker erythro-9-(2-hydroxy-3-nonyl) adenine (EHNA), was used to verify adenosine release.

Electrophysiological experiments confirmed that 4-AP increased the width of the action potential by increasing Ca²⁺ influx into the cell, allowing more adenosine to be released²⁶. Interestingly, adenosine release without 4-AP was glutamate receptor independent whereas adenosine release after 4-AP was AMPA receptor dependent. Release in the presence of 4-AP was also found to be activity-dependent by blocking Ca²⁺ influx and using TTX to block voltage-gated sodium channels²⁶.

In 2012, Klyuch et al. studied how both mechanisms (train and single-spike) of adenosine release in the cerebellum were controlled by the metabotropic receptors A₁, GABA_B, and mGlu4⁹⁴. They discovered that metabotropic receptors (A₁, GABA_B, mGlu4) modulate adenosine release, including the adenosine release which is independent of ionotropic glutamate activation (train evoked)⁹⁴. The adenosine receptor A₁, together with GABA_B and mGlu4, potentiated adenosine release but A₁ is most important in adenosine modulation. Blocking metabotropic receptors induced train stimulus evoked adenosine release which was previously found to be independent of ionotropic glutamate activation in 2011²⁶. Metabotropic receptor

inhibition also attenuated single spike adenosine release which is dependent on ionotropic glutamate receptor activation⁹⁴. Adenosine release in the cerebellum is highly complex and involves several endogenous neuromodulators.

Further characterization of activity-dependent adenosine release in the cerebellum revealed that a portion of release is not due to extracellular breakdown of ATP⁸⁹. Activity-dependent adenosine release in the cerebellum of mice lacking the CD73 gene which encodes ecto-5'-nucleotidase (which converts AMP to adenosine) revealed ATP independence⁸⁹. The adenosine release that was independent of ATP was modulated by mGlu4 activation. These findings further support the complexity of adenosine signaling within the brain and that direct exocytosis may be possible.

1.2.2.2 Adenosine is released during hypoxia in the hippocampus.

Adenosine release during hypoxia has been an accepted phenomenon for several years^{3,95,96}. Hypoxia is a physiological condition in which adequate oxygen is not delivered to the tissue. Previous studies of adenosine during hypoxia heavily relied on slow temporal resolution techniques such as HPLC^{3,97}. More recently, adenosine biosensors have been used to understand the time course of adenosine signaling during hypoxia^{9,90,98,99}.

In 2000, Dale et al. discovered and validated adenosine release during hypoxia in the hippocampus using amperometric biosensors⁹⁰. Hypoxic episodes of different durations were studied and adenosine increased steadily during both 5 minute and 10 minute episodes⁹⁰. Doubling the hypoxic episode time resulted in doubled adenosine release, confirming the relationship between hypoxia and adenosine. The increase in adenosine correlated with a decrease in synaptic transmission⁹⁰.

Removal of extracellular Ca^{2+} significantly increased adenosine release whereas increased Ca^{2+} reduced adenosine release. This suggests that adenosine release is not dependent on Ca^{2+} but the amount is regulated by extracellular Ca^{2+} ⁹⁰. Later, Pearson et al. showed that repeated exposures to hypoxia in the hippocampus resulted in weakened depression of synaptic transmission and adenosine release¹⁰⁰. Release is partially restored after recovery or exogenous adenosine application. These findings suggest a depletable but replenishable pool of adenosine¹⁰⁰.

Smaller amperometric enzyme sensors were used in 2003 by Frenguelli et al. to confirm adenosine release during hypoxia⁹. The smaller sensors provided a more accurate depiction of adenosine release during hypoxia because they were inserted in the tissue, instead of being placed on top⁹. The improved sensor also led to the discovery of the post-hypoxia purine efflux (PPE)⁹. PPE is a large increase in adenosine production as the brain returns to normoxia. The function of PPE is unknown, but it was mostly attributed to reoxygenation of the brain causing changes in nitric oxide, adenosine, or intracellular pH⁹. Together these studies provide information on rapid adenosine signaling during hypoxia.

1.2.2.3 Adenosine is released during hypoxia in the nucleus tractus solitarius (NTS) of the brainstem.

In vivo measurements in the NTS region of the brainstem confirmed adenosine release as a result of hypoxia¹⁰¹. Adenosine release was much smaller in the rostral region of the ventrolateral medulla (VLM) than the NTS. Adenosine release in both regions was not correlated with a decrease in respiration, so adenosine release was not believed to modulate the hypoxia-induced decrease in respiration during hypoxic ventilatory depression. Adenosine was measured on the surface of the region and

within the region, and greater amounts of adenosine were detected on the surface, unlike previous studies in this region without hypoxia⁷. The different concentrations of adenosine point to different structures within this region releasing adenosine. Overall, this study demonstrated adenosine release in a region other than the hippocampus during hypoxia and that adenosine release was not the cause of decreased respiration during hypoxia. Therefore, adenosine was found not to be important during hypoxic ventilatory depression that leads to apnoea.

1.2.2.4 Adenosine is released during ischemia.

Amperometric enzyme biosensors have also been used to study adenosine release during ischemia or oxygen/glucose deprivation^{10,38,102}. Ischemia is inadequate blood flow to a tissue that causes a decrease in oxygen. Ischemic attack always results in hypoxia; however, hypoxia is not always caused by ischemia if for example the oxygen content of the arterial blood decreases as with anemia. Ischemia is often simulated experimentally by reducing oxygen and glucose. Similar to hypoxia, ischemic conditions caused adenosine to rise at the same time excitatory synaptic transmission decreased³⁸. The decrease in synaptic transmission was not as dramatic in the presence of an A₁ receptor antagonist and the rate of recovery was also enhanced from 60 minutes to 15 minutes³⁸. This studied provided evidence that adenosine is neuroprotective during ischemia.

Adenosine release precedes ATP release during ischemia in the hippocampus⁹⁸. Amperometric enzyme biosensors were used to compare ATP and adenosine release during ischemia in the hippocampus. ATP release did not occur until after adenosine release and ATP release required extracellular Ca²⁺ while adenosine release was enhanced by removal of extracellular Ca²⁺. Ionotropic

glutamate receptor inhibition increased ATP release but only slightly enhanced adenosine release. Because adenosine was released before ATP and was larger, adenosine is not a result of ATP metabolism. Long periods of ischemia resulted in an anoxic depolarization and ATP was only released at this point.

Boison et al. used amperometric adenosine sensors *in vivo* to show increase adenosine in transgenic mice model with reduced adenosine kinase in the forebrain (fb-adk-def)¹⁰³. Transgenic mice were better protected during ischemic-induced stroke, likely due to elevated adenosine levels. All together, these studies describe the important role adenosine has during ischemia and may provide information for therapeutics in the future.

1.2.2.5 Adenosine modulates chemoreceptor responses.

In 2002, the first *in vivo* measurements were made using amperometric adenosine sensors⁷ on the dorsal surface of the brainstem and the nucleus tractus solitarii (NTS) of the medulla oblongata. Adenosine release was measured in response to a defense reaction, induced by stimulating the hypothalamus defense area (HDA). The defense reaction involves an increase in respiration, heart rate, and blood pressure. The NTS is responsible for regulating many cardiovascular and respiratory responses. In the NTS, adenosine modulated baroreceptor and chemoreceptor reflexes involved in responding to pressure and chemical stimuli, respectively. Thus, adenosine release in the brainstem correlates with cardiovascular defense responses.

1.2.2.6 Adenosine is linked to modulating seizures induced by CO₂.

Respiration rate and blood flow are regulated by carbon dioxide (CO₂) levels and vice versa. Hypercapnia, an increase in CO₂, causes a decrease in neuron excitability, whereas hypocapnia, a decrease in CO₂, increases neuron excitability in the hippocampus¹⁰⁴. Decreasing CO₂ is a common method for inducing seizure likely because this causes CNS vasoconstriction and reduced blood brain flow, while increasing CO₂ is often used in sedation as an anesthetic. The level of CO₂ controls tissue pH, and pH has also been linked to neuronal excitability. Dulla et al. showed that increasing CO₂, decreased pH and increased adenosine in the hippocampal slices¹⁰⁴. The increase in adenosine correlated with the inhibition of synaptic transmission. These effects were modulated by A₁ receptors, ATP receptors, and ecto-ATPase. Decreases in adenosine levels during hypocapnia suggest a link between adenosine and hyperventilation-induced epileptic seizures. During hypercapnia, ATPase blockers did not change adenosine release, and a cocktail of A₁ and ATP receptor antagonists were needed to completely inhibit release. The combination of these findings leads to the conclusion that adenosine and ATP work in concert with one another as neuromodulators during hypercapnia¹⁰⁴.

1.2.2.7 Increase in extracellular adenosine levels provides anticonvulsant behavior during epilepsy.

Basal synaptic adenosine levels are regulated by astrocytic adenosine kinase which regulates seizure activity¹⁰⁵. One of the main pathways for regulating adenosine is phosphorylation of adenosine to AMP by adenosine kinase (ADK). Etherington et al. showed that inhibition of ADK increased extracellular adenosine which inhibited excitatory neurotransmission in the hippocampus and seizure activity

evoked by either Mg^{2+} free aCSF or high frequency stimulation was greatly attenuated¹⁰⁵. ADK is primarily located in glial fibrillary acidic protein (GFAP)-positive astrocytes, so astrocytes are thought to be important during seizure activity. Because ADK regulates adenosine during evoked seizures and adenosine induces anticonvulsant activity, ADK regulation may be novel therapy for epilepsy.

1.2.2.8 Adenosine is involved in the sleep-wake cycle

Sleep can be broadly divided into two categories: slow wave sleep and rapid eye movement sleep. Sleep is divided into those two main categories based on four criteria: posture, changes in electroencephalogram (EEG), increase in response threshold to external stimuli, and rapid reversibility¹⁰⁶. These four criteria are often used to determine sleep/wake activity in mammals. Behaviors during sleep are controlled by either homeostatic mechanisms or circadian rhythms. Adenosine is involved primarily during slow wave sleep^{106,107}. Schmitt et al. discovered that wakefulness regulates extracellular adenosine levels through an astrocytic-SNARE-dependent mechanism in hippocampal slices¹⁰⁸. To understand this, the authors compared extracellular adenosine concentrations using amperometric biosensors in wild-type mice and transgenic mice, which have a double negative transgene specific to disrupt SNARE complex formation in glia (dnSNARE). Both sets of mice were sleep deprived and their adenosine levels compared. Extracellular adenosine was significantly larger in sleep deprived wild-type mice than in dnSNARE mice. This study showed that sleep deprivation increased adenosine and that this release was dependent on neurotransmission from astrocytes in the hippocampus¹⁰⁸.

Dale's group recently characterized the mechanism of adenosine release during the sleep-wake cycle in the basal forebrain⁵⁹. The basal forebrain is involved in the

ascending arousal system¹⁰⁹. Previous studies have linked nitric oxide (NO) signaling to increased adenosine release during sleep¹¹⁰. The relationship between sleep and adenosine was studied in three rodent models: rats, mice, and hamsters⁵⁹ and results were generally similar in all the rodents. Adenosine levels were measured at seven different stages of the diurnal cycle, spanning the light and dark stages, by sacrifice and brain slice preparation at those time points. Extracellular adenosine release increased after ionotropic and group I metabotropic glutamate receptor agonists but did not change from orexin, histamine, and neurotensin administration, suggesting not all depolarizing stimuli contribute to adenosine release. Adenosine release varied during the diurnal cycle. Adenosine release was greatest at the end of the dark cycle and less during the light cycle.

Dale's group also showed that the rise in adenosine in the basal forebrain due to sleep deprivation was dependent on NO produced from inducible nitric oxide synthase (iNOs)⁵⁹. Blocking iNOs, scavenging NO, or using a non-specific inhibitor of NO caused decreased adenosine during sleep deprivation. Figure 1.10 shows comparisons of adenosine release for controls (non-sleep deprived), sleep deprived, sleep deprived with iNOs inhibition (by 1400 W), and non-sleep deprived with iNOs inhibition. The diurnal dependent variation of adenosine may be independent of iNOs because adenosine did not change during control conditions (no sleep deprivation, Figure 1.10a,b) after iNOs inhibition. Basal tone of adenosine followed a similar pattern to adenosine release (Figure 1.10d). However, the cortex did not follow the same pattern as the basal forebrain (Figure 1.10e,f). Overall, adenosine release is dependent on NOs during sleep deprivation and changes based on the diurnal sleep cycle

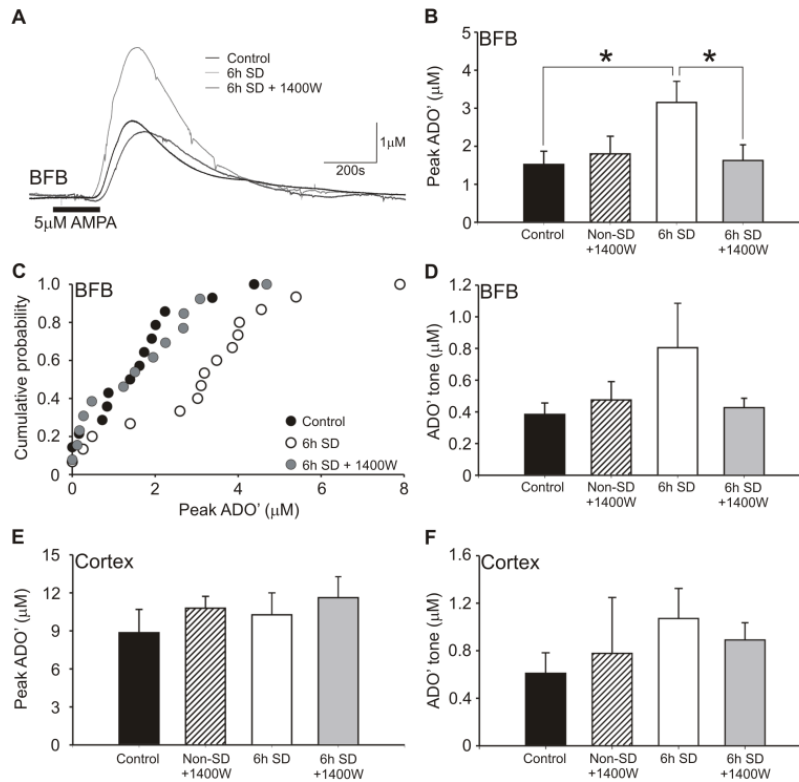


Figure 1.10: Increased adenosine after sleep deprivation is modulated by iNOs production. Adenosine release was measured after 6 hours for control animals (not sleep deprived), sleep deprived, and sleep deprived with 1400W which inhibits iNOs production. A) Shows raw data for all three conditions described above in the basal forebrain. The data is normalized to the 10 μM adenosine calibration. B) Adenosine release was significantly greater in sleep deprived animals. Animals which were not sleep deprived or where iNOs production was inhibited showed less adenosine release. C) Cumulative probability distribution of control individual adenosine responses, sleep deprived, and sleep deprived with iNOs inhibition. D) Basal tone was compared in all four conditions, and the patterned followed that of adenosine release. E) In the cortex, there were no significant differences between adenosine release or F.) basal adenosine tone. Reproduced from Sims et al⁵⁹.

1.3 Contributions of electrochemical detection of adenosine to the field and remaining uncertainties

The advent of rapid real-time monitoring of adenosine *in vivo* has led to new knowledge of the time course of adenosine signaling in the brain. Previous adenosine research relied upon slow temporal techniques such as microdialysis and HPLC^{111,112}. These techniques established a fundamental understanding of the importance of adenosine in the brain, but mechanistic information was more difficult to obtain, especially about rapid signaling. Information on the timescale of adenosine signaling was still unknown; however the long term effects of adenosine were revealed¹¹². Over the last several years, fast-scan cyclic voltammetry with carbon-fiber microelectrodes⁵ and amperometric adenosine biosensors⁸⁸ have gained increased popularity. These studies have revealed that there is rapid signaling of adenosine, a time scale that was previously unknown^{6,7,9,53,91}. More research is needed to fully understand the complicated pathways of adenosine signaling and the function of these transient changes. In this thesis, I develop new techniques to enhance adenosine detection and show how FSCV with carbon-fiber microelectrodes can be used to characterize a new method of adenosine stimulation and to study adenosine modulation of dopamine in the brain.

I first started by developing and optimizing new methods for adenosine detection. Although FSCV at carbon-fiber microelectrodes can accurately and confidently detect adenosine, I sought to enhance adenosine detection by two methods: electrode modification and waveform modification techniques. In Chapters 1 and 2, I developed a novel electrode which consisted of a carbon-fiber coated with Nafion and carbon nanotubes (CNTs) for enhanced dopamine (Chapter 1) and adenosine (Chapter 2) detection. In Chapter 1, I characterize the Nafion-CNT

modified electrode for dopamine detection and compare Nafion to another polymer often used in the literature for dopamine (overoxidized polypyrrole).⁷⁰ In Chapter 2, I apply the Nafion-CNT electrode to adenosine detection using the adenosine waveform.⁵² This was the first time a modified electrode had been optimized for adenosine detection. Nafion-CNT electrodes increased adenosine detection 4-fold, and were also more selective for adenosine over ATP both *in vitro* and in brain slices. Chapter 3 explains a new waveform for enhanced adenosine detection. In this chapter, I implement a sawhorse-shaped waveform instead of the traditional triangle shaped waveform for adenosine detection. This waveform allows a lower switching potential for adenosine oxidation and better discrimination between adenosine and hydrogen peroxide. Overall, these first chapters explain new techniques for enhanced adenosine detection and how they may be used in the future.

The last chapters of this thesis involve developing new strategies to elicit and study adenosine in the brain using FSCV at carbon-fiber microelectrodes. In Chapter 4, I show a new method of evoking adenosine release in the brain by mechanical stimulation via lowering the working electrode. Mechanically stimulated adenosine was also evoked by lowering a glass pipette near the electrode. Mechanically stimulated adenosine was fully characterized and found to be activity dependent and caused from rapid extracellular ATP metabolism. This chapter explains for the first time rapid adenosine changes in the brain in response to a mechanical stimulus. Since adenosine is neuroprotective in nature, this may provide information on adenosine neuroprotection on a rapid time scale.

Adenosine is traditionally classified as a neuromodulator in the brain; however, most studies have used slow temporal resolution techniques to study adenosine

modulation. In Chapter 5, I use FSCV at carbon-fiber microelectrodes to study adenosine modulation of dopamine on a rapid time scale. Exogenous application of adenosine seconds before electrical stimulation of dopamine caused a decrease in dopamine release temporarily. In this chapter, I characterize adenosine modulation of dopamine and find that inhibitory A₁ receptors are responsible for the decrease in dopamine release. Endogenous adenosine caused by mechanical stimulation also caused dopamine release to decrease temporarily. Overall, this is the first time adenosine modulation of dopamine has been studied on a rapid time scale.

In conclusion, this thesis will explain new methods for enhanced adenosine detection and show how FSCV can be used to monitor adenosine function on a rapid time scale.

1.4 References

1. Cunha, R. A. *Neurochem. Int.* **2001**, *38* (2), 107-125.
2. Fredholm, B. B. *Int. Rev. Neurobiol.* **1997**, *40*, 259-280.
3. Koos, B. J.; Kruger, L.; Murray, T. F. *Brain Res.* **1997**, *778* (2), 439-442.
4. Bell, M. J.; Kochanek, P. M.; Carcillo, J. A.; Mi, Z. C.; Schiding, J. K.; Wisniewski, S. R.; Clark, R. S. B.; Dixon, C. E.; Marion, D. W.; Jackson, E. *Journal of Neurotrauma* **1998**, *15* (3), 163-170.
5. Swamy, B. E. K.; Venton, B. J. *Anal. Chem.* **2007**, *79*, 744-750.
6. Pajski, M. L.; Venton, B. J. *ACS Chem. Neurosci.* **2010**, *1* (12), 775-787.
7. Dale, N.; Gourine, A. V.; Llaudet, E.; Bulmer, D.; Thomas, T.; Spyer, K. M. *J. Physiol.* **2002**, *544* (Pt 1), 149-160.
8. Pajski, M. L.; Venton, B. J. *Purinergic Signal.* **2013**, *9* (2), 167-174.
9. Frenguelli, B. G.; Llaudet, E.; Dale, N. *J. Neurochem.* **2003**, *86* (6), 1506-1515.
10. Dale, N.; Frenguelli, B. G. *Current Neuropharmacology* **2009**, *7* (3), 160-179.

11. Dale, N. *J. Physiol.* **2006**, 574 (Pt 3), 633.
12. Cunha, R. A. Adenosine neuromodulation and neuroprotection. In *Handbook of Neurochemistry and Molecular Neurobiology*, Lajtha, A., Vizi, E. S., Eds.; Springer US: 2008; pp 255-273.
13. Franco, R.; Ferre, S.; Agnati, L.; Torvinen, M.; Gines, S.; Hillion, J.; Casado, V.; Lledo, P.; Zoli, M.; Lluís, C.; Fuxe, K. *Neuropsychopharmacology* **2000**, 23 (4 Suppl), S50-S59.
14. Robertson, C. L.; Bell, M. J.; Kochanek, P. M.; Adelson, P. D.; Ruppel, R. A.; Carcillo, J. A.; Wisniewski, S. R.; Mi, Z. C.; Janesko, K. L.; Clark, R. S. B.; Marion, D. W.; Graham, S. H.; Jackson, E. K. *Critical Care Medicine* **2001**, 29 (12), 2287-2293.
15. Rudolphi, K. A.; Schubert, P.; Parkinson, F. E.; Fredholm, B. B. *Cerebrovasc. Brain Metab Rev.* **1992**, 4 (4), 346-369.
16. O'Regan, M. *Neurol. Res.* **2005**, 27 (2), 175-181.
17. Lorbar, M.; Fenton, R. A.; Duffy, A. J.; Graybill, C. A.; Dobson, J. G., Jr. *J Mol Cell Cardiol.* **1999**, 31 (2), 401-412.
18. Villarreal, F.; Zimmermann, S.; Makhsudova, L.; Montag, A. C.; Erion, M. D.; Bullough, D. A.; Ito, B. R. *Mol. Cell Biochem.* **2003**, 251 (1-2), 17-26.
19. Lu, Q.; Newton, J.; Hsiao, V.; Shamirian, P.; Blackburn, M. R.; Pedroza, M. *American Journal of Respiratory Cell and Molecular Biology* **2012**, 47 (5), 604-613.
20. Fuxe, K.; Stromberg, I.; Popoli, P.; Rimondini-Giorgini, R.; Torvinen, M.; Ogren, S. O.; Franco, R.; Agnati, L. F.; Ferre, S. *Adv. Neurol.* **2001**, 86, 345-353.
21. Pinna, A.; Volpini, R.; Cristalli, G.; Morelli, M. *Eur. J. Pharmacol.* **2005**, 512 (2-3), 157-164.
22. Blum, D.; Hourez, R.; Galas, M. C.; Popoli, P.; Schiffmann, S. N. *Lancet Neurol.* **2003**, 2 (6), 366-374.
23. Ferre, S.; Ciruela, F.; Canals, M.; Marcellino, D.; Burgueno, J.; Casado, V.; Hillion, J.; Torvinen, M.; Fanelli, F.; de Benedetti, P.; Goldberg, S. R.; Bouvier, M.; Fuxe, K.; Agnati, L. F.; Lluís, C.; Franco, R.; Woods, A. *Parkinsonism & Related Disorders* **2004**, 10 (5), 265-271.
24. Latini, S.; Pedata, F. *J. Neurochem.* **2001**, 79, 463-484.
25. Wall, M.; Dale, N. *Curr. Neuropharmacol.* **2008**, 6 (4), 329-337.
26. Klyuch, B. P.; Richardson, M. J. E.; Dale, N.; Wall, M. J. *J. Physiol.* **2011**, 589 (2), 283-295.

27. Fredholm, B. B.; Abbracchio, M. P.; Burnstock, G.; Daly, J. W.; Harden, T. K.; Jacobson, K. A.; Leff, P.; Williams, M. *Pharmacol. Rev.* **1994**, *46* (2), 143-156.
28. Fredholm, B. B.; Chen, J. F.; Cunha, R. A.; Svenningsson, P.; Vaugeois, J. M. *Int. Rev. Neurobiol.* **2005**, *63*, 191-270.
29. Latini, S.; Pazzagli, M.; Pepeu, G.; Pedata, F. *Gen. Pharmac.* **1996**, *27* (6), 925-933.
30. Gomes, C. V.; Kaster, M. P.; Tome, A. R.; Agostinho, P. M.; Cunha, R. A. *Biochimica et Biophysica Acta-Biomembranes* **2011**, *1808* (5), 1380-1399.
31. Thompson, S. M.; Haas, H. L.; Gahwiler, B. H. *Journal of Physiology-London* **1992**, *451*, 347-363.
32. Hamilton, B. R.; Smith, D. O. *J. Physiol.* **1991**, *432*, 327-341.
33. Calker, D.; Biber, K. *Neurochemical Research* **2005**, *30* (10), 1205-1217.
34. Haselkorn, M. L.; Shellington, D.; Jackson, E.; Vagni, V.; Feldman, K.; Dubey, R.; Gillespie, D.; Bell, M.; Clark, R.; Jenkins, L.; Schnermann, J.; Homanics, G.; Kochanek, P. *J. Neurotrauma* **2008**, *25* (7), 901.
35. Baldwin, S. A.; Beal, P. R.; Yao, S. Y.; King, A. E.; Cass, C. E.; Young, J. D. *Pflugers Arch.* **2004**, *447* (5), 735-743.
36. Thorn, J. A.; Jarvis, S. M. *Gen. Pharmac.* **1996**, *27*, 613-620.
37. Sperlagh, B.; Vizi, E. S. *Current Topics in Medicinal Chemistry* **2011**, *11* (8), 1034-1046.
38. Pearson, T.; Damian, K.; Lynas, R. E.; Frenguelli, B. G. *J. Neurochem.* **2006**, *97* (5), 1357-1368.
39. de Mendonca, A.; Sebastiao, A. M.; Ribeiro, J. A. *Brain Res. Brain Res. Rev.* **2000**, *33* (2-3), 258-274.
40. Deng, Q.; Watson, C. J.; Kennedy, R. T. *J. Chromatogr. A* **2003**, *1005* (1-2), 123-130.
41. Valtysson, J.; Persson, L.; Hillered, L. *Acta Neurochirurgica* **1998**, *140* (4), 387-395.
42. Aden, U.; Halldner, L.; Lagercrantz, H.; Dalmau, I.; Ledent, C.; Fredholm, B. B. *Stroke* **2003**, *34* (3), 739-744.
43. Newby, A. C.; Worku, Y.; Holmquist, C. A. *Adv. Myocardiol.* **1985**, *6*, 273-284.

44. Ferre, S.; Fredholm, B. B.; Morelli, M.; Popoli, P.; Fuxe, K. *Trends Neurosci.* **1997**, *20* (10), 482-487.
45. Ferre, S.; Fuxe, K.; von, E. G.; Johansson, B.; Fredholm, B. B. *Neuroscience* **1992**, *51* (3), 501-512.
46. Quarta, D.; Borycz, J.; Solinas, M.; Patkar, K.; Hockemeyer, J.; Ciruela, F.; Lluís, C.; Franco, R.; Woods, A. S.; Goldberg, S. R.; Ferre, S. *J. Neurochem.* **2004**, *91* (4), 873-880.
47. Okada, M.; Mizuno, K.; Kaneko, S. *Neurosci Lett.* **1996**, *212*, 53-56.
48. Okada, M.; Nutt, D. J.; Murakami, T.; Zhu, G.; Kamata, A.; Kawata, Y.; Kaneko, S. *J. Neurosci.* **2001**, *21* (2), 628-640.
49. Sperlagh, B.; Zsilla, G.; Baranyi, M.; Illes, P.; Vizi, E. S. *Neuroscience* **2007**, *149* (1), 99-111.
50. Von Lubitz, D. K. *Expert. Opin. Investig. Drugs* **2001**, *10* (4), 619-632.
51. Street, S. E.; Walsh, P. L.; Sowa, N. A.; Taylor-Blake, B.; Guillot, T. S.; Vihko, P.; Wightman, R. M.; Zylka, M. J. *Mol. Pain* **2011**, *7*.
52. Ross, A. E.; Venton, B. J. *Analyst* **2012**, *137* (13), 3045-3051.
53. Cechova, S.; Venton, B. J. *J. Neurochem.* **2008**, *105* (4), 1253-1263.
54. Cechova, S.; Elsobky, A. M.; Venton, B. J. *Neuroscience* **2010**, *171* (4), 1006-1015.
55. Street, S. E.; Kramer, N. J.; Walsh, P. L.; Taylor-Blake, B.; Yadav, M. C.; King, I. F.; Vihko, P.; Wightman, R. M.; Millan, J. L.; Zylka, M. J. *J. Neurosci.* **2013**, *33* (27), 11314-11322.
56. Xie, S.; Shafer, G.; Wilson, C. G.; Martin, H. B. *Diamond & Rel. Mat.* **2006**, *15*, 225-228.
57. Dong, H.; Wang, S.; Galligan, J. J.; Swain, G. M. *Front. Biosci. (Schol. Ed.)* **2011**, *3*, 518-540.
58. Park, J.; Quaiserova-Mocko, V.; Patel, B. A.; Novotny, M.; Liu, A.; Bian, X.; Galligan, J. J.; Swain, G. M. *Analyst* **2008**, *133* (1), 17-24.
59. Sims, R. E.; Wu, H. H. T.; Dale, N. *Plos One* **2013**, *8* (1).
60. Stamford, J. A.; Kruk, Z. L.; Millar, J.; Wightman, R. M. *Neurosci Lett.* **1984**, *51* (1), 133-138.
61. Wightman, R. M.; Amatore, C.; Engstrom, R. C.; Hale, P. D.; Kristensen, E. W.; Kuhr, W. G.; May, L. J. *Neuroscience* **1988**, *25* (2), 513-523.

62. Park, J.; Aragona, B. J.; Kile, B. M.; Carelli, R. M.; Wightman, R. M. *Neuroscience* **2010**, *169* (1), 132-142.
63. Dryhurst, G. *Electrochemistry of biological molecules*; Academic Press: New York, 1977. pp. 71-185.
64. Venton, B. J.; Wightman, R. M. *Synapse* **2007**, *61* (1), 37-39.
65. Takmakov, P.; Zachek, M. K.; Keithley, R. B.; Walsh, P. L.; Donley, C.; McCarty, G. S.; Wightman, R. M. *Anal. Chem.* **2010**, *82* (5), 2020-2028.
66. Hashemi, P.; Dankoski, E. C.; Petrovic, J.; Keithley, R. B.; Wightman, R. M. *Anal. Chem.* **2009**, *81* (22), 9462-9471.
67. Cooper, S. E.; Venton, B. J. *Analytical and Bioanalytical Chemistry* **2009**, *394* (1), 329-336.
68. Lugo-Morales, L. Z.; Loziuk, P. L.; Corder, A. K.; Toups, J. V.; Roberts, J. G.; McCaffrey, K. A.; Sombers, L. A. *Anal. Chem.* **2013**, *85* (18), 8780-8786.
69. Hocevar, S. R.; Wang, J.; Deo, R. P.; Musameh, M.; Ogorevc, B. *Electroanalysis* **2005**, *17* (5-6), 417-422.
70. Pears, M. J.; Ross, A. E.; Venton, B. J. *Anal. Methods* **2011**, *3*, 2379-2386.
71. Swamy, B. E. K.; Venton, B. J. *Analyst* **2007**, *132*, 876-884.
72. El-Nour, K. A.; Brajter-Toth, A. *Electroanalysis* **2000**, *12* (11), 305-310.
73. Brajter-Toth, A.; El-Nour, K. A.; Cavalheiro, E. T.; Bravo, R. *Anal. Chem.* **2000**, *72*, 1576-1584.
74. Venton, B. J.; Michael, D. J.; Wightman, R. M. *J. Neurochem.* **2003**, *84* (2), 373-381.
75. O'Neill, C.; Nolan, B. J.; Macari, A.; O'Boyle, K. M.; O'Connor, J. J. *Eur. J. Neurosci.* **2007**, *26* (12), 3421-3428.
76. Wall, M. J.; Dale, N. *J. Physiol* **2007**, *581* (2), 553-565.
77. Mitchell, J. B.; Lupica, C. R.; Dunwiddie, T. V. *J. Neurosci.* **1993**, *13*, 3439-3447.
78. Xu, Y.; Venton, B. J. *Phys. Chem. Chem. Phys.* **2010**, *12* (34), 10027-10032.
79. Chang, S. Y.; Kim, I.; Marsh, M. P.; Jang, D. P.; Hwang, S. C.; Van Gompel, J. J.; Goerss, S. J.; Kimble, C. J.; Bennet, K. E.; Garris, P. A.; Blaha, C. D.; Lee, K. H. *Mayo Clinic Proceedings* **2012**, *87* (8), 760-765.

80. Tawfik, V. L.; Chang, S. Y.; Hitti, F. L.; Roberts, D. W.; Leiter, J. C.; Jovanovic, S.; Lee, K. H. *Neurosurgery* **2010**, *67* (2), 367-375.
81. Nguyen, M. D.; Lee, S. T.; Ross, A. E.; Ryals, M.; Choudhry, V. I.; Venton, B. J. *Plos One* **2014**, *9* (1), e87165.
82. Sweeney, M. I. *J. Neurochem.* **1996**, *67* (1), 81-88.
83. Bourne, J. A. *CNS Drug Rev.* **2001**, *7* (4), 399-414.
84. Zigmond, M. J.; Abercrombie, E. D.; Berger, T. W.; Grace, A. A.; Stricker, E. M. *Trends Neurosci* **1990**, *13*, 290-295.
85. Cools, R. *Neurosci. Biobehav. Rev.* **2006**, *30* (1), 1-23.
86. Funkiewiez, A.; Ardouin, C.; Cools, R.; Krack, P.; Fraix, V.; Batir, A.; Chabardes, S.; Benabid, A. L.; Robbins, T. W.; Pollak, P. *Mov. Disord.* **2006**, *21* (10), 1656-1662.
87. Sciotti, V. M.; Vanwylen, D. G. L. *J. Cereb. Blood Flow Metab* **1993**, *13* (2), 201-207.
88. Llaudet, E.; Botting, N. P.; Crayston, J. A.; Dale, N. *Biosens. bioelectron.* **2003**, *18*, 43-52.
89. Klyuch, B. P.; Dale, N.; Wall, M. J. *J. Neurosci.* **2012**, *32* (11), 3842-3847.
90. Dale, N.; Pearson, T.; Frenguelli, B. G. *J. Physiol* **2000**, *526* (1), -143.
91. Dale, N.; Frenguelli, B. G. *Purinergic Signal.* **2012**, *8* (Suppl 1), 27-40.
92. Neale, S. A.; Garthwaite, J.; Batchelor, A. M. *Neuropharmacology* **2001**, *41* (1), 42-49.
93. Batchelor, A. M.; Garthwaite, J. *Eur. J. Neurosci.* **1992**, *4* (11), 1059-1064.
94. Klyuch, B. P.; Dale, N.; Wall, M. J. *Neuropharmacology* **2012**, *62* (2), 815-824.
95. van Wylen, D. G.; Park, T. S.; Rubio, R.; Berne, R. M. *J Cereb. Blood Flow Metab* **1986**, *6* (5), 522-528.
96. Wallman-Johansson, A.; Fredholm, B. B. *Life Sci.* **1994**, *55* (9), 721-728.
97. Pedata, F.; Latini, S.; Pugliese, A. M.; Pepeu, G. *J. Neurochem.* **1993**, *61* (1), 284-289.
98. Frenguelli, B. G.; Wigmore, G.; Llaudet, E.; Dale, N. *J. Neurochem.* **2007**, *101* (5), 1400-1413.
99. Otsuguro, K.; Wada, M.; Ito, S. *Br. J. Pharmacol.* **2011**, *164* (1), 132-144.

100. Pearson, T.; Nuritova, F.; Caldwell, D.; Dale, N.; Frenguelli, B. G. *J. Neurosci.* **2001**, *21* (7), 2298-2307.
101. Gourine, A. V.; Llaudet, E.; Thomas, T.; Dale, N.; Spyer, K. M. *J. Physiol.* **2002**, *544* (Pt 1), 161-170.
102. Pearson, T.; Currie, A. J.; Etherington, L. A.; Gadalla, A. E.; Damian, K.; Llaudet, E.; Dale, N.; Frenguelli, B. G. *J. Cell Mol. Med.* **2003**, *7* (4), 362-375.
103. Shen, H. Y.; Lusardi, T. A.; Williams-Karnesky, R. L.; Lan, J. Q.; Poulsen, D. J.; Boison, D. *J. Cereb. Blood Flow Metab.* **2011**, *31* (7), 1648-1659.
104. Dulla, C. G.; Dobelis, P.; Pearson, T.; Frenguelli, B. G.; Staley, K. J.; Masino, S. A. *Neuron* **2005**, *48* (6), 1011-1023.
105. Etherington, L. A.; Patterson, G. E.; Meechan, L.; Boison, D.; Irving, A. J.; Dale, N.; Frenguelli, B. G. *Neuropharmacology* **2009**, *56* (2), 429-437.
106. Bjorness, T. E.; Greene, R. W. *Curr. Neuropharmacol.* **2009**, *7* (3), 238-245.
107. Bjorness, T. E.; Kelly, C. L.; Gao, T.; Poffenberger, V.; Greene, R. W. *J. Neurosci.* **2009**, *29* (5), 1267-1276.
108. Schmitt, L. I.; Sims, R. E.; Dale, N.; Haydon, P. G. *J. Neurosci.* **2012**, *32* (13), 4417-4425.
109. Murillo-Rodriguez, E.; Blanco-Centurion, C.; Gerashchenko, D.; Salin-Pascual, R. J.; Shiromani, P. J. *Neuroscience* **2004**, *123* (2), 361-370.
110. Kalinchuk, A. V.; Lu, Y.; Stenberg, D.; Rosenberg, P. A.; Porkka-Heiskanen, T. *J. Neurochem.* **2006**, *99* (2), 483-498.
111. Porkka-Heiskanen, T.; Strecker, R. E.; McCarley, R. W. *Neuroscience* **2000**, *99* (3), 507-517.
112. Pedata, F.; Corsi, C.; Melani, A.; Bordoni, F.; Latini, S. *Ann. N. Y. Acad. Sci.* **2001**, *939*, 74-84.

Chapter 2

Comparison of Nafion- and overoxidized polypyrrole-carbon nanotube electrodes for neurotransmitter detection

We must believe that we are gifted for something, and that this thing, at whatever cost, must be attained

~Marie Curie

Chapter 2: Comparison of Nafion- and overoxidized polypyrrole-carbon nanotube electrodes for neurotransmitter detection

Abstract:

In this chapter, Nafion-CNT modified electrodes were compared to oPPY-CNT modified electrodes for dopamine detection. Permselective polymer coatings improve selectivity and sensitivity of microelectrodes for cationic neurotransmitters. Immobilizing carbon nanotubes (CNTs) into these polymers should further improve sensitivity by increasing the electroactive surface area. The goal of this study was to compare the electrochemical properties of overoxidized polypyrrole (oPPY)-CNT and Nafion-CNT coated microelectrodes. Fast-scan cyclic voltammetry was used to test their response to neurochemicals. For dopamine, the average increase in oxidation current compared to bare electrodes was 3.7 ± 0.5 for oPPY-CNT electrodes (limit of detection (LOD)= 3.3 ± 0.6 nM) and 3.3 ± 0.8 for Nafion-CNT electrodes (LOD= 4 ± 1 nM). The selectivity for dopamine over ascorbic acid was better with oPPY-CNT electrodes. oPPY-CNT electrodes also displayed increased electron transfer kinetics for anions while Nafion-CNT electrodes did not, which proves that polymer deposition can affect the electrocatalytic properties of the CNTs. Both oPPY-CNT and Nafion-CNT electrodes were used to detect stimulated dopamine release in the caudate-putamen of anesthetized rats after 2, 4 and 12 pulse stimulation trains. oPPY-CNT electrodes could also detect small amounts of dopamine after 4 and 12 pulse stimulations in the basolateral amygdala (BLA). Although Nafion-CNT electrodes were easier to fabricate, oPPY-CNT electrodes were more advantageous for dopamine detection because they were reproducibly fabricated, measured higher currents *in vivo*, and maintained selectivity over anions. The addition of CNTs to polymer coatings facilitates measurements of small concentrations of neurotransmitters *in vivo*. This paper was published in Analytical Methods (*Anal. Methods*, 2011,**3**, 2379-2386)

2.1 Introduction

Polymer coatings are a popular strategy for modifying electrode surfaces in order to enhance electrode sensitivity. In neuroscience applications, modification of electrodes with permselective polymers increases the sensitivity and selectivity for cationic neurotransmitters, such as dopamine,^{1,2} while excluding anionic interferents such as ascorbic acid³ and 5-hydroxyindoleacetic acid.⁴ Nafion coatings have been extensively used for dopamine detection because dopamine is attracted to the negatively charged sulfonate groups on the polymer and preconcentrates at the electrode surface.⁵ Nafion modification has the disadvantage of slowing the electrode response due to inhibited diffusion of analytes through the film.⁶ Overoxidized polypyrrole (oPPY) has been proposed as an alternative to Nafion because it can easily coat cylindrical electrodes and has a similar, enhanced sensitivity towards cationic analytes.¹ Overoxidation of polypyrrole causes a loss of conductivity and also introduces carbonyl groups that can attract cations and hinder the diffusion of anions through the film.⁷ Since oPPY films do not have as strong electrostatic reactions with cations as the Nafion films, oPPY was initially proposed to have less of an effect on temporal resolution.¹ However, detection of analytes with fast-scan cyclic voltammetry at oPPY-coated microelectrodes is slower than at bare electrodes.² For both polymers, increases in sensitivity are usually modest when thin coatings of polymer are deposited in order to maintain fast temporal resolution.

Another strategy for increasing the sensitivity of electrodes is to coat the surfaces with carbon nanotubes (CNTs).^{8,9} Carbon nanotubes have many beneficial properties for electrochemistry including high surface area to volume ratios, fast electron transfer kinetics, and the ability to be functionalized.¹⁰ Thus, CNT-modified electrodes often

exhibit increased electron transfer rates¹¹ and increased sensitivity.¹² Carbon nanotubes can be directly grown on electrode surfaces¹³ or deposited in a variety of ways, including evaporative drying¹⁴ or suspension in polymers.^{15,16}

CNTs have been deposited on electrodes using polypyrrole^{15,17,18} or Nafion films.^{16,19} Nafion can be used to solubilize nanotubes by wrapping single nanotubes.¹⁹ CNTs have been deposited on electrode surfaces by applying a drop of Nafion-CNT solution to a larger electrode and allowing it to evaporatively dry^{16,20} or dip coating microelectrodes in the solution.^{21,22} A study by our lab has shown that short (1 s) dipping of electrodes into CNTs suspended in Nafion did not form a Nafion coating but did deposit small amounts of CNTs on the surface.²¹ Other studies have shown longer coating times in Nafion-CNTs results in electrodes that retain the properties of both CNT electrodes, exhibiting electrocatalytic properties for analytes such as hydrogen peroxide,^{16,19} and Nafion coated electrodes, showing some selectivity for cations over anions.^{23,24} Electropolymerized polypyrrole films have been used for CNT immobilization as well, although the polymer does not solubilize the nanotubes. Carboxylic acid-functionalized nanotubes are postulated to act as the anion that initiates polymerization of polypyrrole and can influence the properties of the polymer.¹⁵ CNTs have been incorporated into overoxidized polypyrrole films on glassy carbon electrodes^{25,26} and carbon-fiber microelectrodes.²⁷ While these electrodes have been used with traditional electrochemistry techniques, the suitability of polymer-CNT electrodes for use with rapid electrochemical methods has not been tested.

In this study, we characterized oPPY and Nafion immobilization of CNTs onto microelectrodes surfaces for the detection of neurotransmitters. The objective was to directly compare the two different polymer-CNT electrodes to determine how the polymer contributes to the properties of CNT electrodes. Using fast-scan cyclic

voltammetry (FSCV), we found that both oPPY-CNT and Nafion-CNT electrodes had greater sensitivity for dopamine than either bare electrodes or electrodes only coated with polymers. oPPY-CNT electrodes had catalytic effects for detection of the anions ascorbic acid and dihydroxyphenylacetic acid (DOPAC) while Nafion-CNT electrodes did not. This work demonstrates that the electron transfer properties of polymer-CNT electrodes are affected by the polymer. Polymer-CNT electrodes are useful for measuring small concentrations of neurotransmitters *in vivo*.

2.2: Methods

2.2.1 Chemicals:

Dopamine hydrochloride (DA), ascorbic acid (AA), serotonin hydrochloride (5-HT), norepinephrine (NE), epinephrine (EPI), and 3,4-Dihydroxyphenylacetic acid (DOPAC) were purchased from Sigma-Aldrich (St. Louis, MO). Stock solutions were made in 0.1M HClO₄ and were 10 mM for all compounds except DOPAC and ascorbic acid (100 mM). Daily, solutions of DA (1 μM), AA (100 μM), 5-HT (1 μM), NE (1 μM), and DOPAC (20 μM) were made by diluting the stock solutions in Tris buffer. All other chemicals were purchased from Fisher Scientific unless noted (Suwanee, GA). The Tris buffer solution was 15 mM Tris(hydroxymethyl)aminomethane, 3.25 mM KCl, 140 mM NaCl, 1.2 mM CaCl₂, 1.25 mM NaH₂PO₄, 1.2 mM MgCl₂ and 2.0 mM Na₂SO₄ with the pH adjusted to 7.4. Aqueous solutions were made in deionized water (Milli-Q Biocel, Millipore, Billerica, MA).

2.2.2: Carbon-fiber microelectrodes.

Carbon-fiber microelectrodes (CFMEs) were fabricated from T-650 carbon fibers (a gift from Cytec Engineering Materials, West Patterson, NJ). Fibers were vacuum-aspirated into a glass capillary (1.2 mm diameter, A&M Systems, Carlsborg, WA) and pulled on an

electrode puller (Narishige, PE-21, Tokyo, Japan). The fiber was cut approximately 50 μm from the glass seal to form a cylindrical electrode. The epoxy, made of Epon Resin 828 (Miller-Stephenson, Danbury, CT) with 14% (w/w) 1,3-phenylenediamine hardener (Sigma-Aldrich, St. Louis, MO), was heated to 80°C and electrodes were dipped for 30 s in the epoxy and then immediately in acetone for 3 s in order to remove epoxy from the electroactive area of the exposed fiber. The epoxied electrodes were allowed to cure at room temperature overnight, and then cured at 100°C for 2 hours and at 150°C overnight. Before use, all electrodes were soaked for at least 10 min in isopropanol.

2.2.3 Functionalization of CNTs:

The functionalization of the HiPco single-walled CNTs (high pressure carbon monoxide process, Carbon Nanotechnologies, Inc. Houston, TX) was adapted from the procedures published by Wei *et al.*²⁸ Approximately 20-30 mg of CNTs were suspended in 100 mL of piranha solution (3:1 sulfuric acid: 30% hydrogen peroxide) and placed in a water sonication bath for 24 hours at 0°C. After 19 hours of initial reaction, 5 mL of 30% hydrogen peroxide was added to the mixture. After 24 hours, the CNTs were polished by sonicating in piranha solution at 70°C for 15 minutes. The CNT solution was diluted with 1 L of deionized water and filtered using a vacuum filtration with filter paper (pore size of 0.22 μm , Millipore). The functionalized CNTs were washed with copious amounts of water and air dried overnight.

2.2.5 Preparation of OPPY and OPPY-CNT modified electrodes:

The electropolymerization and overoxidation of polypyrrole onto the CFME were adapted from the procedures by Pihel *et al.*² Pyrrole (Sigma-Aldrich, St. Louis, MO) was purified on an alumina column and then diluted with phosphate-buffered saline (PBS, 0.5 M phosphate, 200 mM KCl, pH 7.0) to 50 mM pyrrole. The electrode was dipped into the

50 mM pyrrole solution while a waveform generator (BK Precision 4011A, Yorba Linda, CA) was used to apply one cycle of a triangular waveform of 0.0 V to 1.0 V and back (vs Ag/AgCl) at a scan rate of 1 V/s. Overoxidation of the polypyrrole was performed by dipping the electrode in 0.5 M sodium hydroxide and applying the same triangular waveform to the electrode for 10 cycles at a repetition rate of 0.5 Hz. The electropolymerization/deposition and overoxidation steps were then repeated for a total of 4 coating cycles. The modified electrodes were stored in PBS overnight.

To modify the electrode surface with OPPY and CNTs, the functionalized CNTs were suspended in PBS by sonicating with a wand tissue sonicator (BioLogics, Manassas, VA) for 60 minutes. Then, pyrrole was added to the suspended CNT solution to make a 50 mM concentration and the solution sonicated for another 60 minutes. The electropolymerization and overoxidation of procedures were the same as for OPPY modification. While a previous study had used 6 repeated coatings for oPPy,² we found that increasing the number of cycles when CNTs were present from 4 to 6 also increased the noise substantially, likely because too thick a coating of nanotubes formed on the surface. Preliminary studies with overoxidized polypyrrole coating showed that adding surfactants to solubilize nanotubes led to unstable oPPY-CNT coatings so suspension in water was preferred.

2.2.6 Preparation of Nafion and Nafion-CNT modified electrodes:

The procedure for Nafion coating CFMEs was adapted from Wiedemann et al.³ and Hashemi et al.⁴ The electrode was dipped in a 5 wt % Nafion solution in methanol (Liquion-1105-MeOH, Ion Power, New Castle, DE) for 5 minutes. The dipping time was chosen because nanotubes could be suspended in Nafion for 5 minutes. The modified electrodes were dried in air for 10 s followed by 10 minutes in an oven set to 70°C. Electrodes were stored in air overnight prior to use. For Nafion-CNT modification, the

functionalized CNTs were suspended in the 5 wt % Nafion solution with a tissue sonication probe for 60 minutes. The coating procedure for the Nafion-CNT was the same as for the Nafion modified electrodes.

Dip-coating Nafion on cylindrical electrodes is problematic and might not result in a full Nafion layer on the entire cylindrical surface.² Another procedure has been developed for Nafion coating cylinders that requires a voltage to be applied,⁴ but we found that applying a 1 V potential to the electrode in a Nafion-CNT solution caused the CNTs to fall out of suspension. Thus, electrodes dipped in Nafion-CNTs in the absence of voltage performed better and dip coating in Nafion without a voltage was chosen as a control.

2.2.7 Electrochemistry measurements:

Fast-scan cyclic voltammograms were collected using a ChemClamp (Dagan, Minneapolis, MN, custom modified with lower gain settings) or GeneClamp (Molecular Devices, Sunnyvale, CA with a custom-modified headstage). Data were collected with a homebuilt data analysis system and TarHeel CV software was used to apply the waveform, collect and analyze data.

For all neurochemical measurements, the electrode was scanned from -0.4 V to 1.3 V and back with a scan rate of 400 V/s and a repetition rate of 10 Hz. The reference electrode was a Ag/AgCl electrode. Electrodes were tested using flow-injection analysis to determine their response to a fast (5 s) concentration change. Cyclic voltammograms were background subtracted by averaging background traces collected 2 s before the compound was injected. Measurements were performed before and after modification so each electrode served as its own control.

2.2.8 In vivo experiments:

All animal experiments were approved by the University of Virginia Animal Care and Use Committee. Male, Sprague Dawley rats (250-300 g) were anesthetized with urethane (1.5 g/kg) for the duration of the experiment. The head and neck of each animal was shaved and the injection site locally infiltrated with bupivacaine (0.25 %, 0.2-0.3 mL s.c., Hospira, Lake Forest, IL) for analgesia. The skin was removed and holes drilled for the working electrode placement in the caudate putamen (AP + 1.2, ML +2.0, DV -4.5) or basolateral amygdala (AP -2.0, ML +5.4, DV -7.5). The stimulating electrode hole was drilled for placement in the substantia nigra (AP -5.4, ML, +1.0, DV -8.0). An Ag/AgCl reference electrode was implanted on the contralateral side. Stimulations were applied using a Dagan Biphasic Stimulator Isolator and were biphasic (2 ms, 300 μ A each phase). The number of pulses applied was either 2, 4, or 12. Stimulations were repeated at 2 minute intervals to allow the brain to recover between stimulations.

2.2.9 Scanning electron microscopy:

Samples were sputter-coated with carbon (Gatan PECS, 682) before images acquired. Images were acquired using a JEOL JSM-6700F cold field-emission microscope (Tokyo, Japan) with an acceleration voltage of 10 kV at a WD of 5.9mm or 4.8mm in secondary electron imaging mode.

2.2.10 Statistics:

All averages are given as mean \pm standard error of the mean (SEM) for n electrodes; and all error bars are given as SEM. GraphPad Prism was used for all statistics (GraphPad Software, San Diego, CA). To compare differences after coatings, peak currents were compared for bare and treated electrodes using paired t-tests. A one-way ANOVA with Bonferonni post-tests was used to compare effects among multiple groups.

2.3 Results and Discussion

2.3.1 Introduction:

The goal of this study was to compare two different polymers for coating carbon-fiber microelectrodes with single-walled carbon nanotubes (SWCNTs). Carboxylic acid functionalized CNTs were used because they have previously been shown to increase the sensitivity of CNT modified microelectrodes.²² The oxidation procedure was modified from Wei et al.²⁸ and was designed to produce short, highly functionalized nanotubes that could be suspended in water. Polymer coating procedures were adapted from the literature and optimized for each polymer.

2.3.2 Comparison of Polymer and Polymer-CNT electrodes:

Figure 2.1 shows example data of electrodes coated with oPPY, oPPY-CNTs, Nafion, and Nafion-CNTs. As expected, oPPY by itself increases the current for 1 μ M dopamine, an increase of about 1.6 fold (Fig. 2.1A). Our procedure used only 4 coating cycles of polypyrrole deposition and overoxidation, but the increase in signal is similar to that previously found with cylindrical electrodes coated with 6 cycles.² When the electrode is coated with 0.2 mg/mL of CNTs suspended in pyrrole, the signal of the electrode increases 3.9-fold (Fig. 2.1B). Nafion causes a small increase in the signal for dopamine, about 1.5-fold (Fig. 2.1C). The magnitude of the increase is small, but similar to previous studies where thin Nafion films were deposited on cylinders.⁴ In Fig. 2.1D, when CNTs were added to the Nafion, the increase in current for dopamine is about 3.1-fold. Therefore, the addition of CNTs to either polymer enhanced the current over either polymer by itself.

The current vs time plot for a flow injection analysis experiment is shown below each CV in Fig. 2.1 to allow the time response of the electrodes to be visualized. To

compare the shape of the response before and after coating, current vs time plots were normalized to the same height and shown as insets in Fig. 2.1. Both the oPPY and Nafion polymers cause a slower initial rise time of the electrode. There has been disagreement in the literature about whether oPPY slows the electrode response as much as Nafion as some studies claimed the time response is not as slow,¹ while others found similar time responses for each polymer.² Response time was quantitated by calculating the rise time from 10% to 90% of peak. Nafion and oPPY only electrodes had an average rise time of 1.4 ± 0.1 s and 1.2 ± 0.1 s respectively, which were not significantly different by an unpaired t test ($p=0.22$). Our results indicate that the initial time response for oPPY and Nafion coated electrodes are about the same, but the Nafion-coated electrodes do not return to baseline as quickly. When CNTs were added to the polymers, the rise times were 1.4 ± 0.1 s and 1.2 ± 0.1 s for Nafion-CNT and oPPY-CNT electrodes respectively. These rise times were not significantly different than Nafion or oPPY only ($p=0.71$, $p=0.79$ respectively, t-test), so the CNTs did not slow the response time. Thus, polymer-CNT electrodes have higher currents but similar time responses to polymer coated electrodes.

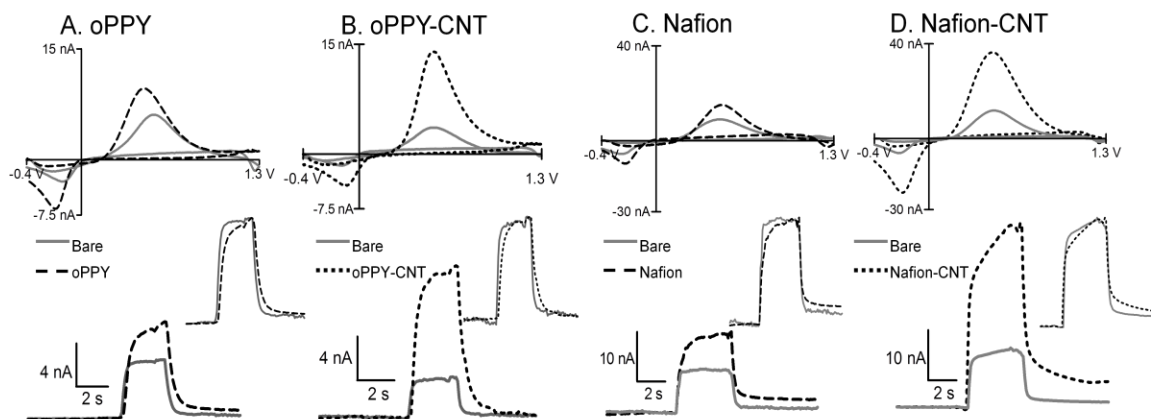


Figure 2.1: Example polymer and polymer-CNT coated electrode data for 1 μM dopamine. The top row shows cyclic voltammograms of an electrode before (solid line) and after (dashed line) modification. The bottom row shows current vs time responses for a flow injection analysis experiment. The insets are normalized to the same height to allow better evaluation of the time response. A. oPPY only increases the oxidation current by about 1.6-fold. The time response of the oPPY coated electrode is slower than the bare electrode. B. oPPY-CNT increased the current 3.9-fold. The response time of the oPPY-CNT electrode is also slower than bare. C. Nafion increases the current about 1.5-fold and slows the electrode time response, causing the signal to not completely return to baseline. D. Nafion-CNT coating increases the signal about 3 fold and also slows the time response.

2.3.3 Optimizing CNT concentrations:

The concentration of CNTs deposited on the electrode surface was optimized by varying the amount of CNTs in suspension. Each electrode was tested before and after coating for these experiments and Figure 2.2 plots the average ratio of the oxidative current after modification to before. A ratio of 1 indicates no change after treatment. oPPY significantly increased the oxidation current for 1 μM dopamine compared to bare electrodes ($p < 0.01$, paired t-test)(Fig. 2.2A). The addition of 0.05 mg/mL CNTs in oPPY appeared to decrease the signal, although it was not significantly different than control ($p > 0.05$, one-way ANOVA with Bonferonni post-test). The small amount of nanotubes may have interfered with the polymer formation without providing substantial benefits of the CNTs. With 0.2 mg/mL of CNTs in oPPY, the dopamine signal was significantly

greater than bare electrodes ($p < 0.001$, paired t-test) and oPPY alone ($p < 0.05$, one-way ANOVA with Bonferroni post-test). The electrodes coated using 0.5 mg/mL CNTs in oPPY had larger signals than bare electrodes ($p < 0.05$, paired t-test) but the data were noisy and the sensitivity varied extensively between electrodes, which led to the large error bars. Therefore, 0.2 mg/mL was chosen as the optimized concentration for oPPY.

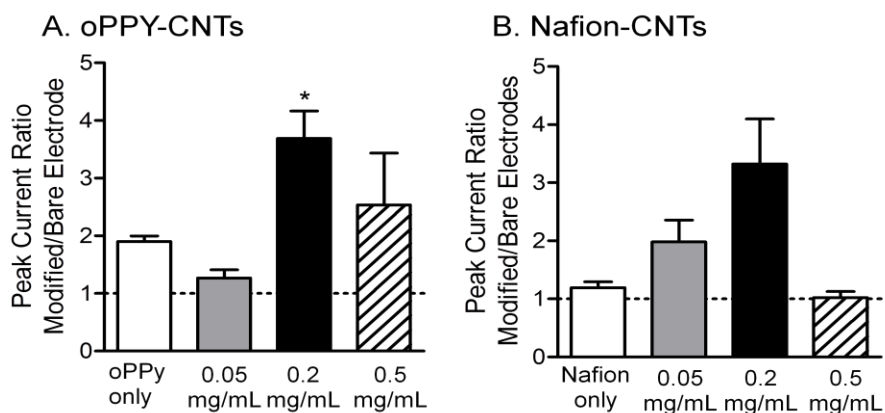


Figure 2.2: Optimization of the amount of nanotubes in the coating solution. The y-axis is a ratio of the oxidation current for 1 μM dopamine after modification divided by the current before. A. oPPY-CNT coatings. Compared to oPPY only ($n=7$), the average improvement for 0.05 mg/mL CNTs ($n=5$) and 0.5 mg/mL CNTs ($n=11$) is not significantly different, but 0.2 mg/mL CNTs ($n=9$) shows significantly greater increases in current (*, $p < 0.05$, Bonferroni post-test after 1-way ANOVA). B. Nafion-CNT coatings. While 0.05 mg/mL CNTs ($n=7$) and 0.2 mg/mL in Nafion ($n=20$) show greater improvements than Nafion only ($n=6$), the variances are large and the differences are not significant (1-way ANOVA, Bonferroni post-test). The 0.5 mg/mL CNTs in Nafion ($n=4$) did not increase the signal and the electrodes were noisy because the nanotubes did not fully suspend.

In Fig. 2.2B, Nafion slightly increased the signal for 1 μM dopamine but the increase was not significant, likely due to cylindrical electrodes that were not fully covered in Nafion. With 0.05 or 0.2 mg/mL of CNTs in the Nafion, increases in the signal were observed and oxidative currents were significantly greater than bare electrodes ($p < 0.01$, paired t-tests). However, due to the large variance among electrodes, when a one-way ANOVA was performed on the data in Fig. 2.2B, the Nafion-

CNT data were not greater than the Nafion alone using post-hoc comparisons ($p > 0.05$). The signal did not increase for 0.5 mg/mL CNTs in Nafion. The nanotubes did not suspend well at this concentration and fell out of suspension within the 5 minutes used for coating. Therefore, the electrodes were not coated well and either their signal increase was not large or agglomerations formed on the surface and they were too noisy to use (S/N ratio less than 10). The optimum concentration was therefore 0.2 mg/mL CNTs in Nafion.

The optimum concentration for CNTs in oPPY as well as Nafion was 0.2 mg/mL and the average increase in oxidative current for dopamine was similar for both polymers. The similarity in improvement may be coincidental since the coating procedures used for each polymer were very different. However, the similarity between the two polymers at optimum conditions also suggests that there may be a maximal beneficial effect of adding CNTs. A monolayer of CNTs is expected to produce the best results and adding too many CNTs to the surface can cause large signal increases, but also large amounts of noise.⁸ Thus, the similar increases in signal may result from an optimized number of nanotubes on the surface.

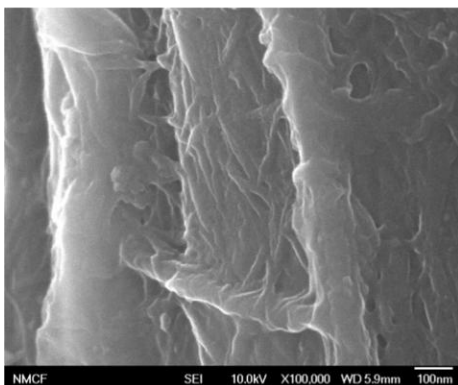
An additional control was performed for each group by coating microelectrodes with carbon nanotube suspensions without polymers. For oPPY, the control was a suspension of 0.2 mg/mL CNTs in PBS buffer and the electrochemical voltage steps and NaOH coating procedure was the same as when pyrrole was present. Electrodes coated with this method did not exhibit increased signals for dopamine and their S/N ratios decreased by about a factor of 2, so these electrodes would not be useful for *in vivo* neurotransmitter experiments. For Nafion, the CNT only control was a suspension of 0.2 mg/mL CNTs in methanol, the solvent for Nafion. Electrodes were dip-coated for 5 min. The signal for dopamine also did not increase for CNT-methanol dipping. The

CNTs did not suspend well in methanol. The electrodes were very noisy, as agglomerations of nanotubes were likely present on the surface. Therefore, polymer-CNT electrodes had better properties for neurotransmitter detection than electrodes modified with CNTs alone. The addition of CNTs to the polymers allowed a more even, reproducible, and less variable coating procedure.

2.3.4 Electrode characterization:

Scanning electron microscopy images of the surfaces were taken for each polymer with 0.2 mg/mL CNTs to examine the surface characteristics of the CNT-polymer electrodes. (Fig.2.3). The images show that CNTs are visible throughout both polymer coatings. A CNT is marked by an arrow in each panel of Fig.2.3 for easy identification. Fig. 2.3A shows a polymer coating formed by oPPy with nanotubes on the surface along with thicker strands of polymer in the vertical direction. Single-walled nanotubes are 1-2 nm in diameter but the diameter of the nanotubes in the image appears to be about 10-20 nm. The wider appearance could be due to bundles of nanotubes or polymer coating of nanotubes. In Fig. 2.3B, CNTs are also evident on the Nafion-CNT electrode, although the Nafion coating does not form the thick strands seen for oPPY. The presence of a clear Nafion coating contrasts with a previous study where electrodes were dipped in Nafion-CNT suspensions for just one second and nanotubes were deposited but a Nafion layer did not form.²¹

A. oPPY-CNTs



B. Nafion-CNTs

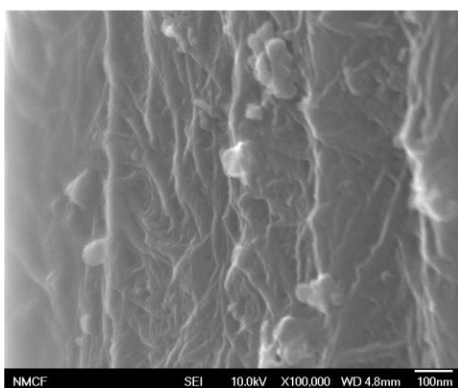
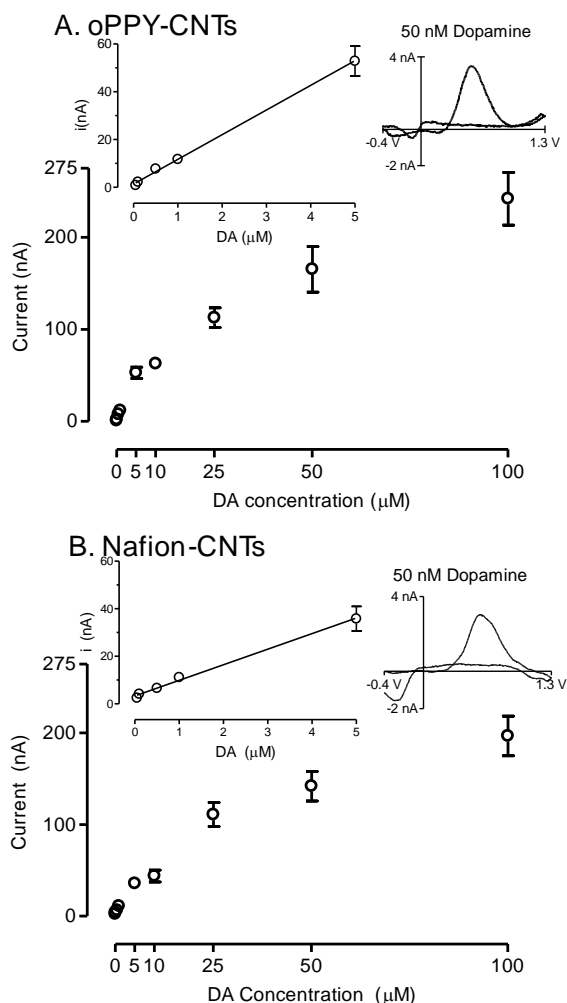


Figure 2.3: Scanning electron micrographs of electrode surfaces. A. oPPY-CNT surface shows polymer coating with CNTs embedded. B. Nafion-CNT surface also shows polymer coating and nanotubes, although the Nafion does not appear to be as thick as the oPPY. Electrodes are shown at 100,000X and the scale bar is 100 nm.

To characterize the linear range of detection, different concentrations of dopamine were tested with oPPy-CNT and Nafion-CNT electrodes (Fig. 2.4). For both polymer-CNT electrodes, the response was linear up to 5 μM dopamine. After 5 μM , the current does not increase as much because the adsorption sites on the surface are likely fully occupied by dopamine. The linear range for oPPY-CNT is larger than previous studies of electrodes coated in oPPY alone,² which were only linear to 1 μM . The larger linear range is likely due to more electroactive sites on the electrode surface.

To test the limit of detection, concentrations as low as 50 nM dopamine were tested. The inset CV in Fig. 2.4 shows that the oxidation peak for 50 nM dopamine is clearly evident for both oPPY-CNT and Nafion-CNT electrodes, although the reduction peak is hard to discern for the oPPY-CNT electrode. The limits of detection (S/N=3), calculated from the 50 nM data, were 3.3 ± 0.6 nM for oPPY-CNTs and 4 ± 1 nM for Nafion-CNTs. Using differential pulse voltammetry (DPV), previous studies of oPPY-CNTs modified microelectrodes had a 0.5 nM LOD.²⁷ FSCV is expected to have a higher LOD than DPV because the fast scanning leads to increased noise.²⁹ For Nafion-CNT microelectrodes, our measured LOD of 4 nM is an improvement of the previously reported LOD of 70 nM with DPV.²³

Figure 2.4: Measuring different concentrations of dopamine. The current vs. concentration response is plotted for 0.05 μ M to 100 μ M dopamine. The inset shows the concentration is linear up to 5 μ M dopamine for both A. oPPY-CNTs and B. Nafion-CNTs. In general, more current is detected for each concentration at oPPY-CNTs than Nafion-CNTs. The insets show example CVs for 50 nM dopamine.



The responses of the polymer-CNT electrodes were also tested for other analytes (Fig. 2.5 and Table 2.1). Serotonin, norepinephrine, and epinephrine are positively charged like dopamine at physiological pH, so the response to each of these analytes was expected to be similar to dopamine. oPPy-CNT and Nafion-CNT electrodes did increase the signal for these analytes, although the increase was not as great as for dopamine (Table 2.1). For epinephrine, polymer-CNT coatings also increased the peak current at 1.3 V, which is due to a cyclization product of epinephrine after oxidation (Fig. 2.5).³⁰ Cations all exhibited the same trends at the polymer-CNT electrodes, showing increase in current due to increases in surface area and electrostatic interactions with the polymer.

DOPAC and ascorbic acid are negatively charged analytes that can act as an interferent for dopamine detection. Previous studies of oPPY coated cylindrical electrodes showed small increases in current for DOPAC and oPPY-CNT electrodes also had a small increase in current (Fig. 2.5).² Nafion-CNT electrodes also had small increases in signal for DOPAC. The increase in DOPAC signal was not as large as that for cationic species in the case of both Nafion-CNT and oPPY-CNT electrodes. For ascorbic acid, Nafion-CNT electrodes had a slight increase in current while oPPY-CNT electrodes had a small decrease in signal. Oxidation peak currents increased to a lesser extent for anions than for cations. Therefore, there is improved discrimination of cations from anions at polymer-CNT electrodes compared to bare electrodes. However, when comparing polymer-CNT electrodes to polymer only electrodes, the discrimination of cations from anions is not as good. For example, Nafion alone leads to a significant decrease in ascorbic acid oxidation current whereas the Nafion-CNT coating causes increases in ascorbic acid current. This decrease in selectivity is likely caused by CNTs

which are present throughout the Nafion, including on the polymer surface. Thus, the negatively charged analytes might not need to diffuse through the Nafion to be detected.

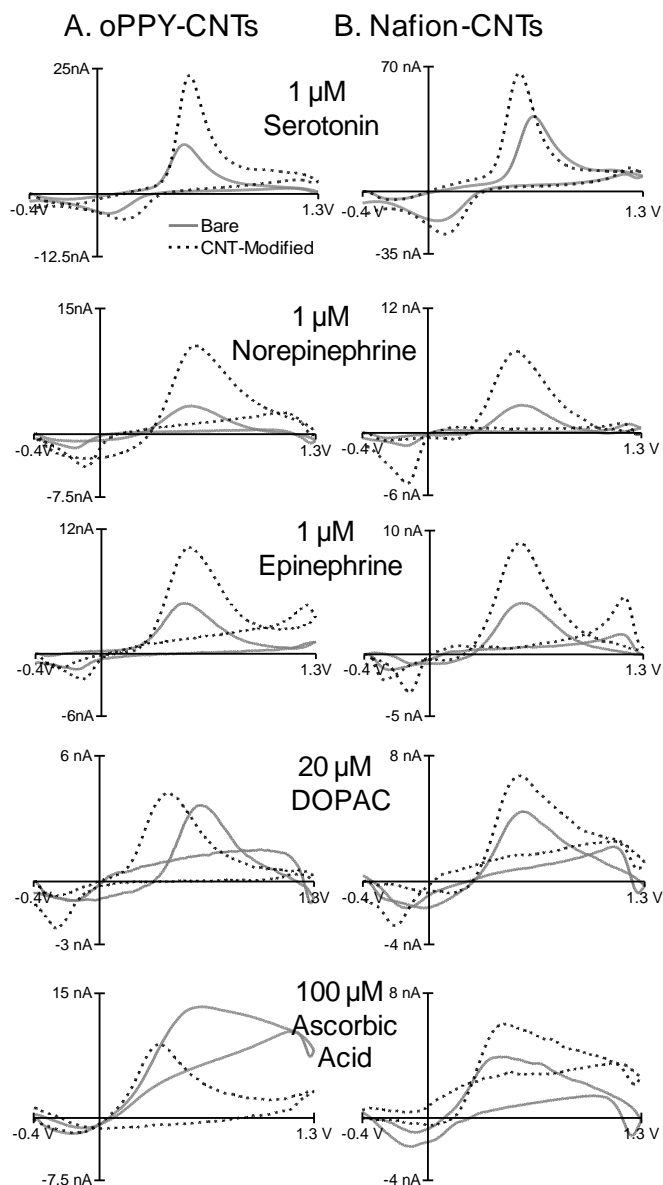


Figure 2.5: Response of polymer-CNT electrodes to other neurochemicals. The bare electrode (solid line) is compared to the modified electrode response (dashed) for A. oPPY-CNT or B. Nafion-CNT. The current for 1 μM serotonin, 1 μM norepinephrine, and 1 μM epinephrine increases for both types of electrodes. For 20 μM DOPAC, the signal for oPPY-CNTs and Nafion-CNT electrodes slightly increases. At the oPPY-CNT electrode, both electron transfer kinetics and reversibility also increase for DOPAC. For 100 μM ascorbic acid, the signal is lower for the oPPY-CNT electrode while electron transfer kinetics are faster. Current for ascorbic acid increases at the Nafion-CNT electrode.

Table 2.1: Average improvement in oxidative current for different neurochemicals.

Analytes	oPPY-CNTs	Nafion-CNTs
Dopamine (1 μ M)	3.6 \pm 0.6	3.3 \pm 0.8
Norepinephrine (1 μ M)	2.7 \pm 0.3	2.1 \pm 0.4
Epinephrine (1 μ M)	2.6 \pm 0.3	2.2 \pm 0.4
Serotonin (1 μ M)	2.0 \pm 0.2	2.2 \pm 0.2
DOPAC (20 μ M)	1.2 \pm 0.1	1.4 \pm 0.1
Ascorbic acid (100 μ M)	0.9 \pm 0.2	1.9 \pm 0.4

Data are average ratio of oxidative signal for coated electrodes divided by bare electrodes. Error is standard error of the mean (n=5).

The example CV traces in Figure 2.5 show a change in the shape of the CV for ascorbic acid and DOPAC after oPPY-CNT coating. The oxidation peak for DOPAC shifted to less positive potentials and the reduction peak was more clearly defined after oPPY-CNT coating. The oxidation peak for ascorbic acid also shifted to lower potentials at all oPPY-CNT electrodes and the peak also appeared more symmetrical. For cationic analytes, large electrocatalytic effects from the CNTs were not observed, but the electron transfer kinetics for anions at oPPY-CNT electrodes were dramatically faster. The kinetics were dependent on the polymer, as the CNTs used to fabricate each electrode were the same but electrocatalytic effects were not observed at Nafion-CNT electrodes. Nafion can wrap the nanotubes, which might be detrimental to rapid electron transfer and analytes closely approaching the nanotubes.¹⁹ These studies demonstrate that the polymer coating can affect the electron transfer kinetics of CNT-coated electrodes.

2.3.5 In vivo use of polymer-CNT microelectrodes:

To validate that oPPY-CNT and Nafion-CNT microelectrodes were useful for neurotransmitter measurements, stimulated dopamine release was detected in anesthetized rat brains. Polymer-CNT coated microelectrodes were implanted in the

caudate-putamen and 12, 4, or 2 pulse stimulations were applied to a stimulating electrode implanted in the substantia nigra. Figures 2.6A and B shows that both oPPY-CNT and Nafion-CNT electrodes could be used to detect dopamine in the caudate-putamen after short stimulations. The inset cyclic voltammograms demonstrate that the CVs acquired for the 4 pulse stimulations are clearly dopamine. Two and four pulse train stimulations are considered a very short stimulation *in vivo* and stimulations of 24 to 60 pulses are more routinely used.³¹ The ability to detect short stimulations allows a better estimation of dopamine efflux after stimulations that mimic physiological phasic firing of dopamine neurons.³² For an average of 4 electrodes in each group, a 4 pulse stimulation produced slightly more current (0.8 ± 0.2 nA) at oPPY-CNT electrodes than at Nafion-CNT electrodes (0.5 ± 0.1 nA). oPPY electrodes have previously been used to detect 2 pulse stimulations in the caudate-putamen, but with a different train frequency (10 Hz rather than 60 Hz).² The S/N ratios for the oPPY-CNT electrodes in this study are better than the previous study.

Measurements of dopamine after short pulse trains were also attempted in the basolateral amygdala (BLA), a brain region that has less dopamine innervation. Dopamine release was detected using oPPY-CNT electrodes but not Nafion-CNT electrodes. Fig. 2.6C shows an example animal where oPPY-CNT electrodes detected 40 nM and 180 nM dopamine for 4 and 12 pulse trains, respectively. Evoked release is smaller in the BLA than in the caudate-putamen and the signals last longer because clearance is slower.³³ To our knowledge, these are the shortest pulse trains that have been used to elicit dopamine release in the BLA. This work demonstrates oPPY-CNT electrodes are useful for measuring small concentrations *in vivo*.

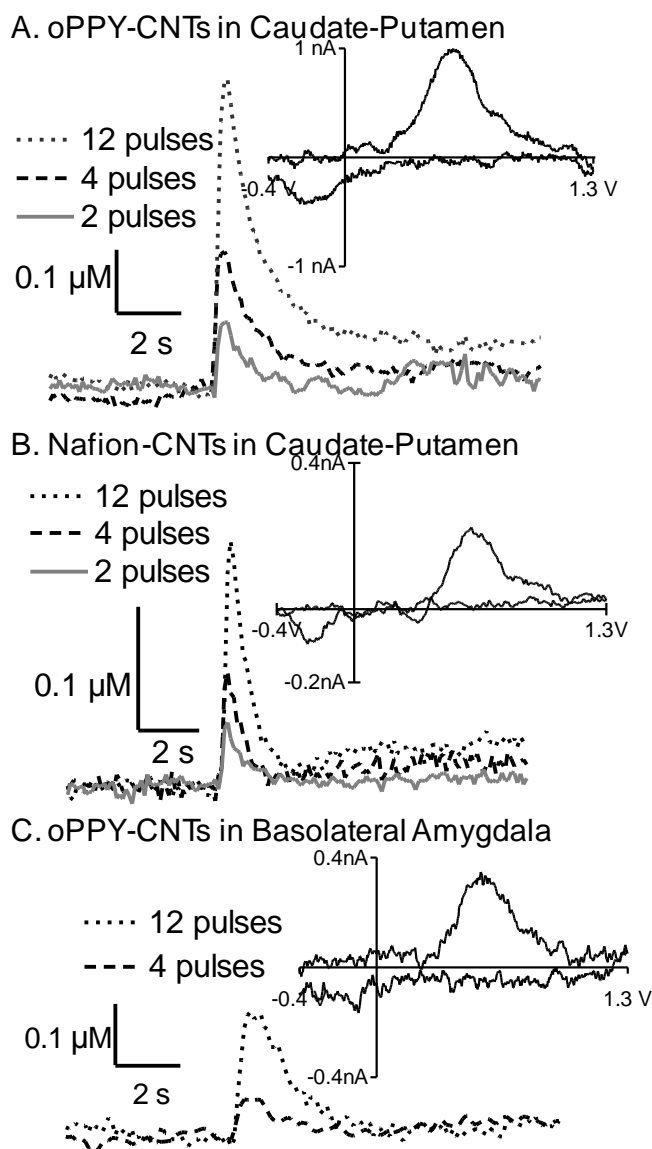


Figure 2.6: In vivo detection of short trains of stimulated dopamine release. Electrical stimulations of dopamine cell bodies elicited in the substantia nigra. A. Response at oPPY-CNT electrodes in the caudate-putamen, B. Nafion-CNT electrodes in the caudate-putamen, and C. oPPY-CNT electrodes in the basolateral amygdala. Stimulation trains of 2 (solid line), 4 (dashed line), or 12 pulses (dotted line) were applied in the caudate-putamen and 4 or 12 pulses were applied in the BLA. In the caudate, higher currents were detected at oPPY-CNT electrodes. The inset CVs are for the 4-pulse stimulations for all panels.

2.4 Conclusions

The magnitude of the signal increase after adding CNTs to each polymer was the same but the procedures for coating the electrodes were very different.

Electropolymerization was used for oPPY while simple dip coating was used for Nafion. The CNTs were suspended in PBS for the polypyrrole coating and they continued to be stable after the addition of pyrrole. However, the Nafion-CNT solutions were not always as stable. The large variation in the Nafion data, especially for the 0.2 mg/mL and 0.5 mg/mL (Fig. 2), could be due to differences in the Nafion solution, as some days CNTs appeared more stably suspended than others. Using a Nafion solution with CNTs better suspended, possibly by lowering the CNT concentration, may give more reproducible coatings and the length of time of coating could be adjusted to deposit the same amount of CNTs. The oPPY-CNT coating procedure produced less variation among electrodes, due to the more ordered deposition by electrochemistry or more stable CNT suspensions. The Nafion-CNT procedure is easier as it simply requires dip coating a batch of electrodes, but the electropolymerization and overoxidation steps for polypyrrole can be performed on multiple electrodes simultaneously², which decreases the amount of time required to make a batch of electrode.

While both oPPY-CNT and Nafion-CNT electrodes increased the sensitivity for dopamine, oPPY-CNT electrodes had advantages over Nafion-CNT electrodes. The reproducibility was better for oPPY-CNTs as was the selectivity for dopamine over ascorbic acid. oPPY-CNT electrodes also increased electron transfer kinetics for anions. Because Nafion is known to wrap nanotubes, it might be electrostatically unfavorable for anions to approach the nanotubes in the Nafion-CNT coating. The differences in kinetics for anions are interesting because while many studies have examined the electrocatalytic effects of nanotubes, few studies have addressed how

immobilization onto surfaces might affect these properties. oPPY-CNT electrodes yielded higher currents *in vivo* and consequently lower concentrations of dopamine could be measured. The experiments using oPPY-CNT electrodes in the basolateral amygdale show that higher sensitivity electrodes facilitate measurements of dopamine after small pulse trains, even in regions with low dopamine innervations. Overall, oPPY-CNT electrodes were a better choice than Nafion-CNT electrodes for repeated *in vivo* use because of the reproducible fabrication, selectivity over anions, and larger currents *in vivo*.

2.5 References

1. Hsueh, C. C.; Brajter-Toth, A. *Anal. Chem.* 1994, 66 (15), 2458-2464.
2. Pihel, K.; Walker, Q. D.; Wightman, R. M. *Anal. Chem.* 1996, 68 (13), 2084-2089.
3. Wiedemann, D. J.; Basse-Tomusk, A.; Wilson, R. L.; Rebec, G. V.; Wightman, R. M. *J. Neurosci Methods* 1990, 35 (1), 9-18.
4. Hashemi, P.; Dankoski, E. C.; Petrovic, J.; Keithley, R. B.; Wightman, R. M. *Anal. Chem.* 2009, 81 (22), 9462-9471.
5. Nagy, G.; Gerhardt, G.; Oke, A. F.; Rice, M. E.; Adams, R. N.; Moore, R. B.; Szentirmay, M. N.; Martin, C. R. *J. Electroanal. Chem.* 1985, 188 (1-2), 85-94.
6. Baur, J. E.; Kristensen, E. W.; May, L. J.; Wiedemann, D. J.; Wightman, R. M. *Anal. Chem.* 1988, 60 (13), 1268-1272.
7. Witkowski, A.; Brajter-Toth, A. *Anal. Chem.* 1992, 64 (6), 635-641.
8. Jacobs, C. B.; Peairs, M. J.; Venton, B. J. *Anal. Chim. Acta* 2010, 662 (2), 105-127.
9. Gooding, J. J. *Electrochem. Acta* 2005, 50, 3049-3060.
10. Lin, Y.; Yantasee, W.; Wang, J. *Front Biosci.* 2005, 10, 492-505.
11. Britto, P. J.; Santhanam, K. S. V.; Ajayan, P. M. *Bioelectrochem. Bioenerg.* 1996, 41 (1), 121-125.
12. Dumitrescu, I.; Unwin, P. R.; Macpherson, J. V. *Chem. Commun.* 2009, (45), 6886-6901.
13. Huang, L. M.; Jia, Z.; O'Brien, S. *J. Mater. Chem.* 2007, 17 (37), 3863-3874.
14. Wu, K.; Fei, J.; Hu, S. *Anal. Biochem.* 2003, 318, 100-106.
15. Peng, C.; Jin, J.; Chen, G. Z. *Electrochim. Acta* 2007, 53 (2), 525-537.
16. Tkac, J.; Ruzgas, T. *Electrochem. Comm.* 2006, 8 (5), 899-903.
17. Wang, J.; Musameh, M. *Anal. Chim. Acta* 2005, 539 (1-2), 209-213.
18. Teh, K. S.; Lin, L. W. *Journal of Micromechanics and Microengineering* 2005, 15 (11), 2019-2027.
19. Wang, J.; Musameh, M.; Lin, Y. *J. Am. Chem. Soc.* 2003, 125 (9), 2408-2409.

20. Su, H. L.; Yuan, R.; Chai, Y. Q.; Zhuo, Y.; Hong, C. L.; Liu, Z. Y.; Yang, X. *Electrochimica Acta* 2009, *54* (17), 4149-4154.
21. Swamy, B. E. K.; Venton, B. J. *Analyst* 2007, *132*, 876-884.
22. Jacobs, C. B.; Vickrey, T. L.; Venton, B. J. *Analyst* 2011.
23. Hocevar, S. R.; Wang, J.; Deo, R. P.; Musameh, M.; Ogorevc, B. *Electroanalysis* 2005, *17* (5-6), 417-422.
24. Wu, K. B.; Hu, S. S. *Microchimica Acta* 2004, *144* (1-3), 131-137.
25. Tu, X. M.; Xie, Q. J.; Jiang, S. Y.; Yao, S. Z. *Biosens. bioelectron.* 2007, *22* (12), 2819-2826.
26. Wen, J. X.; Zhou, L.; Jin, L. T.; Cao, X. N.; Ye, B. C. *J. Chromatogr. B* 2009, *877* (20-21), 1793-1798.
27. Lin, L.; Cai, Y. P.; Lin, R. P.; Yu, L.; Song, C. Y.; Gao, H. C.; Li, X. K. *Microchimica Acta* 2011, *172* (1), 217-223.
28. Wei, Z.; Kondratenko, M.; Dao, L. H.; Perepichka, D. F. *J. Am. Chem. Soc.* 2006, *128* (10), 3134-3135.
29. Kawagoe, K. T.; Zimmerman, J. B.; Wightman, R. M. *J. Neurosci. Methods* 1993, *48* (3), 225-240.
30. Pihel, K.; Schroeder, T. J.; Wightman, R. M. *Anal. Chem.* 1994, *66*, 4532-4537.
31. Garris, P. A.; Wightman, R. M. *J. Neurosci.* 1994, *14* (1), 442-450.
32. Grace, A. A.; Bunney, B. S. *J. Neurosci* 1984, *4* (11), 2877-2890.
33. Garris, P. A.; Wightman, R. M. *J. Physiol* 1994, *478* (Pt 2), 239-249.

Chapter 3

**Nafion-CNT Coated Carbon-Fiber Microelectrodes for
Enhanced Detection of Adenosine**

I have not failed, I've just found 10,000 ways that won't work

~Thomas Edison

Chapter 3: Nafion-CNT Coated Carbon-Fiber Microelectrodes for Enhanced Detection of Adenosine

Abstract:

In this chapter, I further develop the Nafion-CNT electrodes for adenosine detection. Adenosine is a neuromodulator that regulates neurotransmission. Adenosine can be monitored using fast-scan cyclic voltammetry at carbon-fiber microelectrodes and ATP is a possible interferent *in vivo* because the electroactive moiety, adenine, is the same for both molecules. In this study, we investigated carbon-fiber microelectrodes coated with Nafion and carbon nanotubes (CNTs) for enhanced sensitivity of adenosine and selectivity over ATP. Electrodes coated in 0.05 mg/mL CNTs in Nafion had a 4.2 ± 0.2 fold increase in current for adenosine, twice as large as for Nafion alone. Nafion-CNT electrodes were 6 times more sensitive to adenosine than ATP. The Nafion-CNT coating did not slow the temporal response of the electrode. Comparing different purine bases shows that the presence of an amine group enhances sensitivity and that purines with carbonyl groups, such as guanine and hypoxanthine, do not have as great an enhancement after Nafion-CNT coating. The ribose group provides additional sensitivity enhancement for adenosine over adenine. The Nafion-CNT modified electrodes were significantly more selective for adenosine than ATP in brain slices. Therefore, Nafion-CNT modified electrodes are useful for sensitive, selective detection of adenosine in biological samples. This paper was published in the *Analyst* (***Analyst***. 2012 ,**137(13)**,3045-51).

3.1 Introduction

Adenosine is an important nucleoside signaling molecule formed by ATP degradation. It acts as a neuromodulator to regulate cerebral blood flow, modulate neuronal excitability, and control energy delivery to the brain.¹⁻³ Adenosine also protects against neuronal damage caused by oxidative stress and has been studied for possible protective effects in hypoglycemia, hypoxia, and ischemia.³ Traditionally, adenosine has been thought to act on a slow time scale and changes lasting minutes to hours have been measured *in vivo* with microdialysis sampling coupled to HPLC.^{4,5} However, faster adenosine changes have recently been detected *in vivo* and in brain slices using both fast-scan cyclic voltammetry (FSCV) at carbon-fiber microelectrodes and amperometric enzyme sensors.⁶⁻⁸ FSCV can detect changes on the millisecond timescale which provides high temporal resolution for measuring transients *in vivo*. Detection of transient adenosine release is challenging because evoked adenosine changes are low, around 100-300 nM, and other purine species might interfere.⁷ In particular, ATP and adenosine have similar oxidation potentials and cyclic voltammograms (CVs) because the adenine moiety is the electroactive species in both molecules. Other purines such as guanine and hypoxanthine are similar in structure but have different electrochemistry.⁹ The development of an electrode with enhanced sensitivity and selectivity for adenosine will allow more reliable adenosine detection.

Carbon-fiber microelectrodes modified with Nafion have been used extensively to increase sensitivity to neurotransmitters such as dopamine and serotonin, but have not been used to study adenosine or ATP.¹⁰⁻¹⁴ Nafion is a permselective polymer that enhances sensitivity to cations and decreases sensitivity to anions.¹¹ At physiological pH, ATP is negatively charged while adenosine is neutral. Thus, coating carbon-fiber microelectrodes with Nafion is expected to increase the selectivity for adenosine over

ATP because of the charge repulsion between Nafion and ATP. Different coating methods have been explored for depositing Nafion onto carbon-fiber microelectrodes and dip-coating and electropolymerization are the most common.^{10,15} Dip-coating has traditionally been used on disk electrodes, due to the limited surface area the Nafion polymer needs to adsorb,^{14,16} but cylinder electrodes can be dip coated using longer dip coating times.^{17,18}

Carbon nanotubes (CNTs) have also been used to modify carbon-fiber microelectrodes to enhance detection of neurotransmitters.¹⁹⁻²² CNTs offer unique chemical, electrical, and structural properties which can increase sensitivity and promote electron transfer kinetics.²³⁻²⁵ To purify and functionalize CNTs, treatments with strong oxidizing acids are used.²⁶ The resultant oxygen containing functional groups located on the sidewall defects and ends of CNTs change the overall hydrophobicity which affects the suspension of the nanotubes in various solvents.²⁷ CNTs are often dispersed in low concentrations of Nafion and deposited on electrodes to study the effects of CNTs on electrode sensitivity.^{19,28,29} Vertically aligned CNTs supported on thin Nafion-iron oxide layers have also been reported, although in this case the Nafion just aids in depositing iron oxide on the surface and is not deposited in a thick enough layer to exclude anions.^{30,31} Combining CNTs with higher concentrations of Nafion increases sensitivity for dopamine due to the combination of the preconcentration of the analyte in the Nafion and higher surface area of the CNTs.³² However, the combination of Nafion and CNTs has not been studied for purines such as adenosine.

In this study, we developed modified carbon-fiber microelectrodes with Nafion and CNTs to enhance the sensitivity and selectivity for adenosine over ATP. Using FSCV, we found that Nafion-CNT coatings increased the sensitivity for adenosine 4 fold, which was twice as much as Nafion alone. Adenosine had higher sensitivity enhancements than adenine, showing an effect of the ribose unit, and enhanced

sensitivity over guanosine or inosine, two nucleosides that contain carbonyl groups. Nafion-CNT electrodes were significantly more selective for adenosine than for ATP after exogenous application of analyte in brain slices. Thus, the enhanced sensitivity and selectivity of adenosine *in vitro* translates to improved performance in brain slices.

3.2 Methods

3.2.1 Solutions and chemicals:

Purine, histamine, and dopamine standards were purchased from Sigma, dissolved in 0.1 M HClO₄ for 10 mM stock solutions and diluted daily in Tris buffer for testing. All compounds were tested at 5 μM except dopamine, which was 1 μM. The Tris buffer solution was 15 mM Tris(hydroxymethyl)aminomethane, 1.25 mM NaH₂PO₄, 2.0 mM Na₂SO₄, 3.25 mM KCl, 140 mM NaCl, 1.2 mM CaCl₂, and 1.2 mM MgCl₂ with the pH adjusted to 7.4 (all Fisher, Suwanee, GA). For in situ experiments, calibrations were performed in aCSF: 126 mM NaCl, 2.5 mM KCl, 1.2 mM NaH₂PO₄, 2.4 mM CaCl₂ dehydrate, 1.2 mM MgCl₂ hexahydrate, 25 mM NaHCO₃, 11 mM glucose, and 15 mM tris (hydroxymethyl) aminomethane, pH 7.4. All aqueous solutions were made with deionized water (Milli-Q Biocel, Millipore, Billerica, MA).

3.2.2 Preparation of microelectrodes:

Carbon-fiber microelectrodes were fabricated from T-650 carbon-fibers (gift from Cytec Engineering Materials, West Patterson, NJ).²⁹ . Cylinder electrodes, approximately 50 μm long, were used. Electrodes were epoxied with Epon Resin 828 (Miller-Stephenson, Danbury, CT) with 14% (w/w) 1,3-phenylenediamine hardener (Sigma-Aldrich, St. Louis, MO) to ensure a good seal. All electrodes were soaked for at least 10 min in isopropanol (Fisher Scientific) prior to use. Dip coating carbon-fiber microelectrodes with Nafion-CNT was chosen over electropolymerization due to the application voltage causing CNTs to

aggregate and fall out of solution more quickly. The Nafion coating procedure was adapted from Wiedemann *et al.* and Hashemi *et al.*^{10,15} The electrode was dipped in a 5 wt % Nafion solution in methanol (Ion Power, New Castle, DE) for 5 minutes, air dried for 10 s, then baked in an oven at 70°C for 10 minutes. Electrodes were stored overnight at room temperature prior to use. To modify the electrode surface with Nafion and CNTs, the functionalized CNTs were suspended in the 5 wt % Nafion solution with a tissue sonication probe for 60 minutes. High pressure carbon monoxide conversion (HiPco) single-walled CNTs (Carbon Nanotechnologies, Houston, TX) were functionalized by a procedure adapted from Wei *et al.*³³ that was described previously.³² The coating procedure for the Nafion-CNT was the same as for the Nafion modified electrodes.

3.2.3 Functionalization of CNTs.:

25-30 mg of CNTs were suspended in 100 mL of piranha solution (3:1 sulfuric acid: 30% hydrogen peroxide) and placed in a water bath sonicator for 24 hours at 0°C. After approximately 19 hours, 5 mL of 30% hydrogen peroxide was added to the mixture to make up for hydrogen peroxide decomposition. After 24 hours, the CNT solution was “polished” by heating to 70°C for 15 minutes. The CNT solution was diluted with 1 L of deionized water and vacuum filtered with a 0.22 µm filter paper and allowed to dry overnight. (Millipore, Ireland).

3.2.4 Electrochemistry:

Fast-scan cyclic voltammograms were collected using a GeneClamp 500B potentiostat (Molecular Devices, Union City, CA) with a custom-modified headstage. Data was collected from a homebuilt data analysis system and two computer interface boards (National Instruments PCI 6052 and PCI 6711, Austin TX) were used to apply the

waveform. The electrode was scanned from -0.4 V to 1.45 V (vs Ag/AgCl) and back with a scan rate of 400 V/s and a repetition rate of 10 Hz. Measurements were performed before and after modification with Nafion or Nafion-CNTs, so each electrode served as its own control. Electrodes were tested using flow-injection analysis as described previously.³⁴ Prior to data collection, electrodes were cycled with the waveform for 10 min in order to allow the background to stabilize.

3.2.5 Scanning Electron Microscopy:

Scanning electron microscopy images were taken on a JEOL JSM-6700F microscope (Tokyo, Japan) by using an accelerating voltage of 10 kV and a working distance of approximately 6 mm. Electrodes were sputter-coated before imaging with carbon (PECS, 682, Gatan Inc, Pleasanton, CA).

3.2.6 Brain slice experiments:

All experiments were approved by the Animal Care and Use Committee of the University of Virginia. Male Sprague-Dawley rats (250-350 g) purchased from Charles River and brain slices were collected as previously described.⁷ The electrode position in the prefrontal cortex corresponded to approximately the following coordinates from bregma: AP: 4.20 mm, ML: 0.4 to 0.8 mm, and DV: -3.4 to -4.0mm.³⁵ A glass micropipette was pulled from a borosilicate glass capillary to an outer diameter of around 15 μm and positioned in the tissue approximately 30 μm away from the working electrode. The pipette was filled with 100 μM adenosine and 60 pmol adenosine was pressure ejected (500-600 ms, 20-30 psi) using a Picospritzer III (Parker Hannifin Corp., Fairfield, NJ) 10 minutes after electrode implantation. A second injection was repeated

10 minutes later to ensure stability. Two pressure ejections of 60 pmol of ATP were performed 10 min apart, starting 10 minutes after the last adenosine application.

3.2.7 Statistics:

All values are reported as the mean \pm standard error of the mean (SEM). Paired t test were performed for comparing average bare electrode current to the average coated electrode current and for comparing electron transfer effects. All statistics were performed in GraphPad Prism (GraphPad Software, Inc., La Jolla, CA) and considered significant at the 95% confidence level ($p < 0.05$).

3.3 Results and Discussion

3.3.1 Surface structure characterization:

Nafion-CNT carbon-fiber microelectrodes were developed to increase sensitivity and selectivity for adenosine over ATP. Scanning electron microscopy (SEM) images of the electrode provide evidence of CNTs on the surface. Fig. 3.1 shows images for Nafion, 0.05 mg/mL CNT in Nafion, and 0.2 mg/mL CNT in Nafion modified electrodes. Fig. 3.1A shows that the Nafion coating is not uniform but does cover part of the electrode sidewall. The lack of a uniform Nafion layer may be caused by the short dip time and using dip coating instead of electropolymerization.¹⁰ The Nafion-CNT modified electrodes (Fig. 3.1B and 3.1C) show CNT rod-like structures ranging from 30-50 nm in diameter covering the surface. Previously, polymers such as Nafion were shown to wrap CNTs and since individual single-walled CNTs are only 1-2 nm in diameter, the CNTs in Fig. 3.1B and C may be Nafion wrapped.^{25,36,37} Alternatively, the larger diameter may be a result of CNT bundle formation. Fig. 3.1B and Fig. 3.1C show differences in amount of CNT coverage on the electrode surface. The 0.05 mg/mL CNT

coated electrodes have fewer CNTs on the surface than the 0.2 mg/mL CNT coated electrodes.

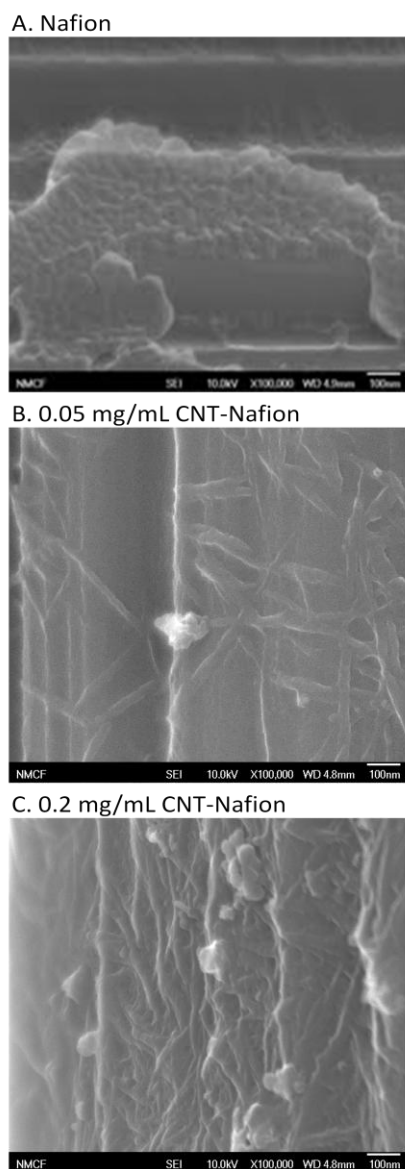


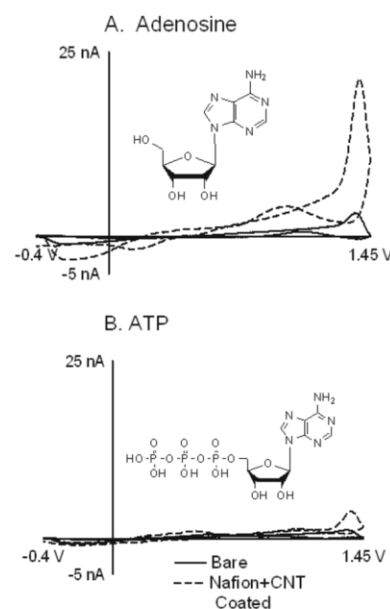
Figure 3.1: Scanning electron microscopy (SEM) images of Nafion and Nafion-CNT modified carbon-fiber microelectrodes at 100,000x resolution. Scale bar is 100 nm. A.) Nafion modified electrodes show a non-uniform layer of Nafion on the surface of the cylinder electrode B.) 0.05 mg/mL CNT in Nafion. Electrodes coated in this solution have a lower density of CNTs than electrodes coated with C.) 0.2 mg/mL CNT in Nafion. CNTs appear as 30-50 nm rod-like structures. The large diameter is attributed to either CNT bundle formation or the effect of Nafion wrapping the CNTs.

3.3.2 Nafion-CNT carbon-fiber microelectrodes increase sensitivity to adenosine:

Fig. 3.2 shows representative CVs for 5 μM adenosine (Fig. 3.2A) and ATP (Fig. 3.2B) on the same scale to illustrate the differences in sensitivity. Adenosine and ATP have similar electrochemistry as both contain an adenine group which is oxidized.⁹

When the electrode is scanned from -0.4 to 1.45 V and back, adenine can undergo a series of three, two-electron oxidations. The first oxidation potential of adenine is 1.3 V, however with FSCV the first oxidation peak of adenosine and ATP is observed around 1.40 V of the cathodic scan.^{9,38} The peak appears on the cathodic scan because of time required for electron transfer and the fast scan rate. When a switching potential of 1.5 V was used in previous experiments, the peak was observed at 1.5 V.³⁸ A slightly lower switching potential was chosen here because it produced more stable background currents and lessened the possibility of hydrolysis of water. The second oxidation peak for adenosine and ATP occurs at 1.0 V on the anodic scan, and the third oxidation peak is seldom seen at our cylindrical T-650 carbon-fiber microelectrodes. Quantitation for adenosine and ATP were performed at the first oxidation peak for all experiments.

Figure 3.2: Nafion-CNT coated electrodes improve sensitivity. The electrode was scanned from -0.4 V to 1.45 V and back at 400 V/s. Nafion-CNT electrodes were fabricated by dip coating in 0.05 mg/mL CNTs in Nafion for 5 minutes. A.) A cyclic voltammogram (CV) of 5 μM adenosine shows the response to a bare electrode (solid) and the same electrode after Nafion-CNT modification (dashed). The oxidative current increased about 4 fold with Nafion-CNTs. B.) A CV of 5 μM ATP shows only a 2 fold increase in sensitivity after Nafion-CNT coating. The response for ATP is about 6-fold less than adenosine after Nafion-CNT coating.



The bare carbon-fiber microelectrodes had a 2.7-fold higher sensitivity for adenosine than ATP although the electrochemistry is similar (Fig. 3.2). At physiological pH, the phosphate groups on ATP are expected to be deprotonated, giving it a negative charge. The lower sensitivity for ATP is likely due to poor adsorption because of the negative charge or steric hindrance of the phosphate groups that prevent the adenine moiety from being properly aligned for oxidation.³⁹

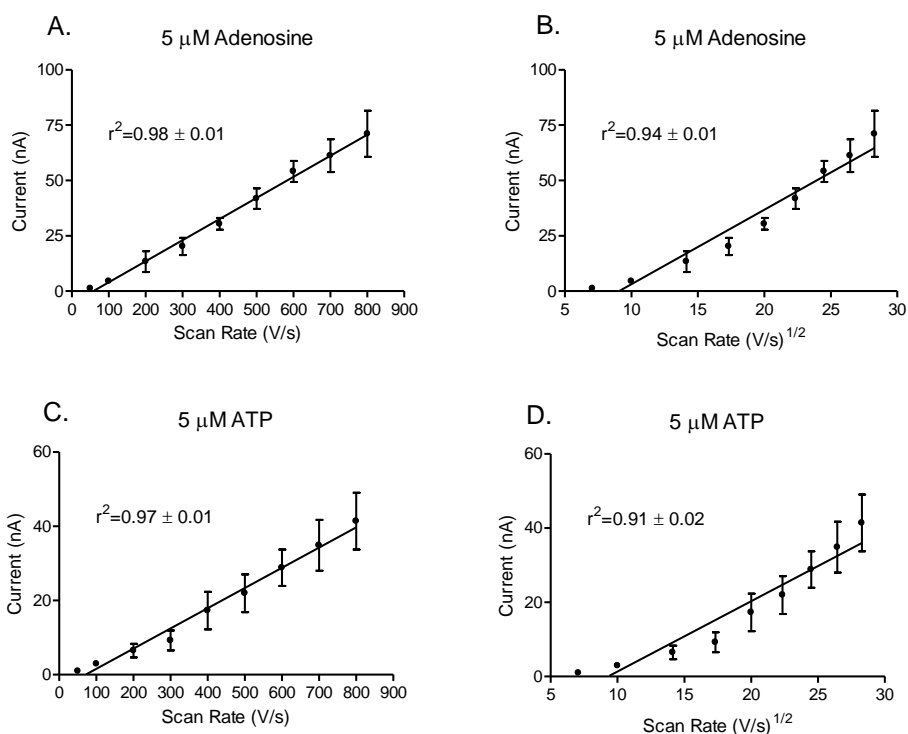


Figure 3.3: The electrochemical reactions observed after Nafion-CNT coated are primarily adsorption controlled. 5 μM adenosine and ATP were tested at Nafion-CNT electrodes for scan rates ranging from 50 V/s to 800 V/s. Plotting current versus scan rate and square root of scan rate shows if reaction is primarily adsorption or diffusion controlled. A and B) For adenosine, the electrochemical reaction at a coated electrode is primarily adsorption controlled because the current versus scan rate plot is more linear. C and D) For ATP, the electrochemical reaction is also primarily adsorption controlled at coated electrodes. (n=3).

Dip coating carbon-fiber microelectrodes in 0.05 mg/mL CNT in Nafion for 5 minutes increased the oxidation current for adenosine and ATP compared to bare carbon-fiber electrodes (Fig. 3.2). However, the increase for adenosine was larger than

for ATP and the signal for adenosine was 6 times greater than the signal for ATP after Nafion-CNT coating. Nafion-CNT coating increased both sensitivity for adenosine and selectivity over ATP. The electrochemical reactions observed for both adenosine and ATP on the Nafion-CNT coated electrode are primarily adsorption controlled (Figure 3.3).

3.3.3 Optimization of CNT concentration:

To test the effects of the amount of CNTs on the current detected, 0.05 mg/mL and 0.2 mg/mL CNTs suspended in Nafion were tested. In Fig. 3.4, the y-axis is a ratio of peak oxidation current of the coated electrode divided by the bare electrode. A ratio higher than 1.0 indicates an increase in current. As a control, electrodes were dip coated with only Nafion, which improved the current for adenosine 1.9 ± 0.3 fold but did not improve the signal for ATP. The data suggest that a thin Nafion layer is deposited onto the electrode, which causes a small increase for adenosine but not for the negatively-charged ATP. The oxidative current increased more for adenosine than for ATP for both CNT concentrations tested (Fig. 3.4). For 0.05 mg/mL CNTs in Nafion, the coated electrode peak oxidation current was significantly greater than the bare electrode for adenosine (paired t-test $p < 0.005$) but not for ATP ($p > 0.05$). The electrodes dipped in 0.2 mg/mL CNTs in Nafion did not have as large a signal improvement as for 0.05 mg/mL CNTs in Nafion and the increase was not significant for either adenosine or ATP (paired t-test, $p > 0.05$).

As a control, electrodes were also coated in 0.05 mg/mL CNTs in methanol, the solvent for Nafion, and the increases in sensitivity were minimal. These electrodes were noisy, possibly because of uneven coatings from poorly suspended CNT solutions. A greater increase in current for the lower CNT concentration in Nafion could be due to the

stability of the Nafion-CNT solution, as the higher concentration of CNTs did not remain suspended for the entire length of coating and formed aggregates, which lead to noisier electrode.⁴⁰ On electrodes with thicker layers of CNTs, the electroactive sites on the CNTs may be harder to access. Thus, lower concentrations of CNTs were chosen for further analysis.

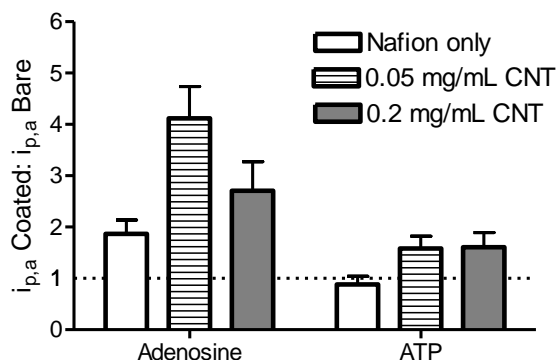


Figure 3.4: Average peak oxidation current ratios for adenosine at microelectrodes modified with Nafion, 0.05 mg/mL CNT in Nafion, or 0.2 mg/mL CNT in Nafion. The y-axis is a ratio of the oxidative current after coating to the current before coating. Nafion-CNT modified electrodes with 0.05 mg/mL (striped) show enhanced sensitivity compared to electrodes coated with 0.2 mg/mL (grey) or Nafion only (white). The ATP current ratio remains about the same for each treatment with CNTs yet decreases slightly after Nafion only coating. (n = 6 for Nafion and Nafion+0.2 mg/mL CNT and n = 18 for Nafion+0.05 mg/mL CNT)

Selectivity, stability, and limit of detection (LOD) were evaluated for the optimized Nafion-CNT coated electrode. The selectivity for adenosine compared to ATP is 3-fold higher for Nafion-CNT modified electrodes than bare electrodes, which allows improved confidence for *in vivo* use. The stability of the coated electrode was evaluated by observing the change in current over a 3 hour time period *in vitro*. The electrode sensitivity was 94 ± 2 % of original signal after 3 hours of cycling (n=3). Biostability was also evaluated by observing the change in sensitivity after the Nafion-CNT electrodes were exposed to the brain slice for 1 hour. The coated electrodes maintained 72 ± 2 % of the original signal after slice exposure whereas bare electrodes had only 57 ± 7 % of their original signal (n=4 each). The LOD of the Nafion-CNT modified electrodes was $7 \pm$

2 nM for adenosine which was significantly different than the bare electrode LOD of 21 ± 3 nM ($p < 0.01$, $n = 5$). The improvement in detection limit will allow more reliable detection of low nanomolar changes *in vivo*.

3.3.4 Time response of Nafion-CNT modified electrodes:

The response time of Nafion-coated and Nafion-CNT electrodes are compared to bare electrodes in Fig. 3.5. Normalizing to the same peak height (inset) allows a better comparison of the shape of the response. During flow injection analysis, a square plug of analyte flows by the electrode which ideally results in a square shaped, oxidation current versus time trace. However, the current versus time trace is not always ideal due to properties such as adsorption of the analyte to the surface and diffusion through the polymer to the electrode surface.⁴¹ Nafion decreases temporal resolution because the analyte must diffuse across the layer⁴² and in Fig. 3.5, Nafion coating did slightly slow the response time to adenosine. Bare electrodes had an average 10% to 90% rise time of 1.2 ± 0.1 s which was significantly different than the Nafion only electrodes rise time of 1.9 ± 0.2 s ($p < 0.01$, $n = 6$). When the electrodes are coated with Nafion-CNTs, rise time does not change from the bare electrode (1.2 ± 0.2 s, $p > 0.05$, $n = 24$). Therefore, the additional sensitivity of adding CNT to the Nafion did not come at the expense of slowing temporal resolution.

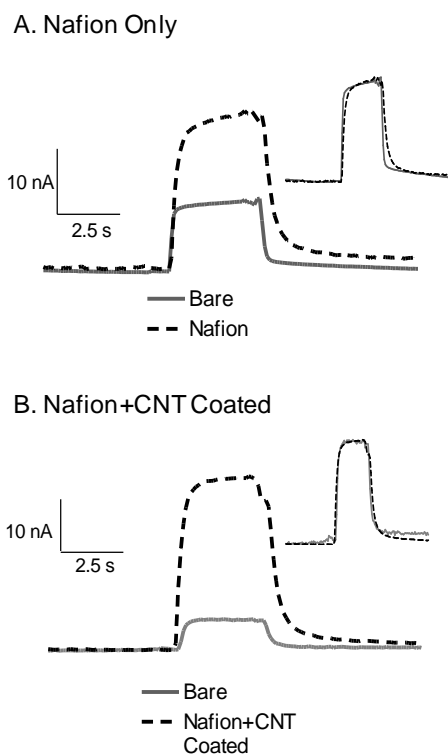


Figure 3.5: Current versus time profiles of A.) Nafion and B.) Nafion-CNT modified carbon-fiber microelectrodes for 5 μ M adenosine. The insets are normalized currents to illustrate differences in shape. For flow injection analysis, buffer is initially flowed by the electrode for 4 s, then analyte flowed for 4 s followed by buffer again. A) The time response after Nafion modification is slightly slower due to slower diffusion. B) Nafion-CNT modified electrodes did not show slower response after modification.

3.3.5 Investigation of other electroactive purines, purine derivatives, and neurotransmitters:

Table 3.1 reports average ratios of coated to bare peak oxidation currents to facilitate comparison of increases in sensitivity after Nafion-CNT coating for multiple species. Anions at physiological pH (ATP, AMP, uric acid) showed lower increases in sensitivity because the Nafion and the negatively charged oxide groups on the CNTs cause repulsion of anions. However, a total repulsion is not observed, likely because the CNTs did increase the electroactive surface area and a complete layer of Nafion was not formed. The improvements for ATP and AMP sensitivity are similar. Adenosine has the highest increase in sensitivity and the improvement was twice as big as that for dopamine. Adenosine signal improvement may be larger than dopamine because of the number or location of adsorption sites exposed to the electrode surface. Histamine and a basic pH change of +0.20 pH units were evaluated as other potential interferents. A 2-

fold increase was seen for histamine after Nafion-CNT coating whereas no increase was seen for the basic pH shift (Fig. 3.6, $n = 3$).

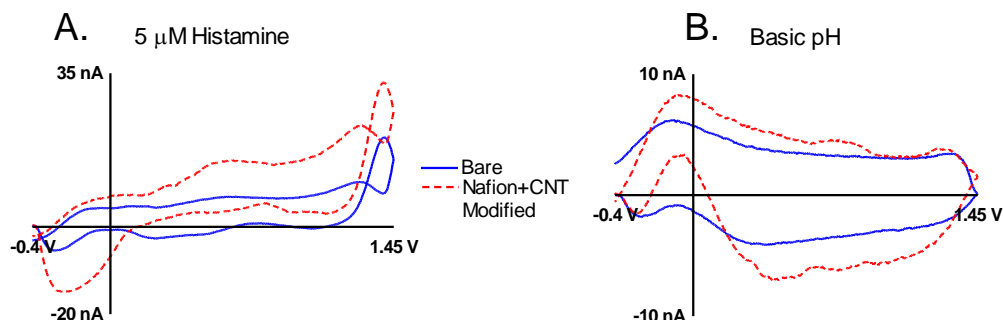


Figure 3.6: Cyclic voltammograms of A.) 5 μM histamine and B.) Basic pH shift of +0.2 pH units before and after Nafion-CNT coating. A 2-fold increase is seen for histamine and no change is observed for the basic pH shift.

Table 3.1 Average current improvement for common purines, purine derivatives, and neurotransmitters

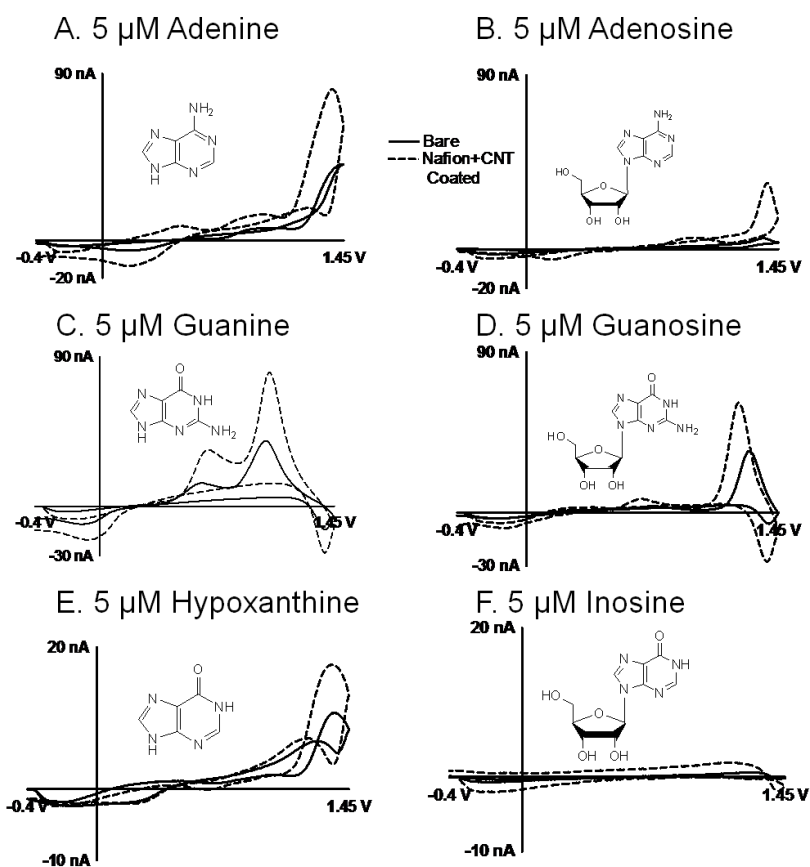
Nafion-CNT/Bare	
Adenosine (5 μM)	4.2 ± 0.9
AMP (5 μM)	1.7 ± 0.7
ATP (5 μM)	1.6 ± 0.2
Uric Acid (5 μM)	1.3 ± 0.1
Dopamine (1 μM)	2.3 ± 0.3
Adenine (5 μM)	2.0 ± 0.3
Guanosine (5 μM)	1.8 ± 0.1
Guanine (5 μM)	1.7 ± 0.1
Inosine (5 μM)	1.5 ± 0.2
Hypoxanthine (5 μM)	1.4 ± 0.1

Average data are the ratio of modified peak oxidation current to bare peak oxidation current for each analyte. Values given are \pm SEM for $n = 18$ for all analytes except for guanine and inosine ($n = 12$).

To study structural effects on sensitivity, purine bases and their corresponding nucleoside were compared: adenine and adenosine, guanine and guanosine, and

hypoxanthine and inosine. Guanine is a purine base found in DNA like adenine and it contains a carbonyl group at the C6 position and an amine group at the C2 position, instead of at the C6 position as in adenine (see Fig. 3.7 for structures). Hypoxanthine is a xanthine derivative which has a carbonyl group at the C6 position like guanine; however, it does not contain an amine group. Inosine is the nucleoside of hypoxanthine and is also a downstream metabolite of adenosine.⁵ Fig. 3.7 shows an example CV for each analyte before and after Nafion-CNT coating and Figure 3.8 shows calibration curves for 50 nM to 10 μ M for all the analytes.

Figure 3.7: Cyclic voltammograms of each purine base and nucleoside. Insets show structures for each analyte. A.) 5 μ M adenine, B.) 5 μ M adenosine, C.) 5 μ M guanine, D.) 5 μ M guanosine, E.) 5 μ M hypoxanthine and F.) 5 μ M inosine. Higher currents were seen for all purine bases for bare electrodes. All analytes show an increase in current after Nafion-CNT coating (dotted line).



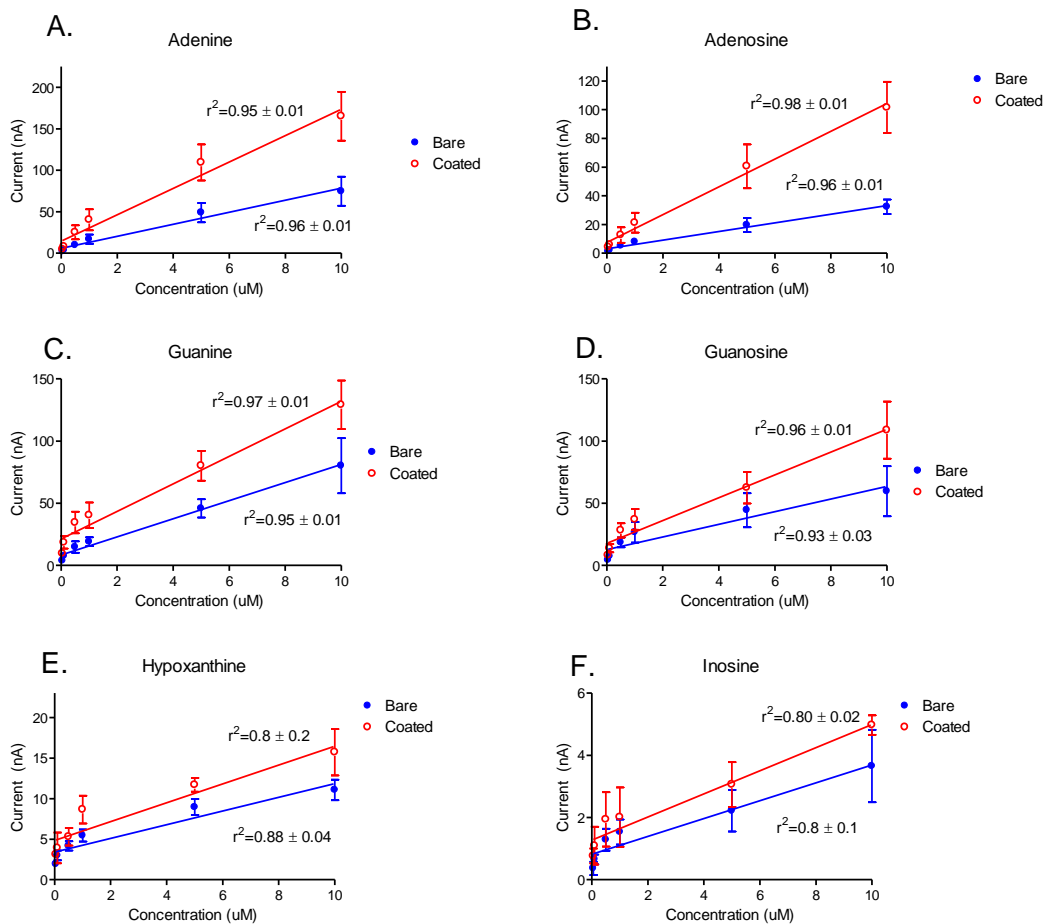


Figure 3.8: Calibration curves for purines and associate nucleosides for both bare and coated electrodes. A) Adenine B) Adenosine C) Guanine D) Guanosine E) Hypoxanthine and F) Inosine ($n = 4$). Hypoxanthine and inosine were the least linear for both bare and coated electrodes because the electrodes were less sensitive to these analytes. Most analytes showed an improvement in linearity after coating (exception: hypoxanthine, inosine, and adenine).

First, the amount of current observed was compared for each purine and corresponding nucleoside. In all cases, higher currents were observed at bare electrodes for each purine base compared to its nucleoside. Bare electrodes are about 3 to 4-fold more sensitive to the purine base adenine than for adenosine (Fig. 3.7 A, B and Fig. 3.8A, B), however guanine had only a slightly higher current than guanosine (Fig. 3.7 C, D and Fig. 3.8C, D). The sensitivity for bare electrodes to hypoxanthine is lower than adenine or guanine, showing the absence of the amine group decreases

sensitivity (note the difference in scale between Fig. 3.7 A/C and E). The oxidation peak for inosine is not well defined, although the broad peaks on the cathodic scan increased with increasing inosine concentration, signifying they are due to inosine detection (Fig. 3.8F).

Second, the effect of different functional groups on purines was characterized. The initial sensitivity for adenine and guanine is similar at bare electrodes, although their oxidation peak potentials are different. The increase in current after Nafion-CNT coating is slightly higher for adenine than guanine (Table 3.1). After Nafion-CNT coating, lower improvements in sensitivity were observed for hypoxanthine than for guanine or adenine (Table 3.1). Comparison of changes in calibration slopes were also made, and the same trends were observed (see Figure 3.8 and Table 3.2). The data demonstrate that amine groups increase the oxidation current for purines, likely by increasing adsorption to the electrode, and that the presence of a carbonyl group decreases the sensitivity enhancements with Nafion-CNT coating.

Table 3.2. Average calibration slope improvement for purines and nucleosides

Adenine	2.2 ± 0.2
Adenosine	3.2 ± 0.1
Guanine	1.5 ± 0.2
Guanosine	1.8 ± 0.3
Hypoxanthine	1.4 ± 0.3
Inosine	1.3 ± 0.2

Average data are the ratio of modified calibration slope to bare calibration slope for each analyte. Values given are \pm SD for $n = 4$.

Third, the effect of the ribose unit on sensitivity enhancement after Nafion-CNT was determined by comparing the purine bases and nucleosides. For guanosine and inosine, the enhancement in signal after Nafion-CNT was about the same as for their

corresponding purine (Fig. 3.7 and Table 3.1). However, adenosine had two times the increase in sensitivity of adenine, when comparing current ratios and about a 1.5 increase in sensitivity over adenine when comparing changes in calibration slopes, indicating a positive effect of the ribose unit. The compounds with the carbonyl group showed no difference for improvement for purines and nucleosides. For adenosine, interactions between the ribose group and the CNTs, particularly repulsion by the oxide groups, might facilitate better orientation of the adenine group on adenosine and enhance oxidation current.

3.3.6 Selectivity of Nafion-CNT modified electrodes in brain slices:

The selectivity of the Nafion-CNT coated electrode for adenosine over ATP was demonstrated in rat brain slices. Adenosine and ATP were pressure ejected into a slice from a micropipette positioned 30 μm away from the working electrode. Both a bare and Nafion-CNT coated electrode were tested in each slice, allowing the selectivity for adenosine over ATP to be determined for a bare and a Nafion-CNT coated electrode in each slice. Figures 3.9 shows the responses of a bare electrode (3.9A) and a Nafion-CNT electrode (3.9B) to exogenously applied adenosine and ATP in the same slice. The Nafion-CNT coated electrode has a 5.1 ± 0.5 fold greater signal for adenosine than ATP compared to the 2.1 ± 0.4 fold difference for the bare electrode (Figure 3.9C). The Nafion-CNT electrodes were significantly more selective for adenosine than bare electrodes in brain slices ($n=4$, $p<0.005$) and the increase in selectivity is about the same as that seen *in vitro*, where the electrode was 6 times more sensitive for adenosine. The Nafion-CNT coated electrode will facilitate future studies that have a greater sensitivity and selectivity for adenosine detection in the brain.

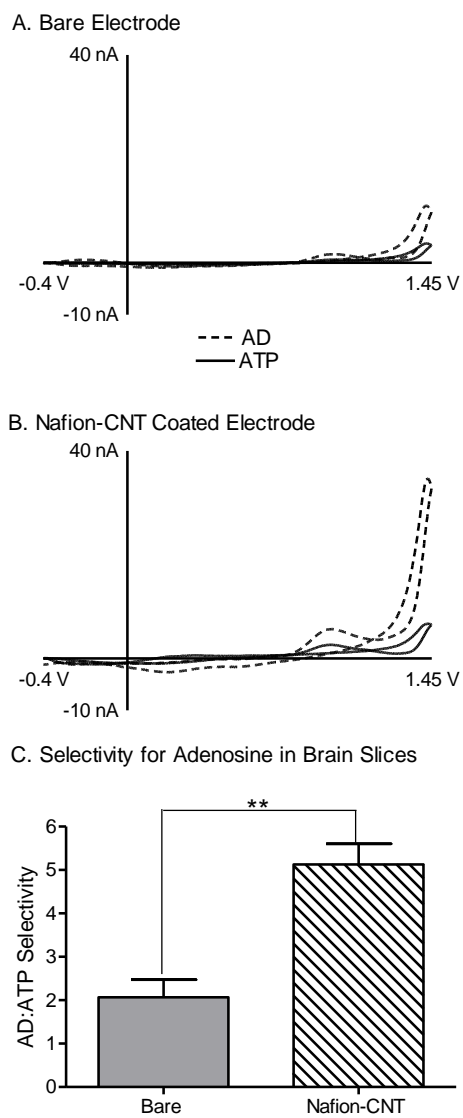


Figure 3.9: Brain slice data comparing bare and coated electrodes selectivity for adenosine. Adenosine and then ATP was pressure ejected into the medial prefrontal cortex 30 μm from the recording electrode. A) CV of adenosine (dashed) and ATP (solid) at a bare electrode show it is 2 times more selective for adenosine. B) The Nafion-CNT coated electrode is 5 times more selective for adenosine over ATP in the same slice as the bare electrode. C) Average selectivity ratio in a slice, given as a ratio of adenosine detected to ATP detected for both bare and coated electrodes ($n=4$, $p<0.005$).

3.4 Conclusions

In this chapter, I show that combining Nafion and CNTs on the surface of carbon-fiber microelectrodes provided enhanced sensitivity and selectivity to adenosine over ATP. A lower concentration of CNTs was optimal for enhanced sensitivity for adenosine. Temporal response was not affected by Nafion-CNT coating which makes these electrodes ideal for *in vivo* use because they maintain a fast response. Comparing pairs of different purine bases shows that the presence of an amine group enhances sensitivity and that purines with carbonyl groups do not have as great an enhancement after Nafion-CNT coating. The ribose group provides additional sensitivity enhancement for adenosine over adenine, but this trend is not observed for other purines and nucleosides. The Nafion-CNT electrodes detected adenosine more selectively than ATP in brain tissue as compared to bare electrodes. Overall, Nafion-CNT electrodes provide more sensitive and selective detection of adenosine which should facilitate more reliable detection of adenosine in biological systems.

3.5 References

1. Pedata, F.; Melani, A.; Pugliese, A. M.; Coppi, E.; Cipriani, S.; Traini, C. *Purinergic Signalling* **2007**, *3*, 299-310.
2. de Mendonca, A.; Sebastiao, A. M.; Ribeiro, J. A. *Brain Res. Brain Res. Rev.* **2000**, *33* (2-3), 258-274.
3. Latini, S.; Pedata, F. *J. Neurochem.* **2001**, *79*, 463-484.
4. Porkka-Heiskanen, T.; Strecker, R. E.; McCarley, R. W. *Neuroscience* **2000**, *99* (3), 507-517.
5. Akula, K. K.; Kaur, M.; Kulkarni, S. K. *J. Chromatogr. A* **2008**, *1209* (1-2), 230-237.
6. Cechova, S.; Venton, B. J. *J. Neurochem.* **2008**, *105* (4), 1253-1263.
7. Pajski, M. L.; Venton, B. J. *ACS Chem. Neurosci.* **2010**, *1* (12), 775-787.
8. Llaudet, E.; Botting, N. P.; Crayston, J. A.; Dale, N. *Biosens. bioelectron.* **2003**, *18*, 43-52.
9. Dryhurst, G. *Electrochemistry of biological molecules*; Academic Press: New York, 1977. pp. 71-185.
10. Hashemi, P.; Dankoski, E. C.; Petrovic, J.; Keithley, R. B.; Wightman, R. M. *Anal. Chem.* **2009**, *81* (22), 9462-9471.
11. Crespi, F.; Martin, K. F.; Marsden, C. A. *Neuroscience* **1988**, *27* (3), 885-896.
12. Brazell, M. P.; Kasser, R. J.; Renner, K. J.; Feng, J.; Moghaddam, B.; Adams, R. N. *J. Neurosci. Methods* **1987**, *22* (2), 167-172.
13. Gerhardt, G. A.; Oke, A. F.; Nagy, G.; Moghaddam, B.; Adams, R. N. *Brain Res.* **1984**, *290* (2), 390-395.
14. Baur, J. E.; Kristensen, E. W.; May, L. J.; Wiedemann, D. J.; Wightman, R. M. *Anal. Chem.* **1988**, *60* (13), 1268-1272.
15. Wiedemann, D. J.; Kawagoe, K. T.; Kennedy, R. T.; Ciolkowski, E. L.; Wightman, R. M. *Anal. Chem.* **1991**, *63* (24), 2965-2970.
16. Baur, J. E.; Kristensen, E. W.; May, L. J.; Wiedemann, D. J.; Wightman, R. M. *Analytical Chemistry* **1988**, *60* (13), 1268-1272.
17. Pihel, K.; Walker, Q. D.; Wightman, R. M. *Anal. Chem.* **1996**, *68* (13), 2084-2089.
18. Kuhr, W. G.; Wightman, R. M. *Brain Res.* **1986**, *381* (1), 168-171.

19. Hocevar, S. R.; Wang, J.; Deo, R. P.; Musameh, M.; Ogorevc, B. *Electroanalysis* **2005**, *17* (5-6), 417-422.
20. Huffman, M. L.; Venton, B. J. *Analyst* **2009**, *134* (1), 18-24.
21. Jacobs, C. B.; Peairs, M. J.; Venton, B. J. *Anal. Chim. Acta* **2010**, *662* (2), 105-127.
22. Wu, K.; Fei, J.; Hu, S. *Anal. Biochem.* **2003**, *318*, 100-106.
23. Hirsch, A.; Vostrowsky, O. *Top. Curr. Chem.* **2005**, *245*, 193-237.
24. Wong, E. W.; Sheehan, P. E.; Lieber, C. M. *Science* **1997**, *277*, 1971-1975.
25. Wang, J. *Electroanalysis* **2005**, *17* (1), 2005-7.
26. Forrest, G. A.; Alexander, A. J. *J. Phys. Chem. C.* **2007**, *111* (29), 10792-10798.
27. Wang, J.; Musameh, M.; Lin, Y. *J. Am. Chem. Soc.* **2003**, *125* (9), 2408-2409.
28. Tkac, J.; Ruzgas, T. *Electrochem. Comm.* **2006**, *8* (5), 899-903.
29. Swamy, B. E. K.; Venton, B. J. *Analyst* **2007**, *132*, 876-884.
30. Chattopadhyay, D.; Galeska, I.; Papadimitrakopoulos, F. *J. Am. Chem. Soc.* **2001**, *123*, 9451-9452.
31. Kim, S. N.; Rusling, J. F.; Papadimitrakopoulos, F. *Adv. Mater.* **2007**, *19*, 3214-3228.
32. Peairs, M. J.; Ross, A. E.; Venton, B. J. *Anal. Methods* **2011**, *3*, 2379-2386.
33. Wei, Z.; Kondratenko, M.; Dao, L. H.; Perepichka, D. F. *J. Am. Chem. Soc.* **2006**, *128* (10), 3134-3135.
34. Strand, A. M.; Venton, B. J. *Anal. Chem.* **2008**, *80* (10), 3708-3715.
35. Paxinos, G.; Watson, C. *The Rat Brain in Stereotaxic Coordinates*; 6 ed.; Academic Press: 2007.
36. Star, A.; Stoddart, J. F.; Steuerman, D.; Diehl, M.; Boukai, A.; Wong, E. W.; Yang, X.; Chung, S. W.; Choi, H.; Heath, J. R. *Angew. Chem. Int. Ed.* **2001**, *40* (9), 1721-1725.
37. Olive-Monllau, R.; Esplandiú, M. J.; Bartroli, J.; Baeza, M.; Cespedes, F. *Sens. Actuat. B: Chem.* **2010**, *146* (1), 353-360.
38. Swamy, B. E. K.; Venton, B. J. *Anal. Chem.* **2007**, *79*, 744-750.
39. Xu, Y. D.; Venton, B. J. *Electroanalysis* **2010**, *22* (11), 1167-1174.
40. Jacobs, C. B.; Vickrey, T. L.; Venton, B. J. *Analyst* **2011**, *136* (17), 3557-3565.

41. Bath, B. D.; Michael, D. J.; Trafton, B. J.; Joseph, J. D.; Runnels, P. L.; Wightman, R. M. *Anal. Chem.* **2000**, 72 (24), 5994-6002.
42. Nagy, G.; Gerhardt, G. A.; Oke, A. F.; Rice, M. E.; Adams, R. N.; Moore, R. B.; Szentirmay, M. N.; Martin, C. R. *J. Electroanal. Chem.* **1985**, 188 (1-2), 85-94.

Chapter 4

Sawhorse waveform voltammetry for selective detection of adenosine, ATP, and hydrogen peroxide

Strive not to be a success, but rather to be of value

~Albert Einstein

Chapter 4: Sawhorse waveform voltammetry for selective detection of adenosine, ATP, and hydrogen peroxide

Abstract

Fast-scan cyclic voltammetry is an electrochemistry technique which allows subsecond detection of neurotransmitters *in vivo*. Triangle shaped waveforms are traditionally used for neurotransmitters such as dopamine. Recently, modified waveforms have become popular to maximize analyte sensitivity and to reduce fouling. The sawhorse waveform has been used to stabilize background current during dopamine detection with faster scan rates. Here, a sawhorse waveform was used to maximize time for adenosine oxidation and to manipulate the shapes of cyclic voltammograms (CVs) of analytes which oxidize at the switching potential. The optimized waveform consists of scanning at 400 V/s from -0.4 to 1.35 V and holding briefly for 1.0 ms followed by a ramp back down to -0.4 V. This waveform allows a lower switching potential for adenosine detection. Hydrogen peroxide and ATP also oxidize at the switching potential and can interfere with adenosine measurements *in vivo*; however, their CVs were different from adenosine with the sawhorse waveform. Principal component analysis (PCA) was used to determine that the sawhorse waveform was better than the triangle waveform at discriminating between adenosine, hydrogen peroxide, and ATP. With calibrations performed in slices, PCA was also able to identify mechanically-evoked adenosine release in brain slices. The sawhorse waveform is useful for adenosine, hydrogen peroxide, and ATP discrimination and will facilitate more confident measurements of these analytes *in vivo*. This paper has been submitted to the Journal of Analytical Chemistry.

4.1 Introduction

Fast scan cyclic voltammetry (FSCV) is an electrochemical technique which allows subsecond measurements of neurotransmitters *in vivo*.¹⁻³ Traditional FSCV uses a triangular shaped waveform which is applied to a carbon-fiber microelectrode at a scan rate of 300-400 V/s.^{4,5} Most FSCV research has focused on studying dopamine dynamics in the brain,⁶⁻⁹ where dopamine is detected at 0.6 V and traditional waveforms are only scanned to 1.0 V.¹⁰ However, recently the waveform was extended to 1.3 V which caused an increase in dopamine oxidative current¹¹. The increase in current was due to increased adsorption from oxygen functional groups and surface renewal from breaking carbon-carbon bonds on the surface.¹² With higher scan rates up to 2400 V/s, a sawhorse shaped waveform was implemented that holds at a 1.3 V switching potential for around a half a millisecond.¹³ The purpose of holding at 1.3 V was to stabilize and renew the electrode surface and not to allow more time for dopamine oxidation, as the surface adsorbed dopamine completely oxidized before the hold time. Waveform optimization has proven to be an important tool for maximizing analyte sensitivity¹² and reducing fouling^{1,14} at the electrode.

FSCV has been extended to several other important but more electrochemically-challenging neurochemicals in the brain such as serotonin¹, hydrogen peroxide¹⁵, and adenosine¹⁶. Adenosine poses a specific challenge due to its relatively high E^0 (~1.30 V)¹⁷, so a switching potential of 1.45-1.50 V with FSCV is necessary.^{16,18,19} Adenosine is a neuromodulatory molecule found in the brain²⁰⁻²² and is neuroprotective during conditions of ischemia^{23,24} and hypoxia^{25,26}. Detection of adenosine using FSCV^{3,16,18} is beneficial for understanding how adenosine functions on the subsecond to second timescale.²⁷ A secondary peak has been observed with FSCV for adenosine detection

and can aid in distinguishing the analyte, however the secondary peak is harder to see at very low concentrations.^{18,28}

Other analytes have cyclic voltammograms (CVs) with peaks around the same potential as adenosine, including ATP and hydrogen peroxide.^{15,16,18} ATP can be released by exocytosis and then metabolized extracellularly to adenosine.²¹ ATP and adenosine have the same electroactive adenine moiety¹⁷ and their CVs are almost identical. However, FSCV detection of adenosine at carbon-fiber microelectrodes is 3-6 times more sensitive than for ATP, due to the negative charge of ATP.¹⁸ Hydrogen peroxide also has a peak that occurs near the switching potential with FSCV.^{15,29,30} Unlike adenosine and ATP, hydrogen peroxide does not have a secondary peak but the relatively slow kinetics of hydrogen peroxide mean that the main peak is detected at a similar potential as the primary peak for adenosine.¹⁵ While scanning to higher potentials might help separate adenosine and hydrogen peroxide, this solution is not practical due to water hydrolysis. Thus, a waveform is needed which could allow for better discrimination between these analytes that does not require a higher switching potential.

In this study, we discriminated adenosine, ATP, and hydrogen peroxide using a sawhorse waveform. The purpose of holding at the switching potential was to allow more oxidation to occur without the need for a higher switching potential. We found that holding the electrode at the switching potential for 1.0 ms allows a lower oxidizing potential to be used for adenosine detection. Higher amounts of current were observed for adenosine with a 1.35 V switching potential at the sawhorse waveform compared to the triangle waveform. Holding for 1.0 ms at the switching potential produced an extra peak in the adenosine CV which was not present for hydrogen peroxide and therefore the two compounds could be distinguished. Principal component analysis (PCA) was used to discriminate between adenosine, ATP, hydrogen peroxide, and dopamine and the sawhorse waveform was better for distinguishing between the analytes.

Mechanically stimulated adenosine in slices was accurately predicted as adenosine using the sawhorse waveform. Overall, adenosine can be detected with higher sensitivity and selectivity at lower potentials with the sawhorse waveform.

4.2 Methods

4.2.1 Chemicals

Adenosine and dopamine standards were purchased from Sigma Aldrich (St. Louis, MO) and ATP was purchased from Tocris Biosciences (Bristol, United Kingdom), dissolved in 0.1 M HClO₄ for 10 mM stock solutions and diluted daily in Tris buffer for testing. 30 % hydrogen peroxide was purchased from Macron Fine Chemicals (Center Valley, PA) and diluted daily in Tris buffer to its final concentration. The Tris buffer solution consists of 15 mM Tris(hydroxymethyl)aminomethane, 1.25 mM NaH₂PO₄, 2.0 mM Na₂SO₄, 3.25 mM KCl, 140 mM NaCl, 1.2 mM CaCl₂ dehydrate, and 1.2 mM MgCl₂ hexahydrate at pH 7.4 (all Fisher, Suwanee, GA). For slice experiments, calibrations and training set solutions were performed in artificial cerebral spinal fluid (aCSF): 126 mM NaCl, 2.5 mM KCl, 1.2 mM NaH₂PO₄, 2.4 mM CaCl₂ dehydrate, 1.2 mM MgCl₂ hexahydrate, 25 mM NaHCO₃, 11 mM glucose, and 15 mM tris (hydroxymethyl) aminomethane, pH 7.4 (all Fisher, Suwanee GA). All aqueous solutions were made with deionized water (Milli-Q Biocel, Millipore, Billerica, MA).

4.2.2 Carbon-fiber microelectrodes

Carbon-fiber microelectrodes were fabricated from T-650 carbon-fibers (gift from Cytec Engineering Materials, West Patterson, NJ)³¹ and cylinder-shaped electrodes, approximately 50-100 μm long, were used. Electrodes were epoxied with Epon Resin 828 (Miller-Stephenson, Danbury, CT) with 14% (w/w) 1,3-phenylenediamine hardener

(Sigma-Aldrich, St. Louis, MO) to ensure a good seal. All electrodes were soaked for 10 min in isopropanol (Fisher Scientific) prior to use.

4.2.3 Electrochemistry measurements

Fast-scan cyclic voltammograms were collected using a ChemClamp (Dagan, Minneapolis, MN) and data was collected using Tarheel CV software (gift of Mark Wightman, UNC) using a homebuilt data analysis system and two computer interface boards (National Instruments PCI 6052 and PCI 6711, Austin TX). The electrode was scanned from -0.4 V to 1.45 V (vs Ag/AgCl) and back with a scan rate of 400 V/s and a repetition rate of 10 Hz for the triangle waveform. For the sawhorse waveform, the electrode was scanned from -0.4 V to 1.35 V and held for 1.0 ms before ramping back down, at a scan rate of 400 V/s and 10 Hz repetition rate.

4.2.4 Brain slice experiments

Male Sprague-Dawley rats (250-350 g, Charles River, Willmington, MA) were housed in a vivarium and given food and water *ab libitum*. All experiments were approved by the Animal Care and Use Committee of the University of Virginia. Rats were anesthetized with isoflurane (1 mL/100 g rat weight) in a desiccator prior to slice preparation and were immediately beheaded. The brain was removed within 2 min and placed in 0-5°C aCSF for 2-4 min for recovery. A vibratome (LeicaVT1000S, Bannockburn, IL) was used to prepare 400 μm slices of the prefrontal cortex. Slices were transferred to oxygenated aCSF (95% oxygen, 5% CO_2) and allowed to recover for approximately an hour before the experiment. A pump (Watson-Marlo 205U, Wilmington, MA) was used to flow 35-37°C aCSF (maintained by an IsoTemp 205 water bath (Fisher Scientific) over the brain slice at 2 mL/min. The electrodes were inserted 50 μm beneath the tissue and the waveform was applied for 20 min before any data collection. The slice was mechanically stimulated by using a micromanipulator to lower a

glass pipette 50 μm . The pipette was ~ 15 μm in diameter and located about 30 μm away from the working electrode. A PCA training set was collected by pressure ejection of adenosine, hydrogen peroxide, and ATP onto brain slices by a Parker Hannifin picospritzer (Picospritzer III, Cleveland, OH). A pulled glass pipette was filled with analyte and placed 30-50 μm from the carbon-fiber microelectrode. The ejection parameters were 10 psi for 100-400 milliseconds and 100-800 nL of analyte (either 25 μM adenosine, ATP, or H_2O_2) was delivered to generate a training set in slices. All training sets were collected after mechanical stimulation.

4.2.5 Principal component analysis

Principal component analysis software was written in LabView Mathscript RT Module (from Mark Wightman and Richard Keithley, UNC Chapel Hill). A training set was compiled for each analyte tested (adenosine, ATP, hydrogen peroxide, and dopamine). Principal components were extracted from the training set and the data was analyzed using principal component regression.³² Mixtures of known concentrations of adenosine with hydrogen peroxide, ATP, or dopamine were analyzed. Every training set has residuals which account for currents from unknown signals, such as noise.³³ The Q-score is the sum of squares of the residuals for each variable. This was calculated, and any signal above Q failed and was not used in the analysis. The program was used to predict concentrations of adenosine and the other analytes within the mixture based on the training set of the individual analytes. In slices, a training set was generated by exogenously applying adenosine, hydrogen peroxide, and ATP in the brain slice. Concentration of mechanically stimulated adenosine signals were predicted using the in slice training set.

4.2.6 Statistics

All values are reported as the mean \pm standard error of the mean (SEM). All statistics were performed in GraphPad Prism (GraphPad Software, Inc., La Jolla, CA) and considered significant at the 95% confidence level ($p < 0.05$). One-way ANOVA with Bonferroni post tests were used to analyze the switching potential optimization and plateau time optimization experiments. Unpaired t-tests were used to compare the switching potentials for the triangle and sawhorse waveform. Unpaired t-tests were also used to compare the PCA predicted adenosine to the actual mechanically stimulated adenosine concentration.

4.3 Results and Discussion

4.3.1 Comparison of the triangle and sawhorse waveform

Fig. 4.1A shows traditional background-subtracted cyclic voltammograms for 5 μM adenosine, 10 μM hydrogen peroxide, 5 μM ATP, and 5 μM dopamine using the triangle waveform (-0.4 to 1.45 V and back at 400 V/s). The waveform trace is plotted on each of the CVs (black dotted line) so that peak positions during the waveform can be analyzed. The main oxidation peak for adenosine, hydrogen peroxide, and ATP is right at or slightly after at the switching potential and all look similar. Adenosine has a secondary peak that appears around 1.0 V, which is more prominent at higher concentrations. ATP has the same oxidation reaction as adenosine and the CVs are similar except that carbon-fiber microelectrodes are more sensitive to adenosine.^{16,18,19} Dopamine has a peak at 0.6 V, away from the switching potential and is shown for comparison purposes as a control.³⁴⁻³⁶

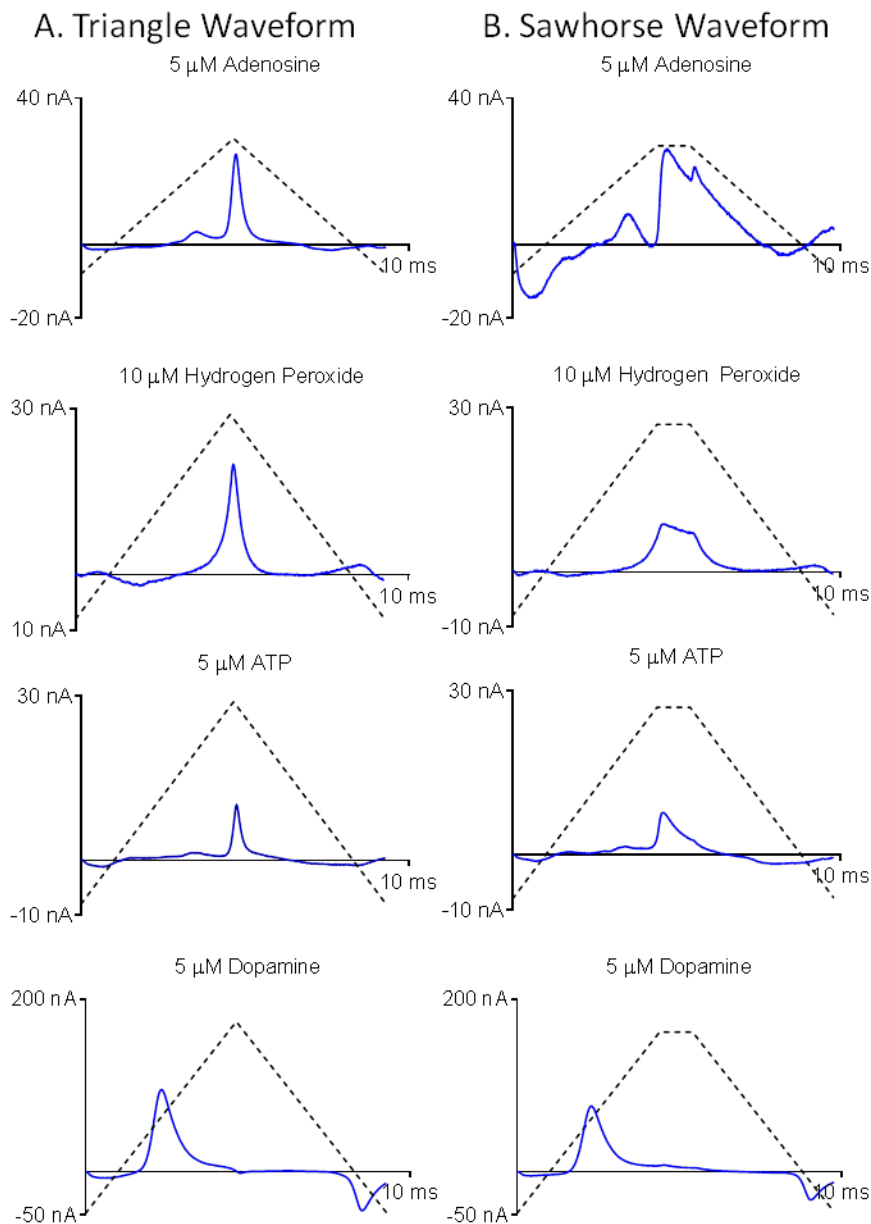


Figure 4.1: Cyclic voltammograms (CVs) for the A) triangle and B) sawhorse waveform. The triangle waveform is the traditional adenosine waveform for FSCV (-0.4 to 1.45 V at 400 V/s). The optimized sawhorse waveform involves scanning from -0.4 V to 1.35 V, holding for 1.0 ms, and ramping back down to -0.4 V at a rate of 400 V/s. The data was collected at two separate electrodes. The dotted black line shows the shape of the waveform over time and the blue line represents the current vs applied waveform time. The CVs are plotted current versus time instead of versus voltage because of the hold time in the sawhorse waveform. 5 μM adenosine, 10 μM hydrogen peroxide, 5 μM ATP, and 5 μM dopamine were tested.

Keithley et al. first introduced the idea of a sawhorse waveform for dopamine detection using FSCV¹³ but the purpose of the sawhorse was to enhance electrode stability at scan rates exceeding 2000 V/s. Here, a modified sawhorse waveform was used to allow more time for analyte oxidation at the switching potential. Figure 4.1B shows background-subtracted cyclic voltammograms for the sawhorse waveform which scans from -0.4 to 1.35 V, holds for 1.0 ms and then scans back down to -0.4 V at 400 V/s. The CVs in this figure are from a different electrode than the CVs for the triangle waveform because scanning to a higher potential can irreversibly change the electrode surface.¹² Traditionally, CVs are plotted as current versus voltage but due to the holding time for the sawhorse, the data are better visualized as a plot of current vs applied waveform time. The waveform is also superimposed on each plot in Fig. 4.1.

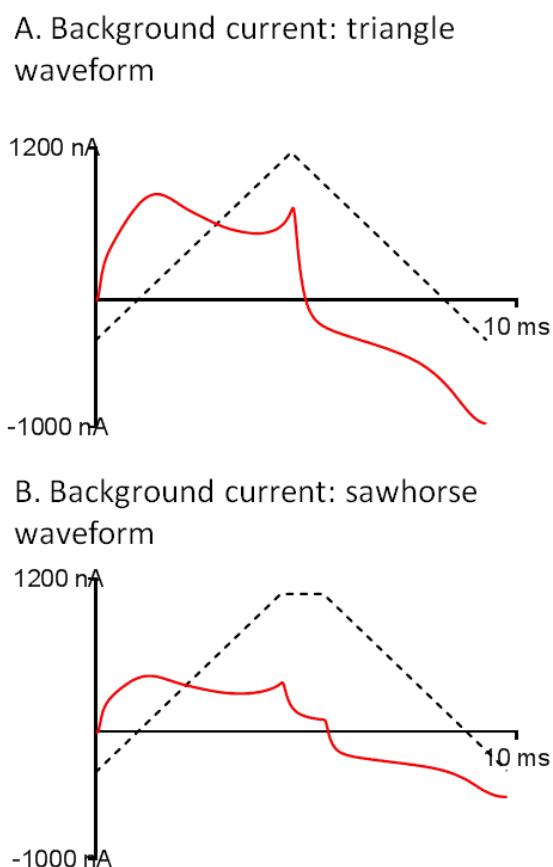
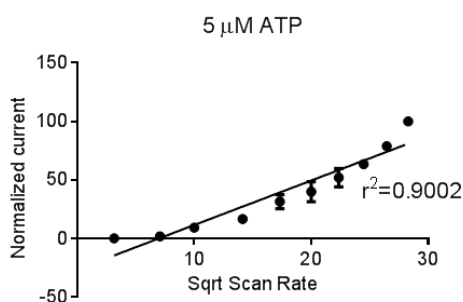
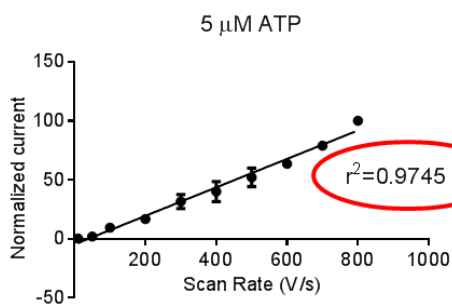


Figure 4.2: Background current for both waveforms. A) Background current for the traditional triangle waveform (-0.4 to 1.45 V at 400 V/s) is plotted in red and the dashed line represents the shape of the waveform over time. B) Background current for the optimized sawhorse waveform (-0.4 to 1.35 V, hold for 1.0 ms at 400 V/s) is plotted in red and the black line denotes the shape of the sawhorse waveform over time. The sawhorse background current shows a drop in capacitive current at the plateau time.

Analytes which oxidize at the switching potential (adenosine, ATP, and hydrogen peroxide) all look similar with the triangle waveform; however, at the sawhorse waveform the analytes are more distinguishable. The first difference between CVs from the sawhorse and triangle waveform is during the holding time. The background charging current decays during the holding potential (Fig. 4.2A, B) due to the exponential decay in capacitive charging. The faradaic current in the background subtracted CVs also decreases. For adsorption controlled species, the peak will return to zero when all of the surface adsorbed species is oxidized. For diffusion controlled species, the current decays much slower. H_2O_2 is diffusion controlled (Figure 4.3) and it falls off slowly with time during the holding potential (Fig. 4.1B). Log plots of current vs time show a significantly slower rate of decay for hydrogen peroxide than for adenosine and ATP (Figure 4.4). Adenosine is primarily adsorption controlled¹⁶ and current drops off faster at the switching potential than for hydrogen peroxide. ATP is also adsorption controlled (Figure 4.3) and because less is adsorbed than adenosine, the signal is back to zero at the end of the holding potential despite the fact that the rate of decay is similar to that for adenosine (Figure 4.4). Dopamine has no peak at the plateau because all the surface adsorbed dopamine was oxidized before that time.

A. ATP Scan Rate Plots



B. Hydrogen peroxide Scan Rate Plots

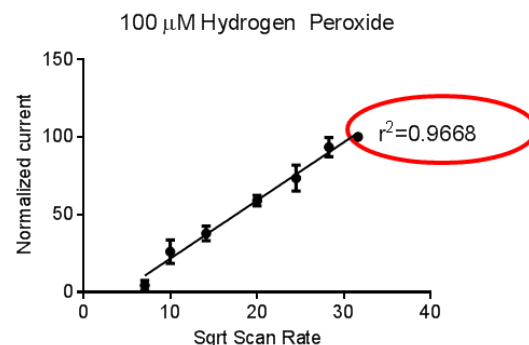
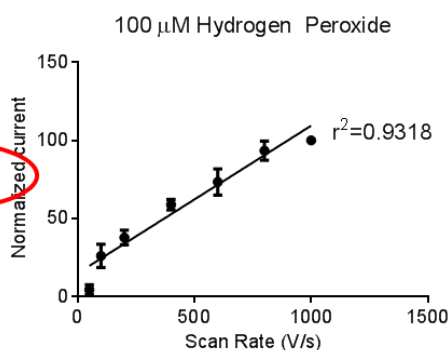


Figure 4.3: Scan rate experiments for both 5 μM ATP and 100 μM hydrogen peroxide. A) 5 μM ATP was tested at a range of scan rates, and the rest of the waveform was held constant (-0.4 V to 1.45 V). The current was normalized to account for variability amongst electrodes. The r^2 value for the plot of normalized current versus scan rate was 0.9745, whereas the r^2 for the plot of normalized current versus the square root of scan rate was 0.9002 ($n = 3$). The data fit better to the current versus scan rate, so ATP is primarily adsorption controlled. B) 100 μM hydrogen peroxide was tested in the same manner; however, the hydrogen peroxide data fit best plot of normalized current versus square root of scan rate ($r^2=0.9668$), therefore hydrogen peroxide is primarily diffusion-controlled ($n = 3$).

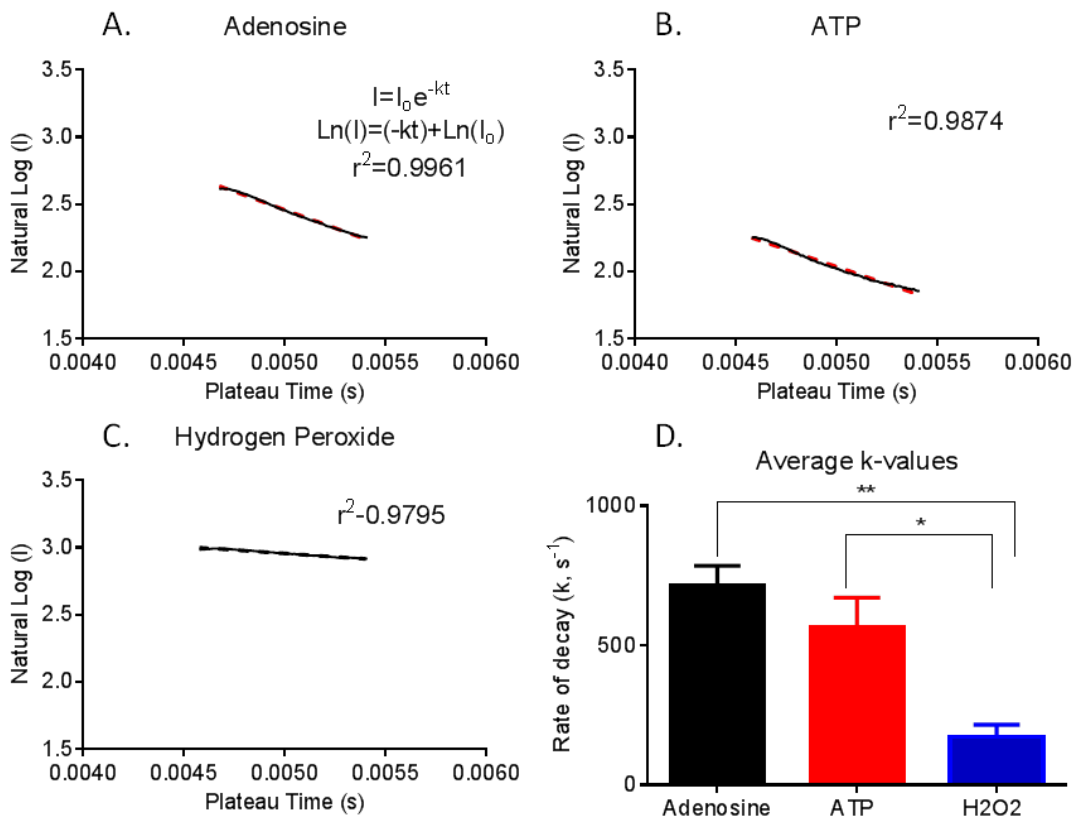


Figure 4.4: Adenosine current decays significantly quicker than hydrogen peroxide. Log plots for current represent if the decay in current is an exponential decay (see equation in panel A). The slope of the line is the rate of decay (k) of the current at the plateau region (Black trace is the analyte and the red dash trace is the fit). A) Plot of the natural log of current versus time for the plateau region of an example adenosine cyclic voltammogram. In this example, the r^2 is 0.9961, and on average the r^2 is 0.9920 ± 0.0020 ($n = 5$). B) ATP is fit to the same equation shown in (A), and the $r^2 = 0.9874$. The average $r^2 = 0.9880 \pm 0.003$ ($n = 4$). C) Hydrogen peroxide is also fit to this equation and the $r^2 = 0.9795$, and on average is $r^2 = 0.9720 \pm 0.004$ ($n = 4$). D) Graph shows average k -values (s^{-1}) for each analyte. Rate of decay was significantly dependent on analyte (one-way ANOVA, $p = 0.0017$, $n = 4-5$). Adenosine and ATP current decays are significantly faster than hydrogen peroxide (one-way ANOVA with Bonferroni post-test, $p < 0.05$).

Upon ramping back down, an extra peak for adenosine occurs in the sawhorse waveform. There is also a large negative current on the forward scan and both of these peaks are background subtraction errors. After adenosine is oxidized, the oxidation product sticks to the electrode.¹⁶ Thus, on the next scan, a secondary oxidation peak for a downstream reaction can be observed at 1.0 V.¹⁶ The adsorption of any species to the

electrode causes a change in the background charging current, which could be due to differences in surface area or exposed surface oxide groups. The extra peaks are much more prominent with the sawhorse waveform, likely due to extra time at a potential sufficient to break surface carbon bonds and add surface oxide groups.¹² Hydrogen peroxide is not adsorption controlled and does not have any of the extra peaks (Figure 4.3). ATP has less of a secondary peak and fewer of the extra peaks than adenosine, likely because less adsorbs due to its charge. The extra peak on the downward scan is also observed for adenine oxidation but is much smaller in current (Fig. 4.5). Adenine is the nucleobase of adenosine and does not contain the ribose unit. Because the extra peak is observed for adenosine, adenine, and ATP but not hydrogen peroxide, it must be due to an adsorption product of the nucleobase.

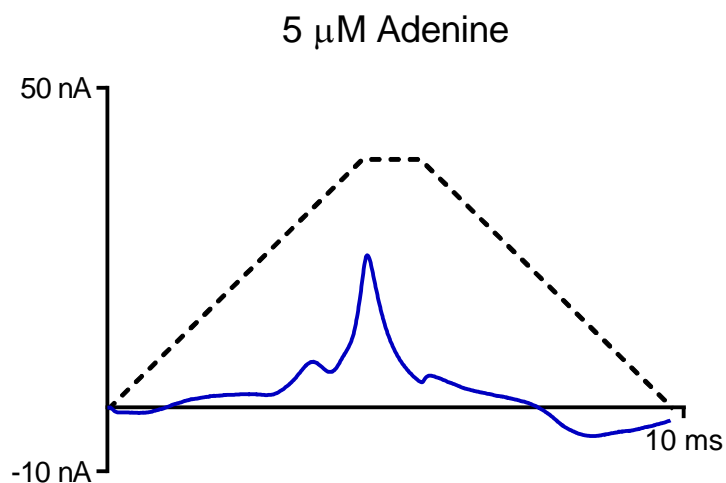


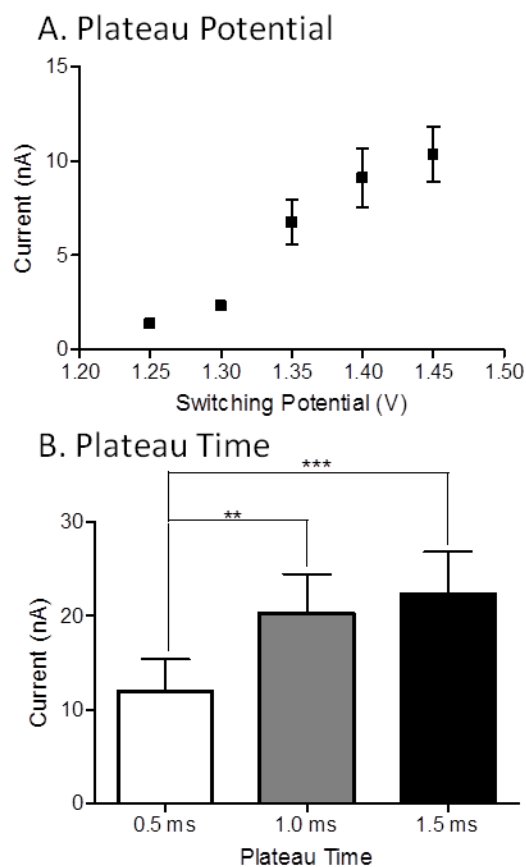
Figure 4.5: Cyclic voltammogram of 5 μ M adenine. The CV is plotted as current versus time (blue) and the waveform is plotted by the dashed line. Adenine current falls off quickly and an extra peak is observed immediately following the plateau.

4.3.2 Sawhorse waveform optimization

The sawhorse waveform plateau potential and time were optimized for sufficient sensitivity and stability of adenosine. Figure 4.6 shows the effect of plateau potential

(Fig. 4.6A) and plateau time (Fig. 4.6B). A range of plateau voltages were tested, from 1.25 V to 1.45 V (n=4). Very little current was detected at 1.25 and 1.30 V, which are below the oxidation potential for adenosine.¹⁷ A noticeable jump in sensitivity was observed at 1.35 V and the current for this potential was significantly higher than both 1.25 V and 1.30 V (one-way ANOVA with Bonferroni post-test, $p < 0.01$ and $p < 0.05$ respectively, n=4). Slightly higher currents were detected at 1.40 and 1.45 V; however the amount of current was not significantly different than 1.35 V (One-way ANOVA with Bonferroni post-test, $p > 0.05$). Thus, 1.35 V was chosen as the optimal plateau potential because it provided significantly more current than lower voltages but was further away from the potential for water hydrolysis. In addition, background currents were more stable at lower potentials.

Figure 4.6: Optimization of the sawhorse waveform switching potential and plateau time. A) A range of plateau voltage spanning from 1.25 V to 1.45 V was tested for 1 μ M adenosine. The plateau time is constant at 1.0 ms. A noticeable jump in current is seen at 1.35 V. Overall current was significantly dependent on switching potential (on-way ANOVA, $p = 0.0273$). The current produced from 1.35 V was significantly higher than both 1.25 V and 1.30 V (one-way ANOVA with Bonferroni post test, $p < 0.01$ and $p < 0.05$ respectively, n=4). Slightly higher currents were detected at 1.40 and 1.45 V; however the amount of current was not significantly different than 1.35 V (one-way ANOVA with Bonferroni post test, $p > 0.05$, n=4). B) Three plateau times were tested: 0.5 ms, 1.0 ms, and 1.5 ms for 5 μ M adenosine. The plateau voltage was held constant at 1.35 V. Overall, current was significantly dependent on plateau time (one-way ANOVA, $p < 0.001$). Both 1.0 ms and 1.5 ms plateau times were significantly higher than 0.5 ms (one-way ANOVA with Bonferroni post-test, $p < 0.01$ and $p < 0.001$ respectively, n=4); however, 1.0 ms was not significantly different than 1.5 ms ($p > 0.05$).



Increasing the plateau time increases the current detected for 1 μM adenosine at a 1.35 V plateau potential (Fig. 4.6B, one-way ANOVA main effect of time, $p = 0.0006$, $n=4$). The shortest plateau time (0.5 ms) resulted in the least amount of current detected. Both 1.0 ms and 1.5 ms plateau times were significantly higher than 0.5 ms (one-way ANOVA with Bonferroni post-test, $p<0.01$ and $p<0.001$ respectively); however, 1.0 ms was not significantly different than 1.5 ms ($p>0.05$). The background current was less stable for 1.5 ms so 1.0 ms was chosen as optimal. This plateau time is longer than that optimized for dopamine by Keithley et al.¹³; however, the purpose here was to allow more time for oxidations so a longer hold time was necessary.

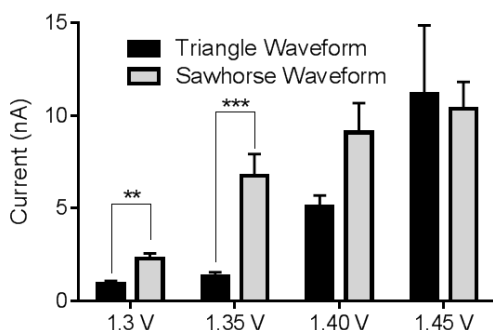


Figure 4.7: Comparison of current at both the triangle and sawhorse waveform at various switching potentials. The plot shows average current for each switching potential tested for both the triangle (black) and sawhorse (grey) waveform for 1 μM adenosine. The sawhorse waveform produced significantly more current for adenosine than the triangle waveform at 1.30 V and 1.35 V switching potential (unpaired t-test $p<0.01$ and $p<0.001$ respectively, $n=6$). The

currents for 1.40 V and 1.45 V were not significantly different between the sawhorse and triangle waveform (unpaired t-test $p>0.05$, $n=6$).

The sawhorse waveform produced significantly more current for adenosine than the triangle waveform at 1.30 V and 1.35 V switching potentials (Fig. 4.7, unpaired t-test $p<0.01$ and $p<0.001$ respectively). With a 1.35 V upper potential, 1.3 ± 0.3 nA/ μM adenosine was detected with the triangle waveform ($n=6$), whereas 6.8 ± 1.1 nA/ μM adenosine was detected with the sawhorse ($n=6$); therefore the sawhorse waveform offers a 5-fold increase in current over the triangle waveform at 1.35 V which is a significant increase (unpaired t-test, $p<0.001$, $n = 6$). The currents for 1.40 V and 1.45 V were not significantly different between the sawhorse and triangle waveform (unpaired t-

test $p > 0.05$). The limit of detection (LOD) for the triangle waveform is 34 ± 10 nM with a switching potential of 1.35 V and is 21 ± 3 nM with 1.45 V,¹⁸ whereas it is 12 ± 4 nM at the sawhorse waveform with a 1.35 V switching potential ($n=6$). The LOD of the sawhorse waveform is significantly different than the triangle waveform with a 1.35 V switching potential (unpaired t-test, $p < 0.05$) but not significantly different than the triangle waveform with a 1.45 V switching potential (unpaired t-test, $p > 0.05$). The sawhorse waveform offers more sensitivity at lower potentials than the triangle waveform.

4.3.3 Analyte differentiation using principal component analysis

Hydrogen peroxide fluctuations *in vivo* have been recorded²⁹ and because their CVs are similar to adenosine, the ability to confidently distinguish between them would be beneficial. Carbon-fiber microelectrodes are more sensitive to adenosine than hydrogen peroxide (6 nA/ μ M and 1.5 nA/ μ M, respectively) but being able to distinguish CVs would increase confidence that hydrogen peroxide interferences could be ruled out during adenosine monitoring *in vivo*. Because the analytes have different shapes for CVs with the sawhorse waveform, principal component analysis (PCA) was used to predict concentrations of analytes in mixtures for both the sawhorse and triangle waveform.

Principal component analysis has been used in the past for discriminating between dopamine and pH changes.^{37,38} PCA was also used to predict dopamine concentrations in the presence of basic pH shifts, ascorbic acid, and dihydroxyphenylacetic acid (DOPAC).³⁷ With PCA, a training set is created spanning the physiologically relevant concentrations of the analytes. For adenosine, ATP, and dopamine the training set was 0.2 μ M, 0.5 μ M, 1 μ M and 5 μ M. The hydrogen peroxide

training set contained 10 μM , 20 μM , 30 μM , and 50 μM to match physiological concentrations and because our electrodes are not as sensitive to hydrogen peroxide. From the training set, eigenvalues are calculated; the largest eigenvalues correspond to the principal components with the highest variance and thus best correlate to the data.³⁹ A residual Q-score from the training set is used to reject data that does not significantly match the principal components. A training set was compiled for each analyte individually with each waveform and then mixtures of analytes were tested and PCA used to predict the concentration of each analyte in the mixture.

Mixtures of adenosine with hydrogen peroxide, ATP, or dopamine were analyzed using both the triangle and sawhorse waveform. Table 4.1 and Table 4.2 show adenosine predictions in the presence of hydrogen peroxide, ATP, or dopamine for the triangle and sawhorse waveform, respectively. The first column of values is from a mixture of 5 μM adenosine and 10 μM hydrogen peroxide. For the triangle waveform, PCA underestimated the adenosine and overestimated the hydrogen peroxide concentration in the mixture (Table 4.1). Table 4.3 gives statistical data using t-tests that show the predicted adenosine and H_2O_2 concentrations are significantly different from the actual values. Small amounts of ATP and dopamine were also predicted, when none were present. In comparison, for the sawhorse waveform, PCA predicted concentrations of adenosine and hydrogen peroxide that were much closer to the actual concentration and negligible amounts of ATP and dopamine were predicted (Table 4.2, column 1, Table 4.3 for statistics). The second column of values represents predicted concentrations from a mixture of 5 μM adenosine and 1 μM ATP. Again, with the triangle waveform, the adenosine concentration was underestimated and the ATP concentration overestimated (Table 4.1). A large portion of the adenosine and ATP mixture was attributed to hydrogen peroxide, which was not present. However, for the sawhorse waveform, the predicted values were closer to the actual values of adenosine and ATP

and very little hydrogen peroxide was predicted (Table 4.2). Lastly, the third column of values in Tables 4.1 and 4.2 represents a mixture of 5 μM adenosine and 1 μM dopamine. As with the other mixtures, the principal component analysis was much better at predicting the concentrations at the sawhorse waveform and did not predict high amounts of hydrogen peroxide or ATP, which were not present.

Table 4.1: Predicted values for triangle waveform

	H₂O₂ (10μM)	ATP (1 μM)	DA (1 μM)
AD (5 μM)	3.2 \pm 0.2	3.7 \pm 0.2	2.8 \pm 0.2
H₂O₂	19.3 \pm 0.7	5.3 \pm 0.3	5.8 \pm 0.2
ATP	0.8 \pm 0.4	1.5 \pm 0.2	1.1 \pm 0.2
DA	1.6 \pm 0.8	0.3 \pm 0.1	1.9 \pm 0.1

Table represents average predicted values of mixtures for the triangle waveform.

Column 1 shows average predictions of the mixture of 5 μM adenosine (AD) and 10 μM hydrogen peroxide (H₂O₂). Column 2 is the mixture of 5 μM adenosine and 1 μM ATP. Column 3 is the mixture of 5 μM adenosine and 1 μM dopamine (DA). Values are mean \pm SEM (n = 4)

Table 4.2: Predicted values for sawhorse waveform

	H₂O₂(10 μM)	ATP (1 μM)	DA (1 μM)
AD (5 μM)	4.4 \pm 0.3	4.5 \pm 0.2	4.9 \pm 0.3
H₂O₂	11 \pm 1.0	0.5 \pm 0.3	0.3 \pm 0.3
ATP	0.6 \pm 0.2	1.2 \pm 0.1	0.3 \pm 0.2
DA	0.00	0.05 \pm 0.03	1.3 \pm 0.3

Table represents average predicted values of mixtures for the sawhorse waveform.

Column 1 shows average predictions of the mixture of 5 μM adenosine (AD) and 10 μM hydrogen peroxide (H₂O₂). Column 2 is the mixture of 5 μM adenosine and 1 μM ATP. Column 3 is the mixture of 5 μM adenosine and 1 μM dopamine (DA). Values are mean \pm SEM (n = 4)

All the values predicted for the triangle waveform (except for the ATP prediction in the adenosine/ATP mixture) were significantly different than the actual concentrations (Table 4.3, unpaired t-test, $p < 0.001$). However, for the sawhorse waveform, predicted values were not significantly different than the actual values (Table 4.3). Thus, the sawhorse waveform in conjunction with principal components analysis is good for discriminating hydrogen peroxide from adenosine and predictions with PCA are more accurate than using the triangle waveform. Adenosine and ATP are the hardest to distinguish with either waveform; however, the sawhorse waveform was able to accurately predict concentrations of ATP and adenosine in a mixture. While pharmacology would also be useful *in vivo* to help discriminate ATP and adenosine, this method is the best electrochemical method currently available for determining both in a mixture.

Table 4.3: Statistics comparing predicted values versus actual values

	AD+H ₂ O ₂ Mixture		AD+ATP Mixture		AD+DA Mixture	
	AD	H ₂ O ₂	AD	ATP	AD	DA
Sawhorse	ns	ns	ns	ns	ns	ns
Triangle	**	**	*	ns	**	**

unpaired t-test n=4 * $p < 0.05$ ** $p < 0.01$

4.3.4 Mechanically stimulated adenosine is predicted as adenosine in brain slices

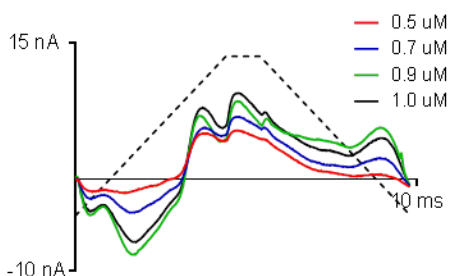
Previously, mechanically stimulated adenosine in the prefrontal cortex was characterized.⁴⁰ Lowering the electrode about 50 μm in the brain slice caused adenosine release that was confirmed to be only adenosine by using pharmacological tests and enzyme sensors specific for adenosine and ATP. Mechanically stimulated adenosine was also detected immediately after lowering a glass pipette of similar size near the

working electrode. Here, we measured mechanically stimulated adenosine in the prefrontal cortex with the sawhorse waveform. An *in slice* training set was generated by exogenously applying adenosine, ATP, and hydrogen peroxide in the slice after mechanical stimulation data had been collected. The analytes were exogenously applied at a range of different amounts to achieve different local concentrations at the electrode, just like *in vitro*, the concentrations at the electrode were calculated based on a pre-calibration factor. Mechanically stimulated adenosine data was analyzed using PCA with the *in slice* training set. The actual mechanically stimulated adenosine concentration was calculated based on a pre-calibration *in vitro* and the predicted concentration was determined using PCA. Figure 4.8A shows an example adenosine training set in slices. Mechanically stimulated adenosine has the same features as the exogenously applied adenosine (Fig. 4.8B). Mechanically-stimulated release does have an extra negative peak at the beginning of the cyclic voltammogram, likely due to an ionic change and this was observed with the triangle waveform in past studies as well.⁴⁰ Figure 4.8C shows the actual concentration of adenosine in comparison to the predicted concentrations of adenosine, hydrogen peroxide, and ATP. Negligible amounts of ATP and hydrogen peroxide were predicted and the signal was predominantly predicted as adenosine. The actual concentration and predicted concentrations of adenosine were not significantly different from one another (unpaired t-test, $p > 0.05$, $n = 8$). This experiment proved that the sawhorse waveform could be used in tissue to predict adenosine concentrations.

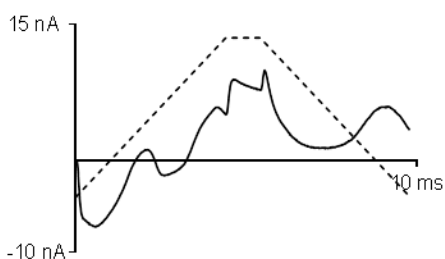
The shape of the adenosine CVs at the sawhorse waveform in slices changed slightly from *in vitro*, likely due to the differences in the tissue environment versus buffer. These differences dictate that an *in situ* training set must be used, as has been used for all previous PCA work. For example, PCA has been used to identify adenosine transients *in vivo*, but the training set was other, large *in vivo* transients detected with the triangle waveform.²⁷ For dopamine, stimulated release was used as the training set to

predict dopamine transients.^{37,41} Here, we use exogenously applied analytes to generate an in slice calibration set and the shapes of the mechanically-stimulated adenosine

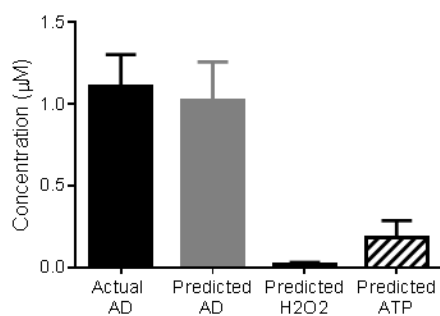
A. Adenosine training set



B. Mechanically stimulated adenosine



C. PCA Predicted values



release match well with the in slice calibration set.

Figure 4.8: Mechanically evoked adenosine using the sawhorse waveform. The medial prefrontal cortex of a rat brain slice was mechanically stimulated by a glass pipette lowered approximately 30 μm away from the carbon-fiber microelectrode. After mechanical stimulation, an in slice training set was collected for adenosine, hydrogen peroxide, and ATP via exogenous application near the electrode. A) An example adenosine training set in a slice. B) An example of a mechanically evoked adenosine CV in a slice. C.) A comparison of the predicted values using PCA for the sawhorse waveform compared to the actual value if the release was all adenosine (black bar). The actual concentration and predicted concentrations of adenosine were not significantly different from one another (unpaired t-test, $p > 0.05$, $n = 8$). Negligible amounts of hydrogen peroxide and ATP were predicted.

4.3.5 Advantages of modified waveforms versus modified electrodes

Electrode modifications with polymers and/or carbon nanotubes have been used extensively in the past to increase sensitivity and specificity but they require extra fabrication time and cost of materials.^{1,18,42,43} Nafion-CNT modified electrodes have enhanced sensitivity and selectivity for adenosine over ATP but the shape of the

voltammograms is not different for ATP and adenosine and the sensitivity for hydrogen peroxide was never characterized.¹⁸ Carbon nanotube yarns have been recently characterized for adenosine and hydrogen peroxide detection. While adenosine also has a secondary peak with those materials, discrimination of the two analytes was not tested.⁴⁴ Enzyme sensors for adenosine or ATP can be used to accurately measure each compound separately, but a single sensor cannot discriminate between mixtures and endogenous H₂O₂ can be an interferent because the enzymes ultimately produce and electrochemically detect H₂O₂.⁴⁵ Overall, the sawhorse waveform provided analyte discrimination of adenosine, ATP and hydrogen peroxide and high sensitivity.

Modified waveforms have been used in the past to increase sensitivity^{46,47} and reduce fouling^{14,48}, but have not been used to increase the analyte currents or aid analyte discrimination. The sawhorse waveform was first implemented to increase electrode stability at high scan rates as holding at the plateau oxidized and renewed the electrode surface.¹³ We used the regular 400 V/s scan rate but focused on maximizing current at the plateau potential. Because of water oxidation, switching potentials over 1.5 V are problematic at carbon-fiber microelectrodes, so the ability to maximize electrochemical signal at lower potentials is useful for analytes with higher potentials. Longer plateau times led to more adenosine oxidation and the shape of the peak was different for an adsorption controlled adenosine than for diffusion controlled hydrogen peroxide. Overall, the sawhorse waveform is useful for studying analytes which oxidize near the switching potential and could be used to further enhance the detection of other neurochemicals *in vivo*.

4.4 Conclusions

In conclusion, a new waveform was developed for adenosine, hydrogen peroxide and ATP detection. The sawhorse waveform allowed a lower switching potential than the traditional triangle waveform to be used and produced lower limits of detection. With the sawhorse waveform, adenosine has a different shape at the plateau potential and extra peaks due to adsorbed products, thus it can be distinguished from dopamine, ATP, and hydrogen peroxide. PCA was used to predict concentrations in mixtures and in slices, confirming that the sawhorse waveform is better for discriminating adenosine in a mixture. Mechanically stimulated adenosine in the prefrontal cortex was accurately predicted as adenosine using the sawhorse waveform in slices. Overall, the sawhorse waveform is highly beneficial for analyte differentiation and could be used in the future *in vivo* to provide better selectivity at lower potentials.

4.5 References

1. Hashemi, P.; Dankoski, E. C.; Petrovic, J.; Keithley, R. B.; Wightman, R. M. *Anal. Chem.* **2009**, *81* (22), 9462-9471.
2. Roberts, J. G.; Lugo-Morales, L. Z.; Loziuk, P. L.; Sombers, L. A. *Methods Mol. Biol.* **2013**, *964*, 275-294.
3. Pajski, M. L.; Venton, B. J. *ACS Chem. Neurosci.* **2010**, *1* (12), 775-787.
4. Venton, B. J.; Troyer, K. P.; Wightman, R. M. *Anal. Chem.* **2002**, *74*, 539-546.
5. Jones, S. R.; Garris, P. A.; Kilts, C. D.; Wightman, R. M. *J. Neurochem.* **1995**, *64* (6), 2581-2589.
6. Bath, B. D.; Michael, D. J.; Trafton, B. J.; Joseph, J. D.; Runnels, P. L.; Wightman, R. M. *Anal. Chem.* **2000**, *72* (24), 5994-6002.
7. Stamford, J. A.; Kruk, Z. L.; Millar, J.; Wightman, R. M. *Neurosci Lett.* **1984**, *51* (1), 133-138.
8. Venton, B. J.; Seipel, A. T.; Phillips, P. E.; Wetsel, W. C.; Gitler, D.; Greengard, P.; Augustine, G. J.; Wightman, R. M. *J. Neurosci.* **2006**, *26* (12), 3206-3209.
9. Venton, B. J.; Wightman, R. M. *Anal. Chem.* **2003**, *75* (19), 414A-421A.
10. Michael, D. J.; Wightman, R. M. *J. Pharm. Biomed. Anal.* **1999**, *19* (1-2), 33-46.
11. Heien, M. L. A. V.; Phillips, P. E. M.; Stuber, G. D.; Seipel, A. T.; Wightman, R. M. *Analyst* **2003**, *128*, 1413-1419.
12. Takmakov, P.; Zachek, M. K.; Keithley, R. B.; Walsh, P. L.; Donley, C.; McCarty, G. S.; Wightman, R. M. *Anal. Chem.* **2010**, *82* (5), 2020-2028.
13. Keithley, R. B.; Takmakov, P.; Bucher, E. S.; Belle, A. M.; Owesson-White, C. A.; Park, J.; Wightman, R. M. *Analytical Chemistry* **2011**, *83* (9), 3563-3571.
14. Cooper, S. E.; Venton, B. J. *Analytical and Bioanalytical Chemistry* **2009**, *394* (1), 329-336.
15. Sanford, A. L.; Morton, S. W.; Whitehouse, K. L.; Oara, H. M.; Lugo-Morales, L. Z.; Roberts, J. G.; Sombers, L. A. *Anal. Chem.* **2010**, *82* (12), 5205-5210.
16. Swamy, B. E. K.; Venton, B. J. *Anal. Chem.* **2007**, *79*, 744-750.
17. Dryhurst, G. *Electrochemistry of biological molecules*; Academic Press: New York, 1977. pp. 71-185.
18. Ross, A. E.; Venton, B. J. *Analyst* **2012**, *137* (13), 3045-3051.

19. Xu, Y. D.; Venton, B. J. *Electroanalysis* **2010**, *22* (11), 1167-1174.
20. Pedata, F.; Pazzagli, M.; Tilli, S.; Pepeu, G. *Naunyn Schmiedebergs Arch. Pharmacol.* **1990**, *342* (4), 447-453.
21. Latini, S.; Pedata, F. *J. Neurochem.* **2001**, *79*, 463-484.
22. Pedata, F.; Melani, A.; Pugliese, A. M.; Coppi, E.; Cipriani, S.; Traini, C. *Purinergic Signalling* **2007**, *3*, 299-310.
23. Pedata, F.; Gianfriddo, M.; Turchi, D.; Melani, A. *Neurol. Res.* **2005**, *27* (2), 169-174.
24. Sweeney, M. I. *Neurosci. Biobehav. Rev.* **1997**, *21* (2), 207-217.
25. van Wylen, D. G.; Park, T. S.; Rubio, R.; Berne, R. M. *J Cereb. Blood Flow Metab* **1986**, *6* (5), 522-528.
26. Wallman-Johansson, A.; Fredholm, B. B. *Life Sci.* **1994**, *55* (9), 721-728.
27. Nguyen, M. D.; Lee, S. T.; Ross, A. E.; Ryals, M.; Choudhry, V. I.; Venton, B. J. *Plos One* **2014**, *9* (1), e87165.
28. Pajski, M. L.; Venton, B. J. *Purinergic Signal.* **2013**, *9* (2), 167-174.
29. Spanos, M.; Gras-Najjar, J.; Letchworth, J. M.; Sanford, A. L.; Toups, J. V.; Sombers, L. A. *ACS Chem. Neurosci.* **2013**, *4* (5), 782-789.
30. Roberts, J. G.; Hamilton, K. L.; Sombers, L. A. *Analyst* **2011**, *136* (17), 3550-3556.
31. Swamy, B. E. K.; Venton, B. J. *Analyst* **2007**, *132*, 876-884.
32. Jolliffe, I. T. *Principal Component Analysis*; Springer-Verlag; New York: 1986.
33. Keithley, R. B.; Heien, M. L.; Wightman, R. M. *Trends Analyt. Chem.* **2009**, *28* (9), 1127-1136.
34. Venton, B. J.; Zhang, H.; Garris, P. A.; Phillips, P. E. M.; Sulzer, D.; Wightman, R. M. *J. Neurochem.* **2003**, *87* (5), 1284-1295.
35. Robinson, D. L.; Venton, B. J.; Heien, M. L. A. V.; Wightman, R. M. *Clinical Chemistry* **2003**, *49* (10), 1763-1773.
36. Owesson-White, C. A.; Roitman, M. F.; Sombers, L. A.; Belle, A. M.; Keithley, R. B.; Peele, J. L.; Carelli, R. M.; Wightman, R. M. *J. Neurochem.* **2012**, *121* (2), 252-262.
37. Heien, M. L.; Johnson, M. A.; Wightman, R. M. *Anal. Chem.* **2004**, *76* (19), 5697-5704.
38. Keithley, R. B.; Wightman, R. M. *ACS Chem. Neurosci.* **2011**, *2* (9), 514-525.

39. Malinowski, E. R. *Analytical Chemistry* **1977**, *49* (4), 606-612.
40. Ross, A. E.; Nguyen, M. D.; Privman, E.; Venton, B. J. *J. Neurochem.* **2014**, *in press*.
41. Keithley, R. B.; Carelli, R. M.; Wightman, R. M. *Anal. Chem.* **2010**, *82* (13), 5541-5551.
42. Jennifer Peairs Ashley E. Ross B. Jill Venton *Analytical Methods* **2011**, *3*, 2379-2386.
43. Xiao, N.; Venton, B. J. *Anal. Chem.* **2012**, *84* (18), 7816-7822.
44. Schmidt, A. C.; Wang, X.; Zhu, Y.; Sombers, L. A. *ACS Nano* **2013**.
45. Llaudet, E.; Botting, N. P.; Crayston, J. A.; Dale, N. *Biosens. bioelectron.* **2003**, *18*, 43-52.
46. Venton, B. J.; Michael, D. J.; Wightman, R. M. *J. Neurochem.* **2003**, *84* (2), 373-381.
47. Hashemi, P.; Dankoski, E. C.; Wood, K. M.; Ambrose, R. E.; Wightman, R. M. *J. Neurochem.* **2011**, *118* (5), 749-759.
48. Jackson, B. P.; Wightman, R. M. *Brain Res.* **1995**, *674* (1), 163-166.

Chapter 5

Mechanical stimulation evokes rapid increases in adenosine concentration in the prefrontal cortex

Challenges are what make life interesting and overcoming them is what makes life meaningful

~Joshua J. Marine

Chapter 5: Mechanical stimulation evokes rapid increases in adenosine concentration in the prefrontal cortex

Abstract

Mechanical perturbations can release ATP, which is broken down to adenosine. In this work, we used carbon-fiber microelectrodes and fast-scan cyclic voltammetry to measure mechanically-stimulated adenosine in the brain by lowering the electrode 50 μm . Mechanical stimulation evoked adenosine *in vivo* (average: $3.3 \pm 0.6 \mu\text{M}$) and in brain slices (average: $0.8 \pm 0.1 \mu\text{M}$) in the prefrontal cortex. The release was transient, lasting 18 ± 2 s. Lowering a 15 μm diameter glass pipette near the carbon-fiber microelectrode produced similar results as lowering the actual microelectrode. However, applying a small puff of artificial cerebral spinal fluid was not sufficient to evoke adenosine. Multiple stimulations within a 50 μm region of a slice did not significantly change over time or damage cells. Chelating calcium with EDTA or blocking sodium channels with tetrodotoxin (TTX) significantly decreased mechanically evoked adenosine, signifying that the release is activity-dependent. An alpha-amino-3-hydroxy-5-methylisoxazole-4-propionate (AMPA) receptor antagonist, 6-cyano-7-nitroquinoxaline-2,3-dione (CNQX), did not affect mechanically-stimulated adenosine; however, the nucleoside triphosphate diphosphohydrolase 1,2 and 3 (NTDPase) inhibitor POM-1 significantly reduced adenosine so a portion of adenosine is dependent on extracellular ATP metabolism. Thus, mechanical perturbations from inserting a probe in the brain cause rapid, transient adenosine signaling which might be neuroprotective. This paper was published in the *Journal of Neurochemistry* (***Journal of Neurochemistry***, 2014, Just Accepted, doi: 10.1111/jnc.12711).

5.1 Introduction

The release of neurotransmitters as a result of a mechanical stimulation, termed mechanosensitive release, has been observed throughout the body¹⁻⁴. Mechanical damage can lead to cell death and be caused by cell stretching¹, swelling⁵, shear stress⁶ or mechanical perturbation⁵. In the brain, mechanosensitive release of neurotransmitters has been observed from both neurons⁵ and astrocytes⁷. Some mechanosensitive release is calcium dependent^{1,7} and a result of exocytosis, such as mechanosensitive glutamate release detected from astrocytes^{7,8}. Other release events are not exocytotic, such as the release of ATP through pannexin channels from neurons after cell swelling⁵. Detection of mechanosensitive release on a rapid time scale has not been explored and would be beneficial in understanding the immediate tissue response to mechanical manipulations.

Mechanosensitive release of ATP has been documented in many parts of the body including the heart⁶, bladder^{4,9} and retinal neuronal cells⁵. Mechanosensitive ATP release is a response to a normal biological function such as inhalation in the lungs³, arterial constriction⁶, or bladder distention⁹. In the brain, mechanosensitive ATP release occurs in response to damage due to swelling, mechanical perturbation, and shear stress^{5,7}. Much of this release is not exocytotic and comes from astrocytes, but some may be calcium dependent and come from neurons^{3,7}. ATP can stimulate P2Y receptors in the extracellular space^{5,10}, but most ATP is quickly broken down to adenosine^{11,12}. Thus, breakdown of ATP is assumed to be the source of most extracellular adenosine during conditions such as brain injury; however, little is known about response to minor tissue injuries such as probe implantation.

Adenosine is an important signaling molecule in the brain which regulates neurotransmission^{13,14} and blood flow^{15,16}. It is also neuroprotective during ischemia

^{13,17,18}, stroke ¹⁹, and traumatic brain injury ^{17,20}. The neuroprotective effects of adenosine are thought to occur primarily through A1 receptors ^{14,21}, which are inhibitory, and increases in adenosine have been detected for minutes to hours after ischemia and brain injury ²². However, direct, calcium-dependent release of adenosine was recently discovered which occurs on the seconds to minute time scale ^{11,23}. There have been reports of rapid adenosine release in response to implantation of electrodes in slices from murine spinal lamina ^{24,25} and deep brain stimulation probes in humans ²⁵, but this release has not been well characterized.

In this study, we characterized the rapid rise in adenosine concentration after mechanical stimulation in the prefrontal cortex of brain slices and *in vivo*. A carbon-fiber microelectrode was lowered to cause mechanical perturbation to the tissue and adenosine measured electrochemically using fast-scan cyclic voltammetry. Mechanical stimulation evoked an increase in adenosine concentration in anesthetized rats and in brain slices. Mechanically evoked adenosine was primarily activity-dependent and partially the result of downstream breakdown of ATP. It was not a downstream effect of glutamate signaling at alpha-amino-3-hydroxy-5-methylisoxazole-4-propionate (AMPA) receptors or released from equilibrative nucleoside transporters (ENTs). Thus, adenosine could provide transient neuromodulation during damage caused by electrode implantation.

5. 2 Methods

5.2.1 Chemicals:

All chemicals were from Fisher Scientific (Fair Lawn, NJ, USA) unless otherwise stated. Adenosine, ATP, and inosine were purchased from Sigma-Aldrich (St. Louis, MO) and dissolved in 0.1 M HClO₄ for 10 mM stock solutions. Stock solutions were diluted daily in

artificial cerebral spinal fluid (aCSF) to calibration concentrations for all brain slice experiments. The aCSF was 126 mM NaCl, 2.5 mM KCl, 1.2 mM NaH_2PO_4 , 2.4 mM CaCl_2 dehydrate, 1.2 mM MgCl_2 hexahydrate, 25 mM NaHCO_3 , 11 mM glucose, and 15 mM tris (hydroxymethyl) aminomethane, pH 7.4 was used in slices and for calibration of electrodes used in slices. Phosphate-buffered saline (PBS) containing 131.25 NaCl mM, 3.0 KCl mM, 10.0 NaH_2PO_4 mM, 1.2 MgCl_2 mM, 2.0 Na_2SO_4 mM, and 1.2 CaCl_2 mM with the pH adjusted to 7.4 was used to calibrate electrodes for *in vivo* experiments. Adenosine was tested at 1.0 μM for brain slice and *in vivo* experiments. For calcium-free experiments, the aCSF solution was made without CaCl_2 and 1 mM ethylenediaminetetraacetic acid (EDTA) was added. Tetrodotoxin (TTX) purchased from Tocris Bioscience (Ellisville, MO), solubilized in 0.2 M citrate buffer (pH 4.8) and frozen as 50 μM aliquots that were diluted to 0.5 μM for experiments. A safety protocol for TTX use was approved by the Office of Environmental Health and Safety at the University of Virginia. The AMPA antagonist, 10 μM 6-cyano-7-nitroquinoxaline-2,3-dione (CNQX), nucleoside triphosphate diphosphohydrolase 1,2 and 3 (NTPDase 1,2 and 3) inhibitor (POM-1), and equilibrative nucleoside transporter inhibitor S-(4-Nitrobenzyl)-6-thioinosine (NBTI) were purchased from Tocris Bioscience (Ellisville, MO).

5.2.2 Electrochemistry:

Carbon-fiber microelectrodes were fabricated from T-650 carbon-fibers as previously described (gift from Cytec Engineering Materials, West Patterson, NJ)²⁶. Cylinder electrodes, 50 μm long and 7 μm in diameter, were used with fast-scan cyclic voltammetry. Fast-scan cyclic voltammograms were collected using a ChemClamp (Dagan, Minneapolis, MN). Data was collected using Tarheel CV software (gift of Mark Wightman, UNC) using a homebuilt data analysis system and two computer interface

boards (National Instruments PCI 6052 and PCI 6711, Austin TX). The electrode was scanned from -0.4 V to 1.45 V (vs Ag/AgCl) and back with a scan rate of 400 V/s and a repetition rate of 10 Hz. Electrodes were equilibrated for 30 min in tissue with the waveform being applied before measurements taken.

5.2.3 Brain slice preparation/experiments:

All animal experiments were approved by the Animal Care and Use Committee of the University of Virginia. Male Sprague-Dawley rats (250-350 g, Charles River, Wilmington, MA) were housed in a vivarium and given food and water *ab libitum*. Rats were anesthetized with isoflurane (1 mL/100 g rat weight) in a desiccator and immediately beheaded. The brain was removed within 2 min and placed in 0-5°C aCSF for 2 min for recovery. Four hundred micrometer slices of the prefrontal cortex were prepared using a vibratome (LeicaVT1000S, Bannockburn, IL), transferred to oxygenated aCSF (95% oxygen, 5% CO₂), and recovered for an hour before the experiment. A pump (Watson-Marlow 205U, Wilmington, MA) was used to flow 35-37°C aCSF over the brain slice at 2 mL/min for all experiments. The electrodes were inserted 75 µm into the tissue. After equilibration, 60 sec of baseline data was collected and the brain slice was mechanically stimulated by lowering the electrode 50 µm with a micromanipulator. See supplementary methods for staining procedure, pharmacology experimental details and picospritzing experiment.

5.2.4 Pharmacology experimental details in slices:

For pharmacology experiments, a pre-drug mechanical stimulation was performed as described, the slice was then perfused with either 1 mM EDTA , 0.5 µM TTX, 10 µM CNQX, 100 µM POM-1, or 10 µM NBTI in aCSF for 30 minutes. The mechanical

stimulation was then repeated. The effect of some of these drugs on electrode sensitivity has previously been reported; EDTA decreased sensitivity for adenosine by 3%, NBTI decreased sensitivity by 68%, and TTX had no effect¹¹. CNQX reduced sensitivity by 40%, NBTI reduced carbon-fiber microelectrode sensitivity by 68%, and POM-1 decreased sensitivity by 30% (data not shown). All bar graphs represent data corrected for drug-induced sensitivity loss.

5.2.5 Picospritzing method:

Pressure ejection of aCSF onto brain slices was tested using a Parker Hannifin picospritzer (Picospritzer III, Cleveland, OH). A pulled glass pipette was filled with aCSF and placed 30 μm from the carbon-fiber microelectrode. The ejection parameters were 10 psi for 100 milliseconds and 100-200 nL of aCSF was delivered.

5.2.6 Staining Experiment.

Slices were obtained and a CFME was inserted in the medial region of the prefrontal cortex (following coordinates from bregma: AP: 4.20 mm, ML: 0.4 to 0.8 mm, and DV: -3.4 to -4.0mm). After equilibration, the electrode was lowered 50 μm into the tissue, raised back up, and lowered again. Once all of the slices were treated in this manner, the slices were washed once with aCSF, then stained at 4 degrees Celsius with LIVE/DEAD fixable aqua dead cell stain kit (Life Technologies Invitrogen, Grand Island NY) (2 μL /mL for 30 minutes) for cells with compromised cell membranes (necrosis) and DAPI (Sigma Aldrich, St. Louis MO) (0.5 μL /mL for 15 minutes) for nuclear staining. The slices were washed twice with cold aCSF and then fixed with 4% paraformaldehyde (Sigma Aldrich, St. Louis MO) in PBS for 15 minutes. The slices were washed twice with aCSF, and then mounted into the imaging chamber of a Zeiss 780 NLO multiphoton imaging system (Thornwood, NY). Z stacks were acquired up to 100 μm into the tissue

at the area of electrode insertion according to the coordinates. An additional Z stack was obtained at a control region in which no electrode had been inserted. Cell death was calculated by dividing the number of cells with compromised cell membranes (bright LIVE/DEAD staining) by the total number of cells (DAPI staining) using ImageJ64.

5.2.7 Enzyme biosensors:

Enzymatic biosensors for adenosine (SBS-ADO-20-50), ATP (SBS-ATP-20-50) and inosine (SBS-INO-20-50) were purchased from Sarissa Biomedical Ltd (Coventry, UK) and were prepared and conditioned as recommended by the manufacturer. These sensors have been previously characterized^{27,28}. Inosine sensors lack adenosine deaminase which is crucial for adenosine detection and were therefore used as a null sensor in a separate set of experiments. Enzyme sensor data was collected using an Axon Axopatch 200B (Molecular Devices, Sunnyvale, CA) and data was collected and analyzed from a homebuilt data analysis system written for amperometry. The sensors were held at 500 mV and the collection frequency was 60 Hz for all measurements. Biosensors were calibrated based on guidelines by Sarissa prior to and after use in brain slices. Adenosine biosensors had a decrease in sensitivity of 57 ± 7 % (n=11) after implantation in brain slices, whereas carbon-fiber microelectrodes had a decrease of 40 ± 7 % (n=5) in sensitivity. On days where ATP sensors were used, 2mM glycerol was added to the aCSF as recommended by the manufacturer. Biosensors were tested for cross-sensitivity with other analytes and the results were found to be negligible. Electrodes were lowered in buffer to verify that movement did not elicit a significant current. Adenosine, ATP, and inosine enzyme sensors were calibrated at 1.0, 5.0, and 10 μ M before and after slice experiments. For slice experiments, gravity flow was used due to noise from the pump and the experiments were performed in exactly the same manner for adenosine, ATP, and inosine biosensors as the carbon-fiber microelectrodes.

5.2.8 In vivo experiments:

Male Sprague-Dawley rats (250-350 g, Charles River, Willmington, MA) were anesthetized with 50% wt urethane in saline solution (1.5 g/kg, i.p). Bupivacaine (0.25 mL, s.c., APP Pharmaceuticals, LLC; Schaumburg, IL, USA) was administered for local analgesia. The rat's temperature was maintained at 37°C using a heating pad with a thermistor probe (FHC, Bowdoin, ME, USA). The working electrode was implanted in the prefrontal cortex: coordinates in mm from bregma: anterior-posterior (AP): +2.7, mediolateral (ML): +0.8, and dorsoventral (DV): -3.0²⁹. A Ag/AgCl reference electrode was inserted on the contralateral side of the brain. The electrode was lowered 100 µm to stimulate mechanosensitive release every 30 minutes for 2 hours.

5.2.9 Statistics:

All values are reported as the mean ± standard error of the mean (SEM). Paired t-test were performed to compare data before and after drugs in the same slices. All statistics were performed in GraphPad Prism (GraphPad Software, Inc., La Jolla, CA) and considered significant at the 95% confidence level (p<0.05). A one-way ANOVA with Bonferroni post tests was performed to compare consecutive mechanical stimulations *in vivo and* across stimulations for both CFME and glass pipettes. A two-way ANOVA was used to compare the two stimulation techniques.

5.3 Results

5.3.1 Mechanically-stimulated adenosine in brain slices and in vivo:

Fast-scan cyclic voltammetry was used to electrochemically detect adenosine in brain slices. A large background current is obtained because of the fast scan rate, but it is removed with background subtraction³⁰. However, basal levels cannot be measured

and the technique instead measures fast changes in concentration. The mechanical stimulation in this study was lowering the carbon-fiber microelectrode 50 μm in the prefrontal cortex of a brain slice. Electrically-stimulated adenosine release has been found to be ATP dependent in the prefrontal cortex³¹, and thus this region has the capability for evoked adenosine release. Adenosine was observed immediately following carbon-fiber microelectrode movement 100% of the time (n=25 slices, 39 mechanical stimulations).

Fig. 5.1A shows a color plot of adenosine release after mechanical stimulation (red arrow) in a brain slice. Applied voltage is on the y-axis, time is on the x-axis, and the green and purple colors represent oxidative current, which is proportional to concentration. Before the electrode was lowered, a background signal was obtained, denoted by the tan color representing no current change. The primary oxidation peak for adenosine occurs immediately after the mechanical stimulation at approximately 1.4 V and the secondary peak occurs at 1.1 V (denoted by the black arrows in Fig. 5.1A and B). The peak positions and shape of the cyclic voltammogram (CV) are characteristic of two, two-electron oxidations for adenosine^{32,33}. The third peak observed at 0.1 V could be the third oxidation peak for adenosine, but that peak is not often observed at our carbon-fiber microelectrodes³². That peak and the blue (negative) currents on the bottom of the color plot are likely due to other chemical and ionic changes that occur with mechanical stimulation. The current after adenosine is released often goes below baseline due to ionic changes³¹. A current vs. time trace at the main oxidation potential for adenosine shows a rapid increase in current immediately following the mechanical stimulation of the electrode. In Fig. 5.1A, the signal lasts about 10 seconds and the peak current corresponds to 0.77 μM adenosine.

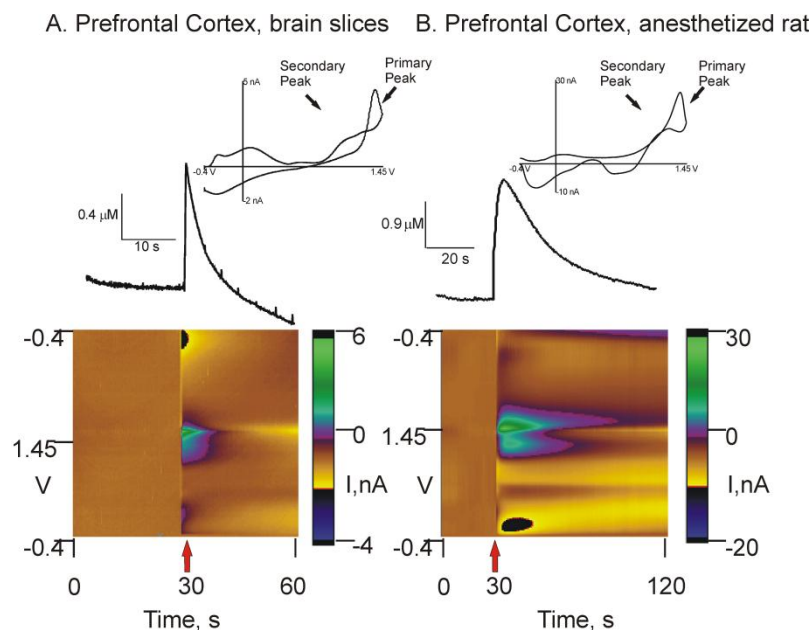
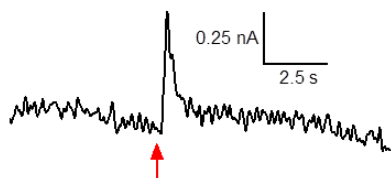


Figure 5.1: Adenosine after mechanical stimulation. The stimulation was quickly lowering a carbon-fiber microelectrode 50 μm in a prefrontal cortex slice (Panel A) or 100 μm in the prefrontal cortex of an anesthetized rat (Panel B) (red arrow denotes when electrode was lowered). A color plot with voltage on the y-axis, time on the x-axis and current in false color is shown. Adenosine occurs immediately after mechanical stimulation and is the green/purple region in the middle of the plot. Plots of the change in concentration for adenosine over time, located above the color plots, show that the adenosine signal lasted approximately 10 seconds with a peak concentration of 0.77 μM for slices (A) and lasted 80 s with a maximal concentration of 2.4 μM *in vivo* (B). The cyclic voltammograms have the typical primary and secondary adenosine oxidation peaks which confirm adenosine was detected.

Mechanosensitive release has most often been attributed to ATP, which can then break down to form adenosine^{3,4}. ATP and adenosine have similar cyclic voltammograms because the adenine group is electroactive in both; however, sensitivity for ATP at carbon-fiber microelectrodes is 3-6 fold less than for adenosine³⁴. To confirm our sensors were measuring adenosine, mechanically-evoked release was measured with selective biosensors for adenosine, ATP, and inosine biosensors in brain slices²⁷. Inosine sensors lack adenosine deaminase, the first enzyme in the cascade that breaks adenosine down to inosine²⁷, and are used as a null sensor to ensure other compounds are not causing a false signal at the adenosine biosensor. While the sensitivity for the

biosensors (adenosine sensitivity: $0.8 \text{ nA}/\mu\text{M}$, ATP: $0.25 \text{ nA}/\mu\text{M}$, inosine: $0.7 \text{ nA}/\mu\text{M}$) was not as good as with the carbon-fiber microelectrodes on our system, adenosine release was observed 50% of the time with mechanical stimulation ($n = 5$ slices, 10 mechanical stimulations, Figure 5.2 and Table 5.1). However, no changes were observed at ATP or inosine biosensors. Thus, the signal detected at carbon-fiber microelectrodes is likely to be adenosine. These data did not rule out ATP metabolism as a source of adenosine because ATP can breakdown to adenosine within 200 ms ³⁵ and the response time of the ATP biosensors are on the magnitude of seconds³⁶. Thus, if ATP is rapidly metabolized to adenosine, then the biosensor is unlikely to detect much ATP.

A. Adenosine Sensor



B. ATP Sensor



C. Inosine Sensor

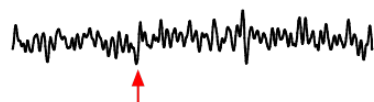


Figure 5.2: Enzyme biosensor measurements of mechanosensitive release. A.) Adenosine, B.) ATP, and C.) inosine enzyme biosensors were lowered $50 \mu\text{m}$ in prefrontal cortex slices. The arrow marks when the electrode was lowered. A. With the adenosine sensor, an increase in current was observed that lasts 6 seconds and corresponds to a peak concentration of $0.5 \mu\text{M}$. B.) With the ATP sensor or C.) with the inosine sensor there was no increase in current for any slices tested ($n=5$ slices, 10 total mechanical stimulations). The inosine sensor served as a null sensor to ensure other compounds were not causing a false signal at the biosensor. The scale bar is the same for all panels.

Table 5.1: Mechanically evoked adenosine

	Concentration (μM)	Concentration Range (μM)	Duration	Duration Range	Percentage of slices detected
CFME <i>in vivo</i> n=5	3.3 ± 0.6	0.3-10	42 ± 5 s	11-110 s	100 %
CFME in slices n=25	0.8 ± 0.1	0.1-3.3	18 ± 2 s	2-46 s	100 %
Adenosine Sensor in slices n=5	0.6 ± 0.03	0.4-0.8	10 ± 2 s	1.8-20 s	50 %

*All values are \pm SEM

Mechanically-evoked adenosine was also observed *in vivo* in the prefrontal cortex of anesthetized rats. Fig. 5.1B shows an example of mechanically-evoked adenosine *in vivo* after the electrode is lowered 100 μm . The peak current corresponds to 2.4 μM adenosine and the duration is approximately 80 s. Average results for carbon-fiber microelectrodes in slices and *in vivo* are summarized in Table 5.1. The concentration and duration of adenosine release is on average much larger *in vivo* compared to brain slices.

Fig. 5.3A shows an example current versus time trace of consecutive mechanical stimulations every 30 minutes *in vivo*. The traces are similar, although there is variation that could be due to different areas of tissue being stimulated. The normalized current versus time trace in the inset shows that the temporal profile of adenosine is relatively stable. Fig. 5.3B shows the average concentration for each successive mechanical stimulation as well as the average for all stimulations (blue bar). There was no significant effect of stimulation number on the concentration of adenosine evoked ($n = 5$ rats, $p = 0.6781$, repeated measures one way ANOVA) or duration (Fig. 5.3C, $n = 5$ rats, $p = 0.6224$, repeated measures one way ANOVA). Thus, the concentration and duration of adenosine signaling is constant for multiple mechanical stimulations.

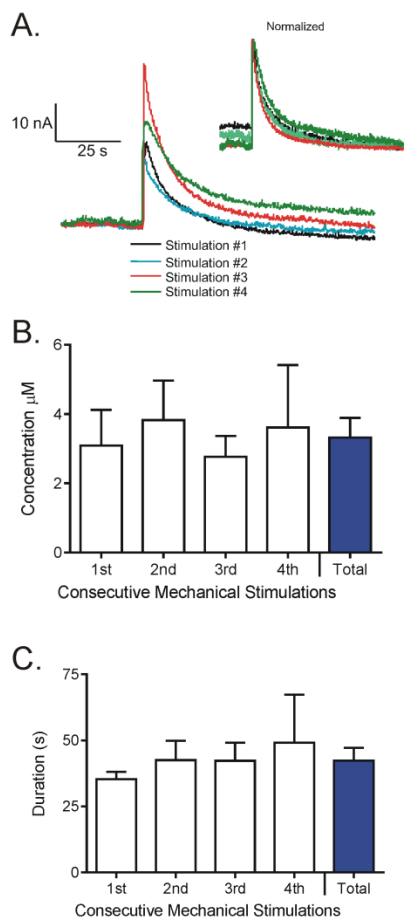


Figure 5.3: Four consecutive stimulations in vivo. In the prefrontal cortex of an anesthetized rat, 4 consecutive mechanical stimulations were performed every 30 minutes for 2 hours. A) Example current versus time traces are shown for four consecutive mechanical stimulations. There is no pattern of release decreasing over time. A) normalized current versus time plot in the inset demonstrates that the temporal profile of the release is not changing. B) Average concentration of adenosine for each stimulation was not significantly different ($n = 5$ rats, $p = 0.6781$, repeated measures one way ANOVA). The last (solid) bar shows the average for all 4 stimulations. C) The duration of adenosine signaling was also not significantly affected by the number of the stimulation ($n = 5$ rats, $p = 0.6224$, repeated measures one way ANOVA). The last (solid) bar is the average for all 4 stimulations.

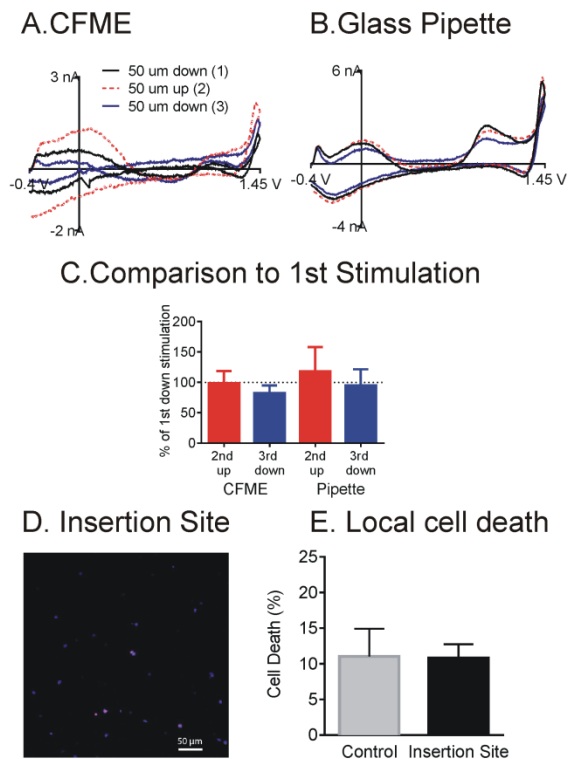
5.3.2 Evaluation of other methods for mechanical stimulation:

Next, we examined the extent to which other mechanical stimulations evoked adenosine. An empty, pulled glass pipette approximately $15 \mu\text{m}$ in diameter was lowered $50 \mu\text{m}$ into the slice near the electrode. A similar increase in adenosine was detected at the carbon-fiber microelectrode when either the carbon-fiber microelectrode itself or a pipette near it was moved (Fig. 5.4A and 5.4B). Repeated mechanical stimulations were also tested. The electrode or glass pipette was lowered $50 \mu\text{m}$, moved back up $50 \mu\text{m}$, and finally lowered again $50 \mu\text{m}$, with 10 min intervals between stimulations for recovery. Figure 5.4A and 5.4B show cyclic voltammograms for both the carbon-fiber microelectrode and glass pipette stimulations, respectively. The cyclic voltammograms for adenosine were similar for all stimulations, which were performed in

the same area of tissue. The magnitude of adenosine measured by repeated stimulations within each technique was not statistically different (repeated measures one-way ANOVA, $F=0.3522$, $p=0.7882$, $n=5$). Carbon-fiber microelectrodes and glass pipettes were also compared and there was no main effect of stimulation technique (repeated measures two-way ANOVA, $F(1,7)=0.2229$, $p=0.6512$) or stimulation number ($F(1,7)=5.046$, $p=0.0595$), and no interaction ($F(1,7)=0.1402$, $p=0.7192$). Thus, mechanically-evoked adenosine can occur by both physically lowering the working electrode or by moving something comparable in size nearby.

Local tissue damage associated with multiple electrode stimulations was characterized by staining for dead cells and was analyzed using multiphoton microscopy. A LIVE/DEAD stain was used to analyze cells with compromised cell membranes (necrosis) and a counter-stain, 4',6-diamidino-2-phenylindole (DAPI), stained for all nuclei. The first 50 μm of the slice tissue was found to be highly damaged, which is expected in slice experiments. A multiphoton Z-stack through the initial dead segment and into the underlying healthy tissue at the point of electrode insertion did not reveal a clear path for electrode insertion. There was no noticeable hole in the tissue and no track of cell death (Fig.5.4D and 5.4E), indicating that the electrode did not disrupt the cell membranes of the cells as it moved up and down through the tissue. Figure 5.4D shows all nuclei stained with DAPI colored blue and dead cells colored red. The percentage of dead cells was counted and compared in the region of electrode implantation and a control region (Fig. 5.4E) and there was no significant difference between these two regions (paired t-test, $p=0.9096$, $n=4$). This is consistent with previous work indicating that FSCV probe insertion does not significantly damage the tissue^{37,38}.

Figure 5.4: Adenosine is mechanically evoked either by both lowering the working electrode or a glass pipette close to the working electrode. Multiple electrode stimulations did not cause significant cell death. Adenosine can be mechanically stimulated by A) moving the carbon-fiber microelectrode and B) moving a 15 μm -diameter glass pipette. Repeated stimulations were tested by moving the carbon-fiber microelectrode (A) or the glass pipette (B) 50 μm down into the tissue, 50 μm back up, and 50 μm back down. Ten minutes of recovery time was given between each move. C) The bar graph compares the second (up) and third (down) stimulation for both techniques. Data is graphed as a percentage of first stimulation and there are no significant differences between the two techniques (repeated measures two-way ANOVA, $F(1,7)=0.2229$, $p=0.6512$) or stimulation number ($F(1,7)=5.046$, $p=0.0595$) and no interaction ($F(1,7)=0.1402$, $p=0.7192$). Repeated adenosine measurements within each technique are not statistically different (repeated measures one-way ANOVA, $F=0.3522$, $p=0.7882$, $n=5$). D) Cell imaging of the insertion site where there was multiple electrode stimulations reveals no obvious significant cell death. Blue represents DAPI staining, showing all nuclei. Red represents dead cells stained with a LIVE/DEAD cell assay and scale bar represents 50 μm . E) There was no significant difference in dead cell percentage between a control region (no electrode insertion) and the electrode insertion site (paired t-test, $p=0.9061$, $n=4$).



Mechanical stimulation of adenosine was not observed by pressure ejecting aCSF into the slice close to the electrode. A glass pipette was implanted, the tissue allowed to recover, and then a picospritzer was used to deliver 100-200 nL volumes of aCSF to the brain slice tissue 30 μm away from the carbon-fiber microelectrode. Low pressures were used to avoid significant tissue damage and the parameters chosen are similar to those used for pressure ejection studies of transport in the literature³⁹. Figure 5.5A shows the concentration over time profile for a mechanical stimulation by lowering the electrode and by pressure ejecting aCSF in the same slice. An increase in adenosine concentration occurred immediately following the electrode lowering;

however, no adenosine changes were observed with aCSF injection. A slight decrease in current was observed followed by a slow return to baseline after aCSF puffing, likely due to a disturbance of the background current by the fluid movement. The cyclic voltammograms (Fig. 5.5B) confirm no adenosine was detected for aCSF application and adenosine was not observed after aCSF application in any slice (n=3).

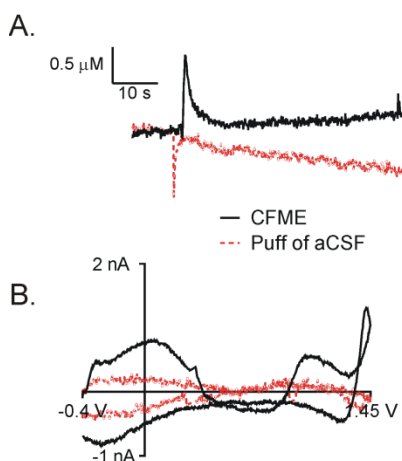


Figure 5.5: Adenosine is not mechanically evoked by small amounts of pressure ejected aCSF. Mechanically evoked adenosine by carbon-fiber microelectrode insertion was compared to pressure ejecting 100-200 nL volumes of aCSF 30 μm from the electrode in the same slice. A) Concentration versus time profile shows an increase in current when the carbon-fiber microelectrode was lowered and only a shift in current was detected after puffing on aCSF. B) Cyclic voltammograms show an adenosine CV for mechanical stimulation with the electrode by no identifiable adenosine with pressure ejection of aCSF.

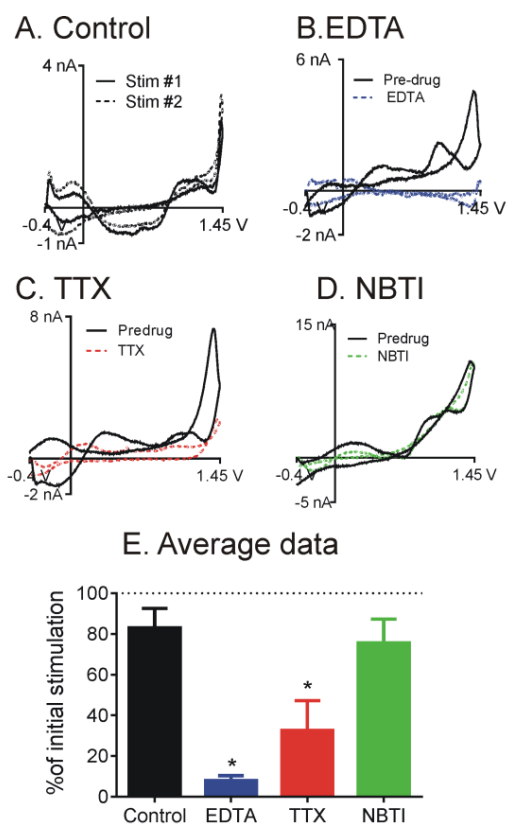
5.3.3 Mechanism of mechanically-evoked adenosine:

Electrically-stimulated adenosine release is activity-dependent in brain slices^{11,40}.

Thus, we tested whether mechanically-evoked adenosine is activity-dependent by bathing the brain slices in calcium-free aCSF with 1 mM EDTA for 30 minutes. To prevent action potentials, 0.5 μM TTX was applied for 30 minutes in separate experiments. In each of these experiments, a baseline of mechanically evoked adenosine was collected, then drug was applied and 30 min later, the electrode was lowered a second time (see Fig. 5.7 for all concentration versus time plots). Control data show that mechanical stimulations 30 minutes apart have the same signal when drugs are not applied (Fig. 5.6A and 5E, n = 5, p = 0.1507, paired t-test). Fig. 5.6B and 5.6C show adenosine cyclic voltammograms from mechanical stimulation before and after perfusion with EDTA and TTX, respectively. EDTA significantly reduced the amount of

adenosine released by 93% (Fig. 5.6E, $n = 6$, $p = 0.0482$, paired t-test) whereas TTX significantly reduced the signal by 61% (Fig. 5.6E, $n = 3$, $p = 0.0337$, paired t-test).

These reductions in adenosine release demonstrate mechanically evoked adenosine is mostly calcium dependent and activity dependent.



electrode sensitivity after NBTI. E.) The bar graph shows average mechanically-evoked release after drug as a % of the initial stimulation. Thus, no change would be 100%. Statistics were performed using paired t-tests comparing the release for pre- and post-drug stimulation. EDTA ($n = 6$, $p = 0.0482$) and TTX ($n = 3$, $p = 0.0337$) significantly decreased mechanically-stimulated adenosine release while there was no effect of NBTI ($n = 5$, $p = 0.1507$).

Figure 5.6: Mechanically evoked adenosine is activity dependent but is not released by equilibrative nucleoside transporters. A predrug mechanical stimulation was performed using a carbon-fiber microelectrode and then slices were perfused with drug and a second mechanical stimulation was performed 30 min later. Release was compared pre and post drug in the same animals using paired t tests. A) Control data. Cyclic voltammograms for mechanically-evoked adenosine are similar for two consecutive mechanical stimulations when the slice was perfused with aCSF. B) Cyclic voltammograms of adenosine show a large decrease in current after perfusion with 1 mM EDTA. C) Cyclic voltammograms of adenosine show a large reduction in mechanically-stimulated adenosine after perfusion with 0.5 μ M TTX. D) There was no change in the adenosine cyclic voltammograms after 10 μ M NBTI, an nucleoside transport inhibitor. The data were corrected for a 68% decrease in

Figure 5.6D shows that blocking equilibrative nucleoside transporters with 10 μ M NBTI did not significantly change the amount of adenosine released compared to the predrug signal (Fig. 5.6E, $n=9$, $p=0.1675$, paired t-test). However, perfusion with NBTI did increase duration of signal (see Figure 5.8) so transport into the cell was blocked.

Activity dependent adenosine release was not facilitated through equilibrative nucleoside transporters.

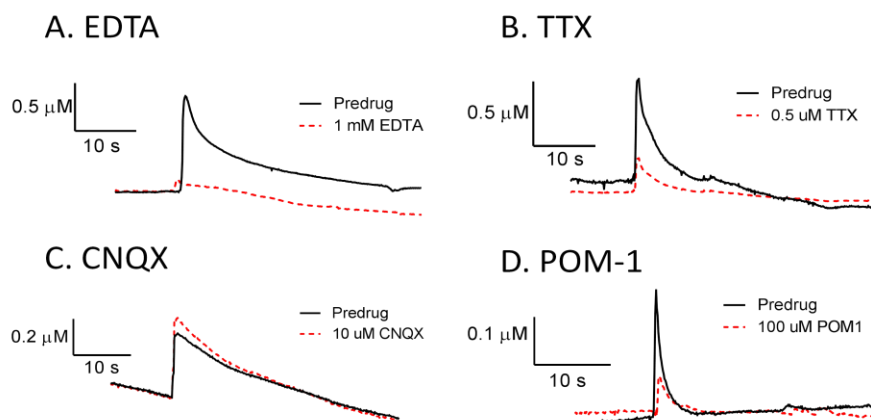


Figure 5.7: Concentration versus time profiles for EDTA, TTX, CNQX, and POM-1. Each graph shows concentration over time before and after 30 minute drug perfusion. A) Concentration goes close to baseline after 1 mM EDTA perfusion and is significantly less at B) 0.5 μM TTX and D) POM-1. C) CNQX does not significantly change the concentration of adenosine detected.

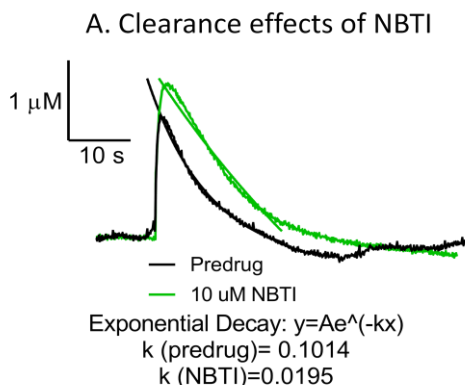


Figure 5.8: Current versus time plots comparing clearance kinetics before and after the transport inhibitor, NBTI, perfusion. Black trace represents the pre-drug current versus time profile for a mechanical stimulation in the prefrontal cortex. The green trace represents the current over time profile for a mechanical stimulation after 30 minutes of 10 μM NBTI perfusion. From the equation, the rate constant of the decay, k , was extracted. The rate constant for the pre-drug trace was much larger than the NBTI trace indicating a much faster decay rate. Comparison of all decay rates before and after NBTI showed a significant decrease in uptake rate ($n=9$, paired t -test, $p=0.0323$).

Next, the dependence of mechanically-evoked adenosine on glutamate or ATP was tested. Activity dependent adenosine release has been proposed to be AMPA

receptor dependent in the cerebellum ⁴¹ and glutamate has been shown to be mechanically released from astrocytes ⁸. To test for AMPA receptor dependence, the antagonist CNQX was used. Fig. 5.9A shows a cyclic voltammogram of mechanically evoked adenosine before and after perfusion with 10 μ M CNQX. Mechanically evoked adenosine after CNQX increased by 20%, but it was not significantly different from the predrug stimulation (Fig. 5.9C, n = 5, p=0.2935). To test for dependence on ATP release, a recombinant NTPDase 1, 2 and 3 inhibitor, POM-1, was used ⁴². Fig. 5.9B shows mechanically evoked adenosine decreased after 100 μ M of POM-1 was perfused and on average significantly reduced mechanically evoked adenosine by 62% (Fig. 5.9C, n = 6, p=0.0098). POM-1 did not completely block all of the adenosine detected so other mechanisms of adenosine accumulation could also contribute to the signal. Less sensitive ATP metabolism inhibitors, ARL 67156 and AOPCP ⁴², were also used but they did not significantly reduce the amount of adenosine detected (data not shown). Overall, our data show mechanically evoked adenosine is not caused by glutamate acting at AMPA receptors but a portion is due to extracellular ATP breakdown.

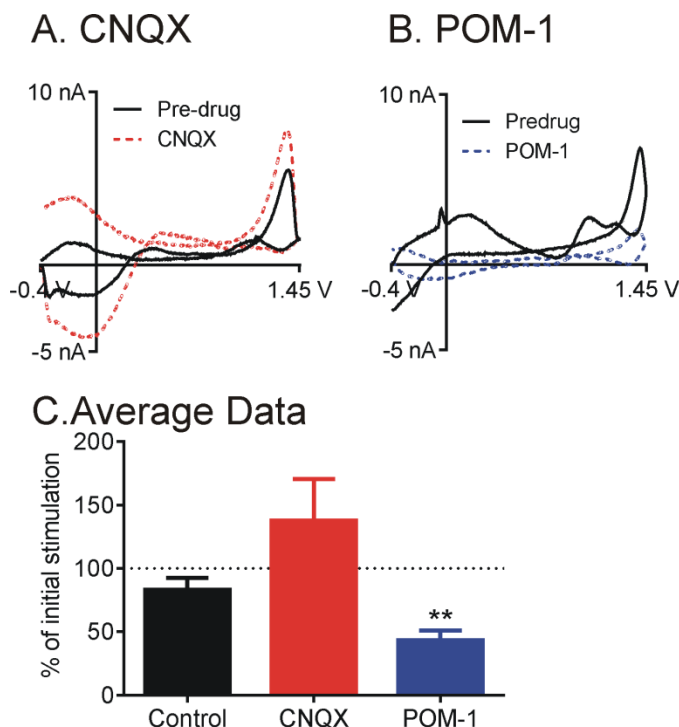


Figure 5.9: Mechanically evoked adenosine is not dependent on AMPA receptors but is a downstream effect of ATP metabolism. A predrug mechanical stimulation was performed using a carbon-fiber microelectrode and then slices were perfused with drug and a second mechanical stimulation was performed 30 min later. Release was compared pre and post drug in the same animals using paired t tests. A) Cyclic voltammograms of adenosine show no change in current after 10 μM CNQX, an AMPA antagonist. The data were correct for a 40 % decrease in electrode sensitivity after

CNQX. B) Cyclic voltammograms (corrected for 30 % decrease in sensitivity) show that perfusion with 100 μM POM-1 does change mechanically-stimulated adenosine. C.) Bar graph shows the average data as a % of the initial, pre-drug stimulation. The statistics are paired t-tests that compare the pre-drug and post-drug mechanically evoked adenosine in the same slice. There is a significant effect of POM-1 ($n=6$, $p = 0.0098$) but no significant effect of CNQX ($n = 5$, $p = 0.2935$).

5.4 Discussion

Mechanosensitive release of purines due to physical perturbation of cells has been mostly attributed to ATP release, which slowly builds up over time²⁻⁴. In this study, we demonstrate that in the prefrontal cortex, mechanical stimulation elicits a rapid, transient release of ATP which is immediately metabolized to adenosine. In brain slices, peak adenosine release was on average $0.8 \pm 0.1 \mu\text{M}$ and lasted 18 ± 2 s. Mechanically-evoked adenosine was activity-dependent but was not dependent on equilibrative nucleoside transporters or a downstream effect of AMPA receptors. Pharmacologically blocking ATP metabolism demonstrated that mechanically evoked adenosine was largely a downstream effect of ATP release. This implies a large releasable pool of ATP

that breaks down quickly to adenosine. These studies provide new insight that ATP is released and rapidly metabolized to adenosine in the extracellular after electrode implantation and that adenosine could act as a signaling molecule during tissue damage.

5.4.1 Mechanically evoked adenosine occurs via different methods:

In this experiment, we primarily mechanically stimulated the tissue by lowering the working electrode 50-100 μm in tissue. This method of stimulation would be relevant to any type of probe implantation, for example electrochemical, electrophysiological, or deep brain stimulation (DBS) probes. Because lowering the carbon-fiber microelectrode could change the background current, the response was compared to lowering a glass pipette of similar size near the stationary microelectrode. The evoked adenosine was similar for both techniques and thus the signal is not an artifact of moving the electrode. However, simply puffing on small amounts of aCSF, close to the electrode did not evoke any adenosine response. The aCSF puff might slightly move cells, but did not cause sufficient damage to elicit adenosine release.

Traditional mechanical perturbation techniques, including cell swelling⁵, cell stretching³, and shear stress^{2,4}, are modeled after normal biological functions. Our study does not directly mimic one of these processes, but an interesting phenomenon was observed in the experiments where the electrode or glass pipette was lowered and raised multiple times. The adenosine increase after pulling the pipette up was slightly larger than for lowering it down. While this phenomenon would need to be characterized much further, it suggests some cell stretching may be a cause of adenosine increase when raising the electrode. These experiments also show that the tissue is not dying, as the same response can be measured repeatedly, and staining reveals no significant increase in local cell death after multiple electrode stimulations. Thus, the electrode insertion is not causing a significant amount of permanent tissue damage, in line with

previous reports of minimal tissue damage associated with carbon-fiber microelectrode insertion *in vivo*^{37,38}.

An adenosine response to probe implantation has been suggested in the past but never fully characterized. Tawfik et al. discovered that adenosine was elevated immediately after electrode implantation, preceding the microthalamotomy effect in the ferret thalamus⁴³. The microthalamotomy effect is observed in essential tremor and Parkinson's disease patients and refers to the immediate relief from tremors following electrode implantation during DBS procedures²⁵. Chang et al. implanted a DBS probe into 7 human patients and also saw the microthalamotomy effect along with release of adenosine in all patients²⁵. Future studies could probe whether adenosine is a cause or effect of the microthalamotomy effect during implantation in DBS. Elevated levels of adenosine were also discovered during and after acupuncture in the tibialis anterior muscle close to the knee⁴⁴. While this study was outside the central nervous system and used bigger needles, adenosine was detected and quantified on the 10-30 min. time scale using microdialysis coupled to HPLC. Thus, other forms of probe implantation cause increases in adenosine, which may be similar or complementary to the transient adenosine release observed in this study.

5.4.2 Mechanical stimulation evokes large, transient adenosine changes:

Mechanically-stimulated adenosine varied widely in both slices and *in vivo*. The concentration of adenosine detected in slices ranged from 0.1 μM to 3.3 μM and *in vivo* from 0.3 to 10 μM . Larger amounts of adenosine were released *in vivo* but the stimulation was 100 μm compared to 50 μm in slices, which would result in more cells being stimulated. The activity dependent nature of release suggests that intact circuits *in vivo* may also facilitate larger amounts of release. The large range is not surprising because the density of adenosine releasing cells around the electrode could vary based

on electrode location. Also, speed of insertion was not tightly controlled which could cause varying tissue responses. The average amount of adenosine released by mechanical stimulation was higher than previously detected with electrical stimulation¹¹; thus, tissue perturbation causes higher amounts of release than electrical stimulation.

The duration of adenosine release varied from 2 s to 110 s in brain slices and *in vivo*. The duration was correlated with the concentration, as larger amounts of adenosine lasted longer because more time was needed to clear the adenosine from the extracellular space. Mechanically-evoked adenosine signaling is fast compared to other studies that measure mechanically-evoked ATP release³. Mechanosensitive ATP release is usually detected using luciferin-luciferase assay techniques², which allow measurements to be taken only every 30 s. The duration of the adenosine response is similar to electrically evoked adenosine signaling that has been shown in multiple brain regions^{11,31,41}. Mechanical evoked release is easier than electrical stimulation and could be used to study the function of transient adenosine signaling, including any neuroprotective effects.

5.4.3 Mechanism and function of mechanically evoked adenosine release:

Mechanically evoked adenosine in the prefrontal cortex is primarily activity dependent. Chelating calcium with EDTA or preventing action potentials with TTX blocked most of the adenosine detected. Activity-dependent adenosine release was completely blocked by TTX in other regions^{23,45} while mechanically-stimulated release in the prefrontal cortex was reduced by 65%; therefore, there may be a portion that is not activity dependent. Calcium chelators were more effective in blocking release, reducing it by over 90%, indicating most of the release is calcium dependent. Adenosine can also be released via equilibrative nucleoside transporters (ENTs)^{45,46}; however, inhibiting equilibrative nucleoside transporters with NBTI did not significantly change

mechanically-evoked adenosine, ruling this mechanism out. Activity-dependent release of ATP, which breaks down to adenosine, was also explored. Blocking ATP metabolism with POM-1 significantly reduced the amount of adenosine detected. However, as with TTX, POM-1 did not completely block all adenosine; so while ATP metabolism contributes to the signal, some adenosine may be formed by another mechanism. Stimulated adenosine release can also be a downstream action of glutamate acting at ionotropic receptors^{11,41,47}. Blocking AMPA receptors with CNQX had no effect on mechanically-stimulated adenosine release, so this release was not AMPA receptor dependent. Future studies could examine the effect of other glutamate receptors such as NMDA receptors, which could also regulate adenosine release⁴⁵, as well as other neurotransmitters to examine if adenosine is a downstream effect of other receptor activation. Our studies show that mechanically-evoked adenosine release in the prefrontal cortex is primarily activity-dependent and mostly due to downstream breakdown ATP. This is in contrast to measurements of slower adenosine build up during seizures that suggest that release from ENTs is the primary mechanism and not breakdown of ATP⁴⁶. Thus, the mechanism of transient release may be different than other forms of adenosine signaling.

This work demonstrates that a local mechanical stimulation causes an elevation of adenosine concentration for less than a minute; thus transiently activating adenosine receptors. The function of rapid adenosine signaling after probe implantation remains unknown; however, adenosine signaling resulting from various forms of damage has been well documented in the literature⁴⁸⁻⁵⁰. In particular, activation of A₁ receptors is inhibitory, which could dampen neurotransmission that causes excitotoxicity in the brain⁵¹. Adenosine could also stimulate blood flow after probe implantation, which would deliver nutrients for tissue repair. The immediate nature of the response allows for rapid activation of the pathway, but the fast duration would not allow long-term depression of

neuronal activity. Further investigations of downstream effects of rapid adenosine signaling after mechanical stimulation as well as interactions of adenosine with other signaling molecules that are released would be interesting to better understand the function of adenosine as a rapid modulator in the brain.

5.5 Conclusion

Mechanically evoked adenosine was observed immediately following mechanical stimulations in the prefrontal cortex in both brain slices and *in vivo*. Adenosine could be evoked by moving the microelectrode or a glass pipette implanted near the microelectrode and stimulations could be repeated, indicating the tissue was not dying. Pharmacological studies confirm most of the adenosine detected is an extracellular breakdown product of ATP. Mechanically evoked adenosine was calcium dependent and activity-dependent but was not dependent on AMPA receptors. The study shows that implantation of a probe into brain tissue causes a transient adenosine response which could be neuroprotective.

5.6 References

1. Stalmans, P.; Himpens, B. *Invest. Ophthalmol. Vis. Sci.* **1997**, *38* (1), 176-187.
2. Woo, K.; Dutta, A. K.; Patel, V.; Kresge, C.; Feranchak, A. P. *J. Physiol* **2008**, *586* (11), 2779-2798.
3. Ramsingh, R.; Grygorczyk, A.; Solecki, A.; Cherkaoui, L. S.; Berthiaume, Y.; Grygorczyk, R. *Am. J. Physiol. Lung Cell Mol. Physiol.* **2011**, *300* (4), L587-L595.
4. Olsen, S. M.; Stover, J. D.; Nagatomi, J. *Ann. Biomed. Eng.* **2011**, *39* (2), 688-697.
5. Xia, J. S.; Lim, J. C.; Lu, W. N.; Beckel, J. M.; Macarak, E. J.; Laties, A. M.; Mitchell, C. H. *J. Physiol* **2012**, *590* (10), 2285-2304.
6. Wan, J. D.; Ristenpart, W. D.; Stone, H. A. *Proceedings of the National Academy of Sciences of the United States of America* **2008**, *105* (43), 16432-16437.
7. Newman, E. A. *J. Neurosci.* **2001**, *21* (7), 2215-2223.
8. Montana, V.; Ni, Y.; Sunjara, V.; Hua, X.; Parpura, V. *J. Neurosci.* **2004**, *24* (11), 2633-2642.
9. Ferguson, D. R.; Kennedy, I.; Burton, T. J. *J. Physiol.* **1997**, *505* (2), 503-511.
10. Pankratov, Y.; Lalo, U.; Verkhratsky, A.; North, R. A. *Pflugers Arch.* **2006**, *452* (5), 589-597.
11. Pajski, M. L.; Venton, B. J. *ACS Chem. Neurosci.* **2010**, *1* (12), 775-787.
12. Latini, S.; Pedata, F. *J. Neurochem.* **2001**, *79*, 463-484.
13. Rudolphi, K. A.; Schubert, P.; Parkinson, F. E.; Fredholm, B. B. *Cerebrovasc. Brain Metab Rev.* **1992**, *4* (4), 346-369.
14. Okada, M.; Mizuno, K.; Kaneko, S. *Neurosci Lett.* **1996**, *212*, 53-56.
15. Sciotti, V. M.; Vanwylen, D. G. L. *J. Cereb. Blood Flow Metab* **1993**, *13* (2), 201-207.
16. O'Regan, M. *Neurol. Res.* **2005**, *27* (2), 175-181.
17. Fredholm, B. B. *Int. Rev. Neurobiol.* **1997**, *40*, 259-280.
18. Parkinson, F. E.; Rudolphi, K. A.; Fredholm, B. B. *Gen. Pharmacol.* **1994**, *25* (6), 1053-1058.

19. Von Lubitz, D. K.; Simpson, K. L.; Lin, R. C. *Ann. N. Y. Acad. Sci.* **2001**, 939, 85-96.
20. Lin, Y.; Phillis, J. W. *Brain Res.* **1992**, 571 (2), 272-280.
21. Cechova, S.; Elsobky, A. M.; Venton, B. J. *Neuroscience* **2010**, 171 (4), 1006-1015.
22. Quarta, D.; Borycz, J.; Solinas, M.; Patkar, K.; Hockemeyer, J.; Ciruela, F.; Lluís, C.; Franco, R.; Woods, A. S.; Goldberg, S. R.; Ferre, S. *J. Neurochem.* **2004**, 91 (4), 873-880.
23. Wall, M. J.; Dale, N. *J. Physiol* **2007**, 581 (2), 553-565.
24. Street, S. E.; Walsh, P. L.; Sowa, N. A.; Taylor-Blake, B.; Guillot, T. S.; Vihko, P.; Wightman, R. M.; Zylka, M. J. *Mol. Pain* **2011**, 7.
25. Chang, S. Y.; Kim, I.; Marsh, M. P.; Jang, D. P.; Hwang, S. C.; Van Gompel, J. J.; Goerss, S. J.; Kimble, C. J.; Bennet, K. E.; Garris, P. A.; Blaha, C. D.; Lee, K. H. *Mayo Clinic Proceedings* **2012**, 87 (8), 760-765.
26. Swamy, B. E. K.; Venton, B. J. *Analyst* **2007**, 132, 876-884.
27. Llaudet, E.; Botting, N. P.; Crayston, J. A.; Dale, N. *Biosens. bioelectron.* **2003**, 18, 43-52.
28. Frenguelli, B. G.; Llaudet, E.; Dale, N. *J. Neurochem.* **2003**, 86 (6), 1506-1515.
29. Paxinos, G.; Watson, C. *The Rat Brain in Stereotaxic Coordinates*; 6 ed.; Academic Press: 2007.
30. Millar, J.; Stamford, J. A.; Kruk, Z. L.; Wightman, R. M. *Eur. J. Pharmacol.* **1985**, 109 (3), 341-348.
31. Pajski, M. L.; Venton, B. J. *Purinergic Signal.* **2013**, 9 (2), 167-174.
32. Swamy, B. E. K.; Venton, B. J. *Anal. Chem.* **2007**, 79, 744-750.
33. Dryhurst, G. *Electrochemistry of biological molecules*; Academic Press: New York, 1977. pp. 71-185.
34. Ross, A. E.; Venton, B. J. *Analyst* **2012**, 137 (13), 3045-3051.
35. Dunwiddie, T. V.; Diao, L. H.; Proctor, W. R. *J. Neurosci.* **1997**, 17 (20), 7673-7682.
36. Llaudet, E.; Hatz, S.; Droniou, M.; Dale, N. *Anal. Chem.* **2005**, 77 (10), 3267-3273.
37. Peters, J. L.; Miner, L. H.; Michael, A. C.; Sesack, S. R. *J. Neurosci Methods* **2004**, 137, 9-23.

38. Jaquins-Gerstl, A.; Michael, A. C. *J. Neurosci. Methods* **2009**, *183* (2), 127-135.
39. Zahniser, N. R.; Larson, G. A.; Gerhardt, G. A. *J. Pharmacol. Exp. Ther.* **1999**, *289* (1), 266-277.
40. Klyuch, B. P.; Dale, N.; Wall, M. J. *J. Neurosci.* **2012**, *32* (11), 3842-3847.
41. Klyuch, B. P.; Richardson, M. J. E.; Dale, N.; Wall, M. J. *J. Physiol.* **2011**, *589* (2), 283-295.
42. Wall, M. J.; Wigmore, G.; Lopatar, J.; Frenguelli, B. G.; Dale, N. *Neuropharmacology* **2008**, *55* (7), 1251-1258.
43. Tawfik, V. L.; Chang, S. Y.; Hitti, F. L.; Roberts, D. W.; Leiter, J. C.; Jovanovic, S.; Lee, K. H. *Neurosurgery* **2010**, *67* (2), 367-375.
44. Goldman, N.; Chen, M.; Fujita, T.; Xu, Q.; Peng, W.; Liu, W.; Jensen, T. K.; Pei, Y.; Wang, F.; Han, X.; Chen, J. F.; Schnermann, J.; Takano, T.; Bekar, L.; Tieu, K.; Nedergaard, M. *Nat. Neurosci.* **2010**, *13* (7), 883-888.
45. Wall, M. J.; Dale, N. *J. Physiol.* **2013**, *591* (Pt 16), 3853-3871.
46. Lovatt, D.; Xu, Q.; Liu, W.; Takano, T.; Smith, N. A.; Schnermann, J.; Tieu, K.; Nedergaard, M. *Proc. Natl. Acad. Sci. U. S A* **2012**, *109* (16), 6265-6270.
47. Wall, M.; Dale, N. *Curr. Neuropharmacol.* **2008**, *6* (4), 329-337.
48. Frenguelli, B. G.; Wigmore, G.; Llaudet, E.; Dale, N. *J. Neurochem.* **2007**, *101* (5), 1400-1413.
49. Shen, H. Y.; Lusardi, T. A.; Williams-Karnesky, R. L.; Lan, J. Q.; Poulsen, D. J.; Boison, D. *J. Cereb. Blood Flow Metab.* **2011**, *31* (7), 1648-1659.
50. Haselkorn, M. L.; Shellington, D.; Jackson, E.; Vagni, V.; Feldman, K.; Dubey, R.; Gillespie, D.; Bell, M.; Clark, R.; Jenkins, L.; Schnermann, J.; Homanics, G.; Kochanek, P. *J. Neurotrauma* **2008**, *25* (7), 901.
51. Sperlagh, B.; Zsilla, G.; Baranyi, M.; Illes, P.; Vizi, E. S. *Neuroscience* **2007**, *149* (1), 99-111.

Chapter 6

Adenosine transiently modulates stimulated dopamine release in the caudate putamen via A1 receptors

A person who never made a mistake never tried anything new

~Albert Einstein

Chapter 6: Adenosine transiently modulates stimulated dopamine release in the caudate putamen via A₁ receptors

Abstract

Adenosine is an important neuromodulator and neuroprotector in the brain. Adenosine has been shown to modulate neurotransmitter release such as dopamine in the brain via A₁ and A_{2A} receptors, but that modulation has only been characterized on a slow time scale. Recent evidence points to a rapid signaling mode of adenosine, lasting only seconds, that suggests it may have a rapid modulatory role as well. Here, fast-scan cyclic voltammetry was used to characterize the extent to which transient adenosine changes modulate stimulated dopamine release (5 pulses at 60 Hz) in rat brain slices of the caudate putamen. Exogenous adenosine was applied for 50-100 ms (2.5-5.0 pmol) and the effect of the time interval between adenosine application and dopamine stimulation tested by monitoring the stimulated dopamine concentration. Adenosine only modulated dopamine when it was applied 2 or 5 s before stimulation. Longer time intervals and bath application of adenosine did not decrease dopamine release. Mechanical stimulation of endogenous adenosine release also decreased stimulated dopamine release by $37 \pm 3 \%$, compared to $54 \pm 6 \%$ for the exogenous application and dopamine inhibition was fully recovered within 10 minutes. The A₁ receptor antagonist, DPCPX, blocked the modulation of dopamine release; whereas dopamine modulation was unaffected by the A_{2A} receptor antagonist, SCH 442416. Thus, transient adenosine changes can transiently modulate phasic dopamine release via A₁ receptors. These data demonstrate that adenosine can have a rapid but transient modulatory role in the brain.

6.1 Introduction

Adenosine is a neuromodulator which has been shown to modulate two very important processes in the brain: cell metabolism^{1,2} and neurotransmission³⁻⁶. Adenosine modulation has been well characterized in the literature⁷; however, rapid changes in adenosine were more recently discovered and the function of rapid release is still relatively unknown. Electrochemical techniques such as amperometric biosensors and fast-scan cyclic voltammetry (FSCV) have shown that adenosine can be released and cleared on fast time scales, from a few seconds to a minute⁸⁻¹⁰. Traditionally, these methods relied on either electrical stimulation or chemical stimulation of adenosine to evoke a rapid response; however, Street et al. discovered rapid adenosine transients in spinal cord slices using FSCV, which did not require a stimulus¹¹. Nguyen et al. detected spontaneous transient adenosine release both in the prefrontal cortex and in the caudate putamen of an anesthetized rat and found that spontaneous adenosine events occur every 2-3 minutes on average¹². Adenosine release lasted just a few seconds and this proves that there is a rapid mode of signaling for adenosine in multiple brain regions. However, the mechanism of how transient changes in adenosine modulate neurotransmitter release was not explored.

Slower time resolution measurements of adenosine have revealed that it can modulate many neurotransmitters^{13,14}. Microdialysis coupled to HPLC has provided information on adenosine modulation of basal levels of dopamine, serotonin, glutamate, and GABA^{3-6,15}. With this technique, adenosine was shown to modulate neurotransmission, and the mechanisms were primarily regulated by the A₁ and A_{2A} receptors. A₁ is the most abundant receptor in the brain and inhibits neurotransmission by blocking adenylyl cyclase activity and A_{2A} is the second most abundant adenosine receptor in the brain and has an excitatory effect, activating adenylyl cyclase activity⁷.

Specifically, adenosine has been shown to modulate basal dopamine levels in the caudate putamen⁶ and the nucleus accumbens⁵ by the A₁ and A_{2A} receptors; however, changes in basal levels were not recorded until greater than 20 minutes. Interactions between the A₁ and A_{2A} receptor have been shown to regulate dopamine release and these interactions are dependent on glutamate NMDA receptor activation in the nucleus accumbens⁵. In other studies, the inhibitory effects of the A₁ receptor was shown to overpower the excitatory effects of A_{2A} receptor activation, and consequently A_{2A} receptor drug effects were masked in the presence of activated A₁ receptors⁶; however, the measurements were taken at 20 minute intervals. Rapid modulation of dopamine by adenosine, on the second time scale, has not been investigated.

In this study, we use FSCV to measure adenosine modulation of dopamine release in the caudate putamen. Adenosine was exogenously applied to slices of the caudate putamen to mimic adenosine transients and the effect of these transients on stimulated dopamine release measured. Adenosine temporarily inhibits dopamine release by about 50 % if it is applied 2-5 s before the stimulation. Perfusing the slice with 5 μM adenosine for 30 minutes did not affect stimulated dopamine release, which suggests that transient changes in adenosine were responsible for the rapid dopamine modulation. Mechanically evoked adenosine also transiently inhibited dopamine release. Blocking the A₁ receptors by 8-Cyclopentyl-1,3-dipropylxanthine (DPCPX) blocked the modulatory effects of transient adenosine, resulting in no change in stimulated dopamine release; however, blocking A_{2A} receptors with SCH 442416 had no effect. Thus, transient changes in adenosine causes temporary inhibition of dopamine release in the caudate putamen via A₁ receptors, proving that adenosine can modulate on a rapid time scale.

6.2 Methods

6.2.1 Chemicals

All chemicals were from Fisher Scientific (Fair Lawn, NJ, USA) unless otherwise stated. Adenosine and dopamine were purchased from Sigma-Aldrich (St. Louis, MO) and dissolved in 0.1 M HClO₄ for 10 mM stock solutions. Stock solutions were diluted daily in artificial cerebral spinal fluid (aCSF) to 1 μM for electrode calibrations for brain slice experiments. The aCSF consisted of 126 mM NaCl, 2.5 mM KCl, 1.2 mM NaH₂PO₄, 2.4 mM CaCl₂ dehydrate, 1.2 mM MgCl₂ hexahydrate, 25 mM NaHCO₃, 11 mM glucose, and 15 mM tris (hydroxymethyl) aminomethane and was adjusted to pH 7.4. 8-Cyclopentyl-1,3-dipropylxanthine (DPCPX) (Sigma Aldrich) and SCH 442416 (Tocris Biosciences, Ellisville, MO) stock solutions were made in dimethylsulfoxide (DMSO) and diluted in aCSF on the day of the experiment.

6.2.2 Electrochemistry

Cylinder microelectrodes were made from carbon-fibers as previously described (gift from Cytec Engineering Materials, West Patterson, NJ)¹⁶ and were 50 μm long and 7 μm in diameter. Fast-scan cyclic voltammetry (FSCV) was used with carbon-fiber microelectrodes. Cyclic voltammograms (CVs) were collected using a ChemClamp (Dagan, Minneapolis, MN). Data was collected using Tarheel CV software (gift of Mark Wightman, UNC) using a homebuilt data analysis system and two computer interface boards (National Instruments PCI 6052 and PCI 6711, Austin TX). The electrode was scanned from -0.4 V to 1.45 V (vs Ag/AgCl) and back with a scan rate of 400 V/s and a repetition rate of 10 Hz. Electrodes were equilibrated for 30 min in tissue with the waveform being applied before measurements taken.

6.2.3 Brain slice experiments

All animal experiments were approved by the Animal Care and Use Committee of the University of Virginia. Male Sprague-Dawley rats (250-350 g, Charles River, Wilmington, MA) were housed in a vivarium and given food and water *ab libitum*. Rats were anesthetized with isoflurane (1 mL/100 g rat weight) in a desiccator and beheaded immediately. The brain was removed within 2 min and placed in 0-5°C aCSF for 2 min for recovery. Four hundred micrometer slices of the caudate putamen were prepared using a vibratome (LeicaVT1000S, Bannockburn, IL), transferred to oxygenated aCSF (95% oxygen, 5% CO₂), and recovered for an hour before the experiment. aCSF (maintained at 35-37°C) was flown over the brain slices using a pump (Watson-Marlow 205U, Wilmington, MA) at a rate of 2 mL/min for all experiments. The carbon-fiber electrode was inserted 75 µm into the tissue. Dopamine was stimulated using a biphasic stimulating electrode, with wires spaced 800 µm apart and placed 300 µm from the working electrode (PlasticsOne, Inc., Roanoke, VA). Two stimulations of dopamine, spaced 10 minutes apart, were performed prior to exogenous or endogenous adenosine application to ensure signal stability. Pulse trains of 5 biphasic pulses, each 200 µA and 4 ms long (2 ms per phase), were applied at a frequency of 60 Hz using a stimulus isolator (Dagan). For exogenous application of adenosine experiments, 25 µM adenosine was pressure ejected onto brain slices either 2, 5, 10, 30, or 60 s prior to dopamine stimulation using a Parker Hannifin picospritzer (Picospritzer III, Cleveland, OH). Each pressure ejection time before dopamine stimulation was completed in a separate set of slices. The picospritzing pipette was placed 20-30 µm from the working electrode. Low pressures and short puff-times were used to minimize tissue damage from the pressure application. The ejection parameters were 10 psi for 50-100 milliseconds and 100-200 nL of 25 µM adenosine was delivered (2.5-5.0 pmol). High

concentrations of adenosine are needed with exogenous application in order to detect any at the carbon-fiber microelectrode due to diffusion and rapid uptake. For mechanical stimulation of adenosine in slices, an empty pulled glass pipette was inserted into the slice 20-30 μm from the working electrode, and lowered 50 μm with a micromanipulator 2 s prior to dopamine stimulation.

6.2.4 Pharmacology experiments

For pharmacology experiments, two pre-drug dopamine stimulations were collected, followed by perfusion of either 200 nM 8-Cyclopentyl-1,3-dipropylxanthine, DPCPX, (Sigma Aldrich, St. Louis MO) or 1 μM SCH 442416 (Tocris Biosciences, Ellisville MO) for 30 minutes. Dopamine was stimulated to measure if the drugs affected stimulated dopamine release. Next, adenosine was exogenously applied 2 s prior to the next dopamine stimulation (10 minutes later) in the presence of the drug. As a control, dopamine stimulation were repeated without drug to make sure dopamine is stable over the length of the experiment.

6.2.5 Statistics

All values are reported as the mean \pm standard error of the mean (SEM). Paired t-test were performed to compare the initial dopamine stimulation to the dopamine stimulation immediately after exogenous adenosine application or after mechanical adenosine stimulation, compare initial dopamine stimulation versus the last stimulation within each set of control experiments, and to compare initial dopamine stimulation to the dopamine stimulation immediately after exogenous adenosine application in the presence of either DPCPX or SCH 442416. All statistics were performed in GraphPad Prism V6 (GraphPad Software, Inc., La Jolla, CA) and considered significant at the 95% confidence level ($p < 0.05$).

6.3 Results

Adenosine is an important neuromodulator in the brain and can be released and cleared on a rapid time scale^{7,9,17}. FSCV is a technique which allows for electrochemical monitoring of electroactive species on the millisecond timescale^{18,19}. Both adenosine and dopamine are electroactive and can be co-detected with FSCV (see figure 6.1 for an example color plot and cyclic voltammograms)^{20,21}. Adenosine has a set of two electron oxidations¹⁶ at carbon-fiber microelectrodes (primary at 1.40 V and secondary at 1.0 V) while dopamine has one oxidation peak at 0.6 V and a reduction peak at -0.2 V²². Adenosine requires a higher switching potential than dopamine, so to detect both dopamine and adenosine, a waveform which scans from -0.4 to 1.45 V is needed²¹. The waveform is applied at 400 V/s with a repetition rate of 10 Hz.

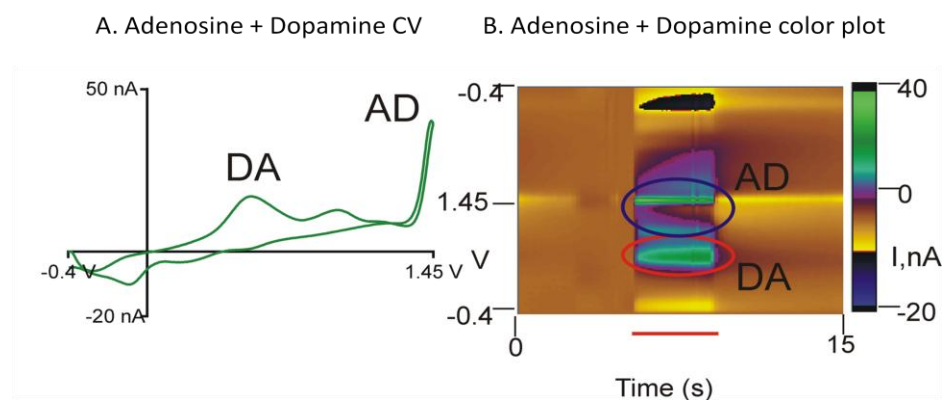


Figure 6.1: Adenosine and dopamine can be co-detected using FSCV. A) Cyclic voltammogram for both 5 μM adenosine and 1 μM dopamine in flow cell. The primary oxidation peaks for adenosine and dopamine are clearly separated. B) The color plot shows both adenosine and oxidation oxidation in false color (green), time on x-axis, and waveform application on the y-axis. Adenosine oxidation is circled in blue and labeled AD, and dopamine oxidation is circled and red and labeled (DA).

To study dopamine modulation, exogenous adenosine transients were applied to the slice at specified intervals before dopamine release was stimulated in the caudate putamen. Figure 6.2 shows a schematic of the experiment. Example of a 3-dimensional color plot shows the waveform voltage on the y-axis, time on the x-axis, and current in

false color. The green-blue color represents oxidative current. Here, adenosine was exogenously applied 5 seconds prior to dopamine stimulation (60 Hz, 5 pulses, 4 ms width). Associated cyclic voltammograms are shown for both of the analytes. Exogenous adenosine application was within the concentration and duration range of spontaneous adenosine events detected *in vivo* (1.2 μM adenosine lasting approximately 3 s). On average, the concentration of adenosine detected at the electrode was $1.0 \pm 0.1 \mu\text{M}$ and lasted $4.6 \pm 0.3 \text{ s}$ ($n = 19$), which are within range of larger spontaneous adenosine events *in vivo*¹².

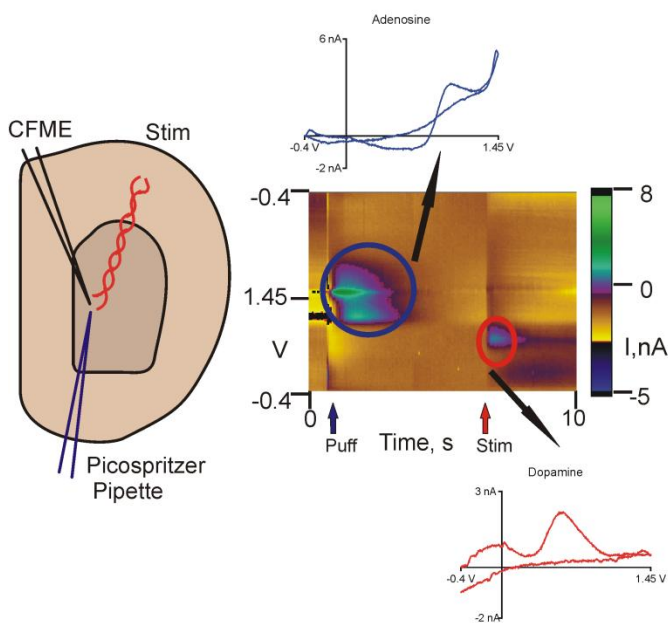


Figure 6.2: Schematic for exogenous application of adenosine in brain slices. A) A bipolar stimulating electrode, carbon-fiber microelectrode (CFME), and picospritzer pipette are all placed in a slice of the caudate putamen. The CFME and stimulating electrode form a shallow triangle and the picospritzer pipette is placed 20–30 μm away from the CFME. To study neuromodulation, 25 μM adenosine is exogenously applied with a picospritzer (10 psi, 50–100 ms, 100–200 nL) prior to dopamine stimulation (60 Hz, 5 pulses, 4 ms pulse width). B) A color plot shows voltage on y-axis, time on x-axis, and current in false color. A blue arrow indicates puff time and the red arrow indicates time of stimulation. Here, adenosine was puffed on 5 s prior to dopamine stimulation. Adenosine has two oxidative peaks (primary 1.4 V and secondary at 1.0 V) and dopamine oxidizes at 0.6 V. Adenosine CV is shown above (blue trace) and the dopamine CV is shown below (red trace). The transient lasted only a few seconds and the local concentration at the electrode was 1.2 μM .

axis, time on x-axis, and current in false color. A blue arrow indicates puff time and the red arrow indicates time of stimulation. Here, adenosine was puffed on 5 s prior to dopamine stimulation. Adenosine has two oxidative peaks (primary 1.4 V and secondary at 1.0 V) and dopamine oxidizes at 0.6 V. Adenosine CV is shown above (blue trace) and the dopamine CV is shown below (red trace). The transient lasted only a few seconds and the local concentration at the electrode was 1.2 μM .

6.3.1 Exogenously-applied, transient adenosine modulates dopamine on a rapid time scale

Rapid changes in extracellular levels of adenosine transiently modulate dopamine release in the caudate putamen. The time interval between exogenous application of adenosine and dopamine stimulation was varied. Figure 6.3 shows an example dopamine CV before and after adenosine application and the average dopamine after exogenous, transient adenosine application. In all experiments, dopamine stimulations were performed twice, 10 minutes apart, before adenosine application to ensure the dopamine signal was stable. Dopamine after adenosine application is normalized to the pre-adenosine stimulation in order to account for variation between stimulated release in different animals. The black line in Figure 6.3A shows an example initial stimulated dopamine signal. The red trace shows 10 min later, when adenosine was applied 2 s before dopamine release was stimulated and the dotted black trace shows stimulated release 10 min after that, where dopamine has fully recovered. Overall, dopamine inhibition was significantly dependent on time of adenosine administration (one-way ANOVA, $p = 0.0060$). Dopamine release was inhibited on average $54 \pm 6\%$ when adenosine was applied 2 s prior (paired t-test between initial dopamine signal and after adenosine, $p = 0.006$, $n = 14$) and $35 \pm 6\%$ when adenosine is applied 5 s prior (paired t-test, $p = 0.0129$, $n = 5$). When adenosine was applied 10 s, 30 s, or 60 s before the stimulation, dopamine was not significantly reduced (paired t-test between the initial dopamine and after the adenosine application, $p > 0.05$ in all cases, $n = 4$). Two controls were performed to ensure that the adenosine was causing the inhibitory response. The black bar in Figure 6.3B represents a stimulation control in which dopamine was stimulated every 10 minutes for 40 minutes and no adenosine was applied. On average, there was no significant decrease in

dopamine for the last stimulation compared to the initial dopamine stimulation (paired t-test, $p > 0.05$, $n = 6$). The gray bar in Figure 6.3B represents the average change in dopamine stimulation after puffing on aCSF 2 s prior to dopamine stimulation. There was no significant decrease in dopamine release from the aCSF puff, indicating it was not simply due to tissue disturbance (paired t-test, $p > 0.05$, $n = 4$).

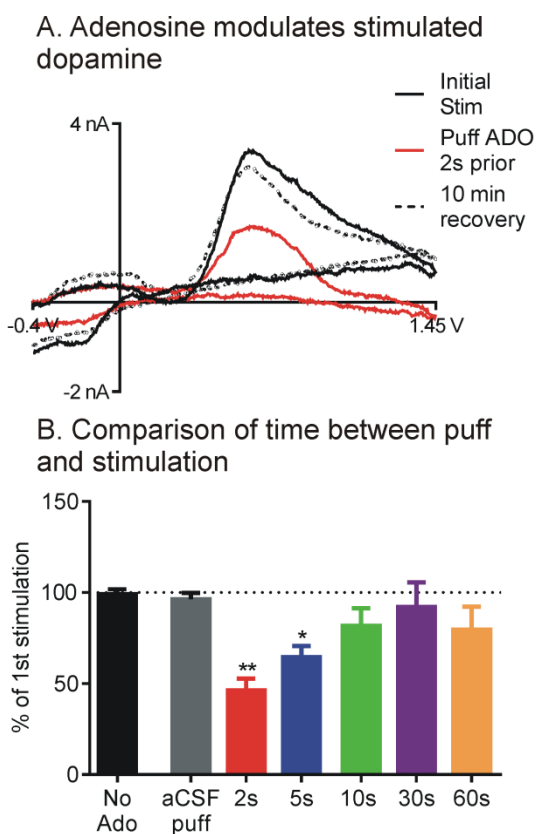


Figure 6.3: Time between exogenous application and dopamine stimulation optimization. A) Example of the optimized procedure, the black trace indicates the initial dopamine stimulation, red trace is the dopamine 2 s after adenosine application, and the dotted trace shows dopamine on the subsequent stimulation (10 minutes later). Dopamine decreases by about 50 %. B) Comparison of puff-times on amount of dopamine inhibition. Overall, dopamine inhibition was significantly dependent on time of adenosine administration (one-way ANOVA, $p = 0.0060$). The y-axis is the percent of initial stimulation and the x-axis shows the time at which adenosine was administered prior to stimulating dopamine. Exogenous application of adenosine at 2 s (red bar) and 5 s (blue bar) significantly decreased dopamine to 46 ± 6 % (paired t test, $p = 0.006$, $n = 14$) and 65 ± 6 % (paired t test, $p = 0.0129$, $n = 5$) of initial stimulation

respectively. If adenosine was applied 10 s or more before the stimulation, dopamine was not significantly changed. The black bar represents a stimulation control and the gray bar represents puffing on aCSF instead of adenosine. Both controls do not significantly change dopamine.

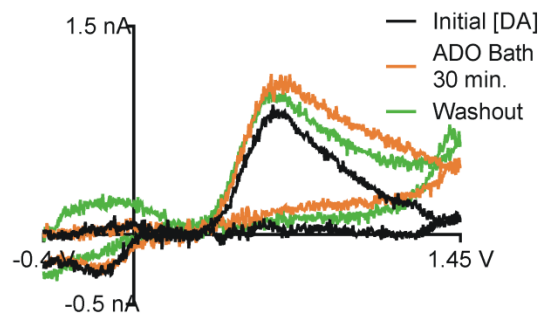
6.3.2 Bath application of adenosine does not modulate dopamine release

Transient changes in adenosine concentration modulated stimulated dopamine release. To test the extent to which an increase in the basal levels of adenosine would

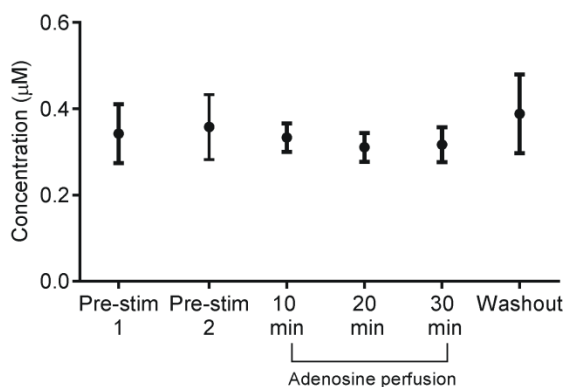
modulate stimulated dopamine release, slices were perfused with 5 μ M adenosine for 30 minutes, with dopamine being stimulated every 10 minutes. Figure 6.4B compares the average pre-adenosine stimulation, dopamine stimulation at different perfusion time points, and stimulation after adenosine washout. Bathing the slice in adenosine did not significantly reduce the amount of dopamine released at 10, 20, or 30 minute perfusions and dopamine concentration was not significantly different than the pre-adenosine or post-adenosine stimulation (washout) (Figure 6.4A and 6.4B, repeated measures one-way ANOVA, $p = 0.5175$, $n = 5$). Figure 6.4C shows the average pre-adenosine stimulations, the dopamine stimulation 2 s after adenosine application, and recovery. Stimulated dopamine concentration after adenosine application was significantly different than both the pre-adenosine stimulations 1 and 2 and the recovery (repeated measures one-way ANOVA, $p = 0.0003$, $n = 14$); however the pre-adenosine stimulations 1 and 2 were not significantly different from one another and were not different from the recovery. The adenosine bath experiments were performed in a separate set of slices than the transient adenosine application experiments. This data suggests that transient behavior is responsible for inhibitory dopamine modulation, because a constant level of elevated adenosine does not affect stimulated dopamine release.

Figure 6.4: Constant perfusion of 5 μM adenosine does not modulate stimulated dopamine release. A) Dopamine is not modulated when 5 μM adenosine in the aCSF is perfused through the slice for 30 minutes (black trace: initial dopamine, orange trace: stimulated dopamine after 30 minute adenosine perfusion, green trace: adenosine washout). B) Comparisons of the average pre-adenosine stimulation, dopamine stimulation at different perfusion time points, and stimulation after adenosine washout are shown. Bathing the slice in adenosine did not significantly reduce the amount of dopamine released at 10, 20, or 30 minute perfusions and dopamine concentration was not significantly different than the pre-adenosine or washout (repeated measures one-way ANOVA, $p = 0.5175$, $n = 5$). C) The average pre-adenosine stimulations, the dopamine stimulation 2 s after adenosine application, and recovery is shown. Stimulated dopamine concentration after adenosine application was significantly different than both the pre-adenosine stimulations 1 and 2 and the recovery (repeated measures one-way ANOVA, $p = 0.0003$, $n = 14$); however the pre-adenosine stimulations 1 and 2 were not significantly different from one another and were not different from the recovery.

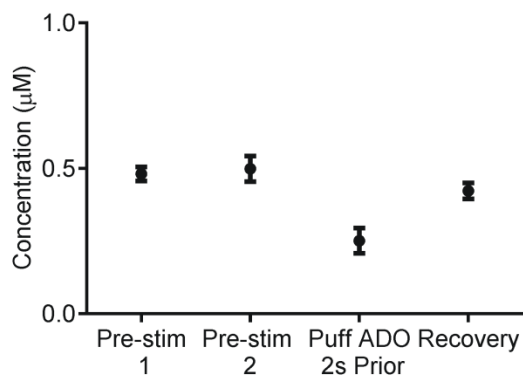
A. Adenosine bath does not affect stimulated DA



B. Average data for adenosine bath



C. Average data for exogenous adenosine 2s prior to DA



6.3.3 Mechanically stimulated (endogenous) adenosine modulates dopamine release

Recently, mechanically evoked rapid increases in extracellular adenosine levels were discovered using FSCV²³. Briefly, lowering either an electrode or glass pipette 50

μm in slices caused an immediate increase in extracellular adenosine levels.

Mechanically evoked adenosine was confirmed with amperometric enzyme sensors and was characterized using pharmacology. Here, we tested the extent to which mechanically evoked adenosine can modulate stimulated dopamine release (Figure 6.5). Like the previous experiments, two baseline dopamine stimulations 10 minutes apart were recorded to make sure the signal was stable (black trace in Figure 6.5A shows the initial dopamine stimulation). Once dopamine stability was confirmed, a glass pipette placed approximately 20-30 μm away from the working electrode was lowered 50 μm deeper into the tissue 2 s prior to the next dopamine stimulation. An immediate increase in extracellular adenosine was detected, on average $1.4 \pm 0.4 \mu\text{M}$ and $6.3 \pm 1.3 \text{ s}$, and the dopamine release was transiently inhibited (Figure 6.5A, red trace). After 10 minutes, dopamine was stimulated again and it recovered to baseline values. Figure 6.5B shows that on average, mechanically evoked adenosine caused a $37 \pm 3 \%$ decrease in dopamine concentration; however, stimulated dopamine release fully recovered after 10 minutes. The stimulated dopamine concentration was significantly different after mechanical adenosine stimulation from the initial dopamine stimulation (paired t-test, $p = 0.0119$, $n = 6$). Overall, this data shows that both exogenously-applied and endogenously-evoked transient adenosine can modulate stimulated dopamine release.

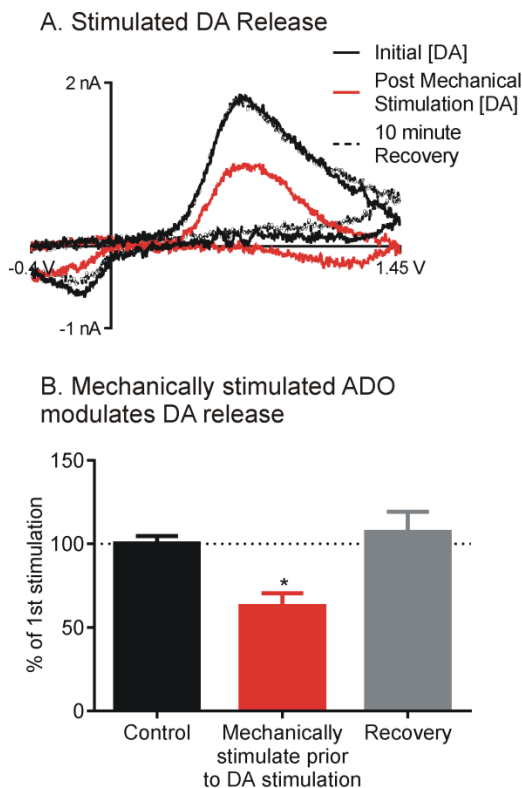


Figure 6.5: Mechanically evoked adenosine transiently modulates dopamine. A) Example data shows dopamine is inhibited by around 50 % after mechanical stimulation by lowering an empty pulled glass pipette (black trace: initial dopamine, red trace: after mechanical stimulation, dotted trace: 10 minute recovery). B) On average, mechanically evoked adenosine causes a significant decrease in dopamine to 63 ± 6 % of initial stimulation (paired t test, $p = 0.0119$, $n = 6$, red bar). Dopamine fully recovers within 10 minutes after mechanical stimulation (gray bar).

6.3.4 Adenosine modulation of dopamine is regulated by A_1 receptors

To test whether dopamine modulation was regulated by the inhibitory A_1 receptor, the A_1 receptor antagonist, DPCPX, was perfused through the slice (Figure 6.6A and 6.6B). First, an initial dopamine stimulation was collected before drug application (Figure 6.6A, black trace). Then, the slice was perfused with 200 nM DPCPX for 30 minutes, and another dopamine stimulation performed to ensure the drug did not have an effect on dopamine release (Figure 6.6A red trace, and 6.6B red bar). Next, adenosine was puffed onto the slice 2 s prior to a dopamine stimulation in the presence of 200 nM DPCPX (Figure 6.6A blue trace and 6.6B blue bar). Overall, there was no significant difference between dopamine stimulation in slices without drug (black bar), dopamine in the presence of DPCPX, or dopamine after adenosine application in the presence of DPCPX (repeated measures one-way ANOVA, $p = 0.5009$, $n = 6$). DPCPX

blocked the inhibition of dopamine release by adenosine; thus, the inhibition of dopamine release is regulated by A₁ receptors.

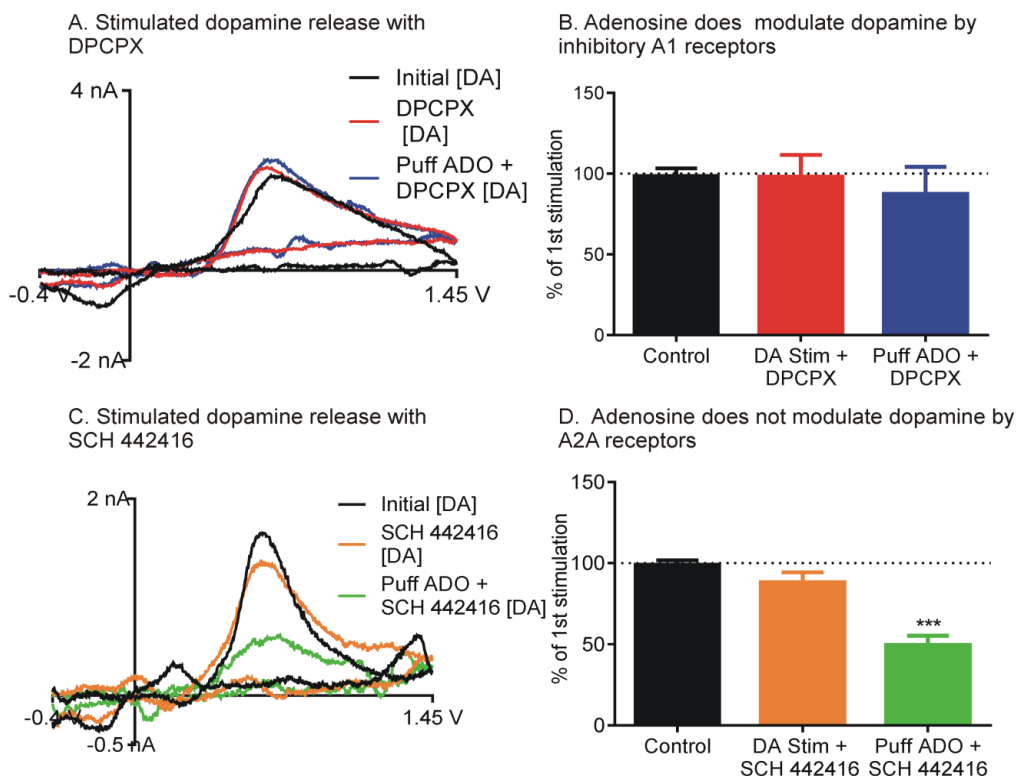


Figure 6.6: Dopamine modulation is regulated by the A₁ receptor and not the A_{2A} receptor in the caudate putamen. A) Dopamine modulation was blocked in the presence 200 nM of the A₁receptor antagonist, DPCPX. Example data show no change in stimulated dopamine release after both drug perfusion and adenosine application (black trace: initial stimulation, red trace: dopamine after DPCPX perfusion for 30 minutes, blue trace: dopamine after exogenous application 2 s prior in the presence of DPCPX). B) On average, there was no significant difference between dopamine stimulation in slices without drug (black bar), dopamine in the presence of DPCPX, or dopamine after adenosine application in the presence of DPCPX (repeated measures one-way ANOVA, $p = 0.5009$, $n = 6$). C) Dopamine modulation was unchanged in the presence of 1 μ M of the A_{2A} antagonist, SCH 442416. Example data show no change in stimulated dopamine release after 30 minutes of drug perfusion, but dopamine is decreased when adenosine was applied 2 s prior in the presence of the drug (black trace: initial dopamine, orange trace: dopamine after SCH 442416 perfusion for 30 minutes, green trace: dopamine after exogenous application 2 s prior in the presence of SCH 442416). D) On average, SCH 442416 alone did not significantly change dopamine release (Figure 6.6D orange bar, repeated-measures one-way ANOVA Bonferroni post test $p = 0.3482$, $n = 6$), however, puffing on adenosine 2 s prior to dopamine stimulation in the presence of the drug still resulted in a decrease in dopamine response (Figure 6.6D, green bar, repeated measures one-way ANOVA Bonferroni post test, $p = 0.0009$, $n = 6$).

The effect of A_{2A} receptors was tested with 1 μ M SCH 442416, an A_{2A} antagonist. The same procedure for DPCPX was repeated for SCH 442416 in a separate set of slices. On average, SCH 442416 alone did not significantly change dopamine release (Figure 6.6D orange bar, repeated-measures one-way ANOVA Bonferroni post test $p = 0.3482$, $n = 6$), however, puffing on adenosine 2 s prior to dopamine stimulation in the presence of the drug still resulted in a 50 ± 6 % decrease in dopamine response (Figure 6.6D, green bar, repeated measures one-way ANOVA Bonferroni post test, $p = 0.0009$, $n = 6$). This data shows that A_{2A} receptors do not affect the rapid modulation of adenosine by dopamine.

6.4 Discussion

In this paper, we show that adenosine transiently modulates dopamine in the caudate putamen. On average, transient adenosine release that occurred 2-5 s before stimulation modulated dopamine release by 54 ± 6 % and dopamine release fully recovered by the next stimulation. Exogenous application of adenosine was controlled to mimic actual spontaneous adenosine events in the brain which typically only last a few seconds¹². Mechanically-stimulated adenosine release also inhibited dopamine. The inhibitory modulation was regulated by the A_1 receptor. This work demonstrates that adenosine can modulate dopamine transients on a rapid time scale.

6.4.1 Adenosine transiently modulates phasic dopamine release

In the past several years, rapid adenosine release in the brain have been well characterized using electrochemical techniques^{9,12,24}. Using FSCV at carbon-fiber microelectrodes, the mechanism of stimulated adenosine release has been characterized in different brain regions^{9,25}. Mechanically evoked adenosine²³ as well as spontaneous adenosine transients have been characterized¹². Amperometric

biosensors have shown rapid adenosine release during hypercapnia²⁶, ischemia²⁷, the sleep-wake cycle²⁸, and epilepsy²⁷. While this research has discovered adenosine signaling on a fast time scale, little is known about the function of these rapid responses of adenosine.

In this work, we characterized a transient modulation of dopamine release by adenosine. Adenosine only modulated electrically-stimulated dopamine release when it was administered 2 or 5 s prior to dopamine stimulation. The exogenous adenosine transients typically lasted 4-5 s and adenosine was therefore present when it had its modulatory effect. Once adenosine had been cleared, like when the adenosine was administered between 10-60 s prior to dopamine stimulation, no modulation was observed. This shows that once adenosine is cleared from the extracellular space, no local modulation is observed. Mechanically stimulated adenosine evoked 2 s prior to stimulation also modulated stimulated dopamine release, thus physiological amounts of adenosine can modulate dopamine. Mechanically-evoked, endogenous adenosine is expected to be localized to a specific region, whereas a larger amount of adenosine was applied exogenously because it was applied 20-30 μm away. A global, but temporary, adenosine elevation would lead to more adenosine receptor activation, which could cause the slightly larger modulation by exogenously applied adenosine. Future studies could test the effect of different adenosine concentrations on dopamine modulation. Overall, transient adenosine modulated stimulated dopamine release only when adenosine was present in the extracellular space.

6.4.2 Rapid dopamine modulation is regulated by A₁ receptors in the caudate putamen

Rapid dopamine modulation is regulated by the inhibitory A₁ receptor. The A₁ receptor antagonist, DPCPX, blocked transient adenosine from modulating dopamine

release. A₁ receptors are expressed throughout the brain, and specifically are highly expressed in the caudate putamen^{7,29}. Most inhibitory actions of adenosine are linked to activation of the A₁ receptor³⁰. In previous studies with microdialysis, basal dopamine levels were modulated by blocking the A₁ receptor, which increased dopamine levels within 20 minutes of perfusion^{6,31}. Here, no change in stimulated dopamine release was observed after 30 minute perfusions with DPCPX. Stimulated dopamine release mimics phasic, or burst firing, which is differently regulated than basal levels (tonic firing)³². Thus, A₁ antagonism may affect basal dopamine levels, which cannot be measured with our background-subtracted technique, but does not affect electrically evoked release within 30 minutes. We show that transient adenosine modulates dopamine via A₁ receptor activation, similar to long-term receptor modulation of dopamine, but on a much faster time scale.

Transient adenosine modulation of dopamine release was not affected by blocking A_{2A} receptors with SCH 442416. A_{2A} receptors are the primary excitatory receptor in the brain and thus were not hypothesized to cause dopamine inhibition. A_{2A} receptors are highly expressed in the caudate putamen, and some evidence shows they can be colocalized with D₂ dopamine receptors³³. Previous studies also show no change in dopamine levels after perfusion with an A₂ antagonist. Past studies have suggested that A₂ receptor action can be masked by A₁ receptors⁶ and more detailed studies could address this with combinations of drugs in the future, but A_{2A} receptors do not appear to be important for the transient modulation of dopamine observed here.

6.4.3 Adenosine perfusion does not modulate stimulated dopamine release

In contrast to the actions of transient adenosine release, bathing the slice in 5 μM adenosine for 30 minutes did not significantly change the amount of stimulated dopamine release. Basal dopamine levels decrease after a 60 minute perfusion with the

stable adenosine analogue 2-chloroadenosine (2-CADO)³⁴. In another study, 50 μM adenosine perfusion significantly decreased extracellular dopamine levels after a 40 minute perfusion⁶. This work showed that the effect of adenosine in modulating basal levels was slow, on the 40 minute to hour time frame, and required large amounts of adenosine. Our electrochemical measurements were not extended past 30 minute adenosine perfusions and basal levels cannot be quantified by FSCV. Thus our experiments show that basal adenosine levels do not modulate phasic release of dopamine on the 30 min time scale. Taken together, these studies point to two different mechanisms of adenosine neuromodulation of dopamine: a slow mechanism that modulates basal dopamine levels after long perfusion times and a rapid modulation of phasic dopamine which occurs only during a temporary increase in adenosine levels. The differences between bath application and transient elevation of adenosine imply that transient receptor activation is the key to modulation of phasic dopamine. Bath application may lead to receptor desensitization or change in function³⁵⁻³⁷, which is why phasic dopamine is not modulated.

6.4.4 Function of transient adenosine release

Adenosine neuromodulation in the brain is complicated and many reports provide evidence for neuromodulation of neurotransmitters⁷. Previous studies have provided information on adenosine modulation of dopamine⁵, serotonin³⁸, glutamate⁵, and GABA¹⁵. Inhibitory modulation has been shown to be mostly regulated by the A_1 receptor^{5,7}. Here, transient adenosine was shown to rapidly modulate stimulated dopamine release by activation of the A_1 receptor. This is the first known function of transient adenosine release in the brain. Other studies could investigate the extent to which adenosine modulates neurotransmitters, like serotonin and glutamate, but on a rapid time scale. Combined with knowledge of adenosine modulation of basal levels,

rapid neuromodulatory studies will paint a clearer picture of adenosine function in the brain and the different time scales of modulation.

6.5 Conclusion

In conclusion, this paper provides evidence for rapid modulation of dopamine in the caudate putamen. Both exogenous and endogenous adenosine transients inhibited stimulated dopamine release by 50 %. The inhibition was reversible, and stimulated dopamine was fully recovered within 10 minutes. Inhibition of dopamine release was regulated by the A_1 receptor, and not by the A_{2A} receptor. This study provides evidence that spontaneous adenosine events in the brain can provide neuromodulation of dopamine neurotransmission on a transient time frame. Future work could focus on how transient adenosine modulates other neurotransmitters in the brain.

6.6 References

1. Cunha, R. A. *Neurochem. Int.* **2001**, *38* (2), 107-125.
2. Newby, A. C.; Worku, Y.; Holmquist, C. A. *Adv. Myocardiol.* **1985**, *6*, 273-284.
3. Ferre, S.; Fredholm, B. B.; Morelli, M.; Popoli, P.; Fuxe, K. *Trends Neurosci.* **1997**, *20* (10), 482-487.
4. Ferre, S.; Fuxe, K.; von, E. G.; Johansson, B.; Fredholm, B. B. *Neuroscience* **1992**, *51* (3), 501-512.
5. Quarta, D.; Borycz, J.; Solinas, M.; Patkar, K.; Hockemeyer, J.; Ciruela, F.; Lluís, C.; Franco, R.; Woods, A. S.; Goldberg, S. R.; Ferre, S. *J. Neurochem.* **2004**, *91* (4), 873-880.
6. Okada, M.; Mizuno, K.; Kaneko, S. *Neurosci Lett.* **1996**, *212*, 53-56.
7. Cunha, R. A. Adenosine neuromodulation and neuroprotection. In *Handbook of Neurochemistry and Molecular Neurobiology*, Lajtha, A., Vizi, E. S., Eds.; Springer US: 2008; pp 255-273.
8. Cechova, S.; Venton, B. J. *J. Neurochem.* **2008**, *105* (4), 1253-1263.
9. Pajski, M. L.; Venton, B. J. *Purinergic Signal.* **2013**, *9* (2), 167-174.
10. Klyuch, B. P.; Dale, N.; Wall, M. J. *J. Neurosci.* **2012**, *32* (11), 3842-3847.
11. Street, S. E.; Walsh, P. L.; Sowa, N. A.; Taylor-Blake, B.; Guillot, T. S.; Vihko, P.; Wightman, R. M.; Zylka, M. J. *Mol. Pain* **2011**, *7*.
12. Nguyen, M. D.; Lee, S. T.; Ross, A. E.; Ryals, M.; Choudhry, V. I.; Venton, B. J. *Plos One* **2014**, *9* (1), e87165.
13. Koos, B. J.; Kruger, L.; Murray, T. F. *Brain Res.* **1997**, *778* (2), 439-442.
14. Bell, M. J.; Kochanek, P. M.; Carcillo, J. A.; Mi, Z. C.; Schiding, J. K.; Wisniewski, S. R.; Clark, R. S. B.; Dixon, C. E.; Marion, D. W.; Jackson, E. *Journal of Neurotrauma* **1998**, *15* (3), 163-170.
15. Sperlagh, B.; Vizi, E. S. *Current Topics in Medicinal Chemistry* **2011**, *11* (8), 1034-1046.
16. Ross, A. E.; Venton, B. J. *Analyst* **2012**, *137* (13), 3045-3051.
17. Klyuch, B. P.; Richardson, M. J. E.; Dale, N.; Wall, M. J. *J. Physiol.* **2011**, *589* (2), 283-295.

18. Keithley, R. B.; Takmakov, P.; Bucher, E. S.; Belle, A. M.; Owesson-White, C. A.; Park, J.; Wightman, R. M. *Analytical Chemistry* **2011**, *83* (9), 3563-3571.
19. Venton, B. J.; Zhang, H.; Garris, P. A.; Phillips, P. E. M.; Sulzer, D.; Wightman, R. M. *J. Neurochem.* **2003**, *87* (5), 1284-1295.
20. Swamy, B. E. K.; Venton, B. J. *Anal. Chem.* **2007**, *79*, 744-750.
21. Cechova, S.; Elsobky, A. M.; Venton, B. J. *Neuroscience* **2010**, *171* (4), 1006-1015.
22. Robinson, D. L.; Phillips, P. E. M.; Budygin, E. A.; Trafton, B. J.; Garris, P. A.; Wightman, R. M. *Neuroreport* **2001**, *12* (18), 2549-2552.
23. Ross, A. E.; Nguyen, M. D.; Privman, E.; Venton, B. J. *J. Neurochem.* **2014**, *in press*.
24. Klyuch, B. P.; Dale, N.; Wall, M. J. *Neuropharmacology* **2012**, *62* (2), 815-824.
25. Pajski, M. L.; Venton, B. J. *ACS Chem. Neurosci.* **2010**, *1* (12), 775-787.
26. Dale, N. *J. Physiol.* **2006**, *574* (Pt 3), 633.
27. Dale, N.; Frenguelli, B. G. *Current Neuropharmacology* **2009**, *7* (3), 160-179.
28. Sims, R. E.; Wu, H. H. T.; Dale, N. *Plos One* **2013**, *8* (1).
29. Rivkees, S. A.; Price, S. L.; Zhou, F. C. *Brain Research* **1995**, *677* (2), 193-203.
30. Gomes, C. V.; Kaster, M. P.; Tome, A. R.; Agostinho, P. M.; Cunha, R. A. *Biochimica et Biophysica Acta-Biomembranes* **2011**, *1808* (5), 1380-1399.
31. O'Neill, C.; Nolan, B. J.; Macari, A.; O'Boyle, K. M.; O'Connor, J. J. *Eur. J. Neurosci.* **2007**, *26* (12), 3421-3428.
32. Floresco, S. B.; West, A. R.; Ash, B.; Moore, H.; Grace, A. A. *Nat. Neurosci.* **2003**, *6* (9), 968-973.
33. Fuxe, K.; Ferre, S.; Canals, M.; Torvinen, M.; Terasmaa, A.; Marcellino, D.; Goldberg, S. R.; Staines, W.; Jacobsen, K. X.; Lluís, C.; Woods, A. S.; Agnati, L. F.; Franco, R. *J. Mol. Neurosci.* **2005**, *26* (2-3), 209-220.
34. Zetterstrom, T.; Fillenz, M. *Eur. J. Pharmacol.* **1990**, *180* (1), 137-143.
35. Klaasse, E. C.; Ijzerman, A. P.; de Grip, W. J.; Beukers, M. W. *Purinergic Signal.* **2008**, *4* (1), 21-37.
36. Mundell, S.; Kelly, E. *Biochim. Biophys. Acta* **2011**, *1808* (5), 1319-1328.
37. Dunwiddie, T. V.; Diao, L.; Kim, H. O.; Jiang, J. L.; Jacobson, K. A. *J. Neurosci.* **1997**, *17* (2), 607-614.

38. Okada, M.; Nutt, D. J.; Murakami, T.; Zhu, G.; Kamata, A.; Kawata, Y.; Kaneko, S.
J. Neurosci. **2001**, *21* (2), 628-640.

Chapter 7

Conclusions and Future Directions

Our greatest weakness lies in giving up. The most certain way to succeed is always to try just one more time
~Thomas Edison

Chapter 7: Conclusions and Future Directions

In this thesis, I have shown new methods for detecting and studying adenosine in the brain using fast-scan cyclic voltammetry (FSCV). In particular, I have developed a new electrode and a new waveform which allows more sensitive and selective adenosine detection. Mechanically evoked adenosine was discovered and transient adenosine was found to rapidly modulate dopamine in brain slices. In this last chapter, I will briefly summarize my overall findings and discuss the future direction of the field.

7.1 Novel analytical tools for optimized adenosine detection

In Chapters 2-4, new analytical methods for studying adenosine were discussed. Chapters 2 and 3 focused on new electrode materials for the enhanced detection of both dopamine and adenosine respectively, and Chapter 4 discussed a new waveform for adenosine detection. The combination of a polymer and carbon nanotubes provided more sensitive neurotransmitter detection without the loss of temporal resolution that polymer coatings can provide.^{1,2} Polymers with carbon nanotubes were also advantageous due to the intrinsic properties of the polymer. For example, Nafion is cation selective, so negatively charged ATP was not as easily detected with the modified electrode. The Nafion-CNT modified electrodes would be ideal to verify adenosine signal if ATP was thought to be an interferent. Electrode modifications have become increasingly popular in the last two decades³⁻⁵, and research is focused on the development of the ideal electrode for whatever the analyte of interest is; however, several advancements are needed before highly reproducible electrodes with a modified surface become standard for detection *in vivo*.

Suspensions of polymer with carbon nanotubes are difficult because carbon nanotubes are not particularly soluble.⁶ Long sonication times, with a tissue probe sonicator, were required in order to fully suspend the carbon nanotubes into the Nafion solution (Chapter 2 and 3).

Prolonged sonication, specifically with a tissue probe sonicator, is damaging to the nanotubes and could cause the outer graphitic layers to be stripped.⁷ Recently, evidence has shown that prolonged sonication times can result in permanent degradation of the carbon nanotube structure.⁷ If the carbon nanotubes are heavily damaged, the electrode will not be coated with properly structured carbon nanotubes, leading to a less than optimal surface. Conversely, if the carbon nanotubes are not well suspended, agglomerations of nanotubes on the surface of the electrode could result in a decreased signal to noise ratio.² If suspension of carbon nanotubes with polymers could be optimized, electrodes would have better signal to noise ratios and higher increases in sensitivity.

Recently, a “true” solvent for carbon nanotubes was published in Nature Nanotechnology.⁶ Chlorosulfonic acid, a type of superacid, provides an ideal solvent for carbon nanotube suspensions without the need for lengthy suspension times. Unfortunately, dip-coating a carbon-fiber electrode into a highly acidic solution could be disastrous and cause stripping of the carbon surface. If highly concentrated suspensions of carbon nanotubes are prepared in strong acid and diluted in water to a reasonable concentration, then electrode modifications may be possible. Also, the effect of strong acids on different polymers like Nafion or overoxidized polypyrrole would need to be explored. Optimizing these conditions will be beneficial in developing a more reproducible and robust electrode modification which doesn't require lengthy sonication times.

Alternative electrode materials have also become increasingly popular over the last several years.^{8,9} Instead of modifying the existing carbon-fiber electrode surface with carbon nanotubes, research has also focused on using carbon-nanotube fibers as electrodes for *in vivo*.⁸ So far, they share similar properties with carbon-fiber electrodes but are more sensitive, selective, and have faster electron transfer kinetics.⁸ Alternative electrodes may be beneficial if

analyte selectivity is not an issue; however, electrode modifications of either carbon-fiber electrodes or carbon nanotube electrodes are still necessary if analyte differentiation is desired.

Chapter 4 describes a new waveform for adenosine detection. Instead of scanning with the triangle-shaped waveform, a modified sawhorse waveform was used. This waveform allowed better sensitivity at lower switching potentials and provided better selectivity for adenosine versus hydrogen peroxide and ATP than the triangle waveform. The sawhorse waveform would be ideal to use if hydrogen peroxide was the primary interferent because principal component analysis easily differentiates these at the sawhorse waveform. Combination of this waveform and a modified electrode with Nafion-CNTs may provide more confidence in adenosine versus ATP measurements.

New waveform modifications which increase selectivity for adenosine versus other interferents like histamine would be beneficial. Histamine is difficult because both adenosine and histamine oxidation kinetics are relatively slow and their oxidation peaks are close to one another.¹⁰ Unfortunately, the histamine oxidation reaction at carbon-fiber microelectrodes is unknown. If the histamine oxidation scheme during electrochemical measurements was established as well as a comprehensive study involving scan rate experiments and adsorption isotherms, then a clearer understanding of how histamine interacts with the electrode surface would be known. Capitalizing on a particular property of adenosine that histamine does not possess may allow a highly selective waveform for adenosine versus histamine. Alternatively, electrode modifications which capitalize on subtle differences of how adenosine and histamine interact with the surface would be useful.

Variations of the sawhorse waveform may also be beneficial for other neurochemicals which are hard to detect such as peptides. Recently, a modified triangle waveform was used to detect gonadotropin-releasing hormone (GnRH) in mouse brain slices.¹¹ Peptides are difficult

because only a few amino acids are electroactive, so many peptides have the same electrochemical signature. A wide variety of controls are needed to verify signals from peptides *in vivo*. Chapter 4 explains how molecules which oxidize at the switching potential behave differently at a potential plateau whether they are adsorption versus diffusion controlled. Peptide oxidation occurs at the switching potential¹¹ so the sawhorse waveform may be ideal for peptide detection *in vivo*. Peptides also vary in size and sequence, so some peptides may sterically interact with the electrode surface differently than others; for example, larger peptides may have a harder time orienting themselves at the electrode while smaller peptides may interact easier. Also, it is unknown whether certain peptides are adsorption-controlled versus diffusion-controlled; however, gaining this knowledge for important peptides that are secreted in high enough concentrations for FSCV detection, may allow the sawhorse waveform to be used. Sawhorse variations may be used to capitalize on differences in peptide interactions with the surface and if done in conjunction with strong biological controls, new waveforms may be useful for peptide detection *in vivo*.

7.2 Adenosine rapid signaling in the brain

Rapid adenosine monitoring has led to the overall understanding that adenosine is not just a slow-acting, retaliatory metabolite. Adenosine can be released and cleared on the order of seconds, much like neurotransmitters. Electrochemical measurements have proven that some adenosine is activity-dependent.^{12,13} Activity dependent release can either result from direct release of adenosine or by downstream effects of other neurotransmitters. The mechanism of release is dependent on the brain region and on the stimulation.¹⁴ For example, adenosine can be stimulated by electrical pulses, elevated K^+ , and AMPA receptor activation. In Chapter 5, a new method of stimulation is discussed which involves mechanically prodding the tissue with either a carbon-fiber electrode or pulled glass pipette. This new method of stimulation provides another mechanism in which

adenosine is released and cleared rapidly; and this contributes to the overall theme that adenosine is not just a slow-acting, retaliatory metabolite.

Mechanically evoked adenosine was fully characterized in the prefrontal cortex in Chapter 5. Previously, Pajski et al. showed that the mechanism of adenosine release is dependent on brain region¹⁴, so experiments which characterize mechanically evoked adenosine in different brain regions are needed. In Chapter 5, we show mechanically evoked adenosine is activity-dependent and a downstream action of ATP; whereas in another region, glutamate may be more important. In the prefrontal cortex, mechanically evoked adenosine is not dependent on glutamatergic AMPA receptors; however, testing both AMPA and NMDA receptors would provide more evidence that glutamate is not involved. Previous studies have shown mechanically evoked ATP in the brain can be from pannexin channels¹⁵, so using drugs like carbenoxolone, which block pannexin channel activity, would help determine if mechanically evoked adenosine is coming from pannexin channels. Briefly, carbenoxolone was tested in the prefrontal cortex (data not shown in Chapter 4), but no change was observed; however, because adenosine varies by brain region, another region may be dependent on pannexin channels.

The point of origin for adenosine release is unknown. Several studies have pointed to astrocytic-release of adenosine¹⁶⁻¹⁸, but some release may be neuronal in origin.¹⁹ Astrocytes have been shown to release neurotransmitters in a calcium dependent manner like neurons, so it is tricky to draw conclusions about adenosine cell origin using FSCV alone.²⁰ Recently, a conditional astrocyte-specific knockout was characterized using a promoter which drives expression of Cre recombinase specifically in astrocytes.²¹ Testing brain slices of mice with astrocyte knockouts may help rule out which regions astrocyte-mediated release of adenosine is more prevalent. Alternatively, fluorescently tagging specific cell-types, like astrocytes, in combination with smaller electrodes, particularly on

the nanoscale, may facilitate electrode placement in regions dense in a specific cell-type. Comparisons of adenosine release in regions highly fluorescent versus release in regions that are not would provide information on where the higher percentage of adenosine is originating from.

In Chapter 4, lowering a carbon-fiber microelectrode or a pulled glass pipette caused mechanically evoked adenosine, but puffing on artificial cerebral spinal fluid did not. New methods to study mechanically evoked adenosine could also be explored. Most research on mechanosensitive ATP release relies on physiological cell changes such as cell swelling in the bladder or shear stress in red blood cells.^{22,23} Instead of evoking adenosine by lowering an object into tissue, adenosine may be evoked by cell swelling in the brain (using a hypotonic solution). Cell swelling in the brain is not characteristic of normal healthy tissue, but it may be useful to study rapid signaling during brain infections which involve brain edema such as meningitis or traumatic brain injury.

Adenosine is not only released in response to an outside stimulus, but have been shown to also spontaneously release *in vivo*.²⁴ Spontaneous adenosine transients were shown to be regulated by the A₁ receptor; however more specific mechanisms of release are hard to characterize *in vivo*. Additionally, several drugs do not cross the blood brain barrier and therefore cannot be used *in vivo* to characterize adenosine events. Characterizing spontaneous adenosine events in slices would be beneficial to understand the mechanism of release because of the added benefit of more pharmacological manipulations.

Characterizing the function of spontaneous adenosine transient release in slices is also easier than *in vivo*. Chapter 5 discusses one function of these transient changes in the brain. In this thesis, we show that adenosine can transiently modulate dopamine in the

caudate putamen. Adenosine also modulates several other neurotransmitters such as serotonin, glutamate, and GABA on a slower time scale.²⁵⁻²⁷ Investigations into the extent to which adenosine transiently modulates other neurochemicals using FSCV would paint a clearer picture of rapid adenosine signaling.

Glutamate and GABA are not electroactive so they cannot be detected using FSCV; however, amperometric enzyme sensors which are selective for glutamate or GABA may help in identification. Recently, an enzyme coated carbon-fiber microelectrode was used for detection of the nonelectroactive molecule glucose using FSCV.²⁸ Enzyme sensors typically have hydrogen peroxide as the end product, and hydrogen peroxide can be detected with FSCV.²⁸ Specific glutamate sensors are available from both Pinnacle²⁹ and Sarissa Biomedical³⁰; however, GABA sensors are not yet commercially available. Using specific enzyme coated carbon-fiber microelectrodes for either glutamate or GABA would allow co-detection of adenosine and a nonelectroactive molecule; so studies of adenosine modulation on a rapid time scale could be studied. Alternatively, combining FSCV and electrophysiology measurements to study adenosine modulation would provide information on excitatory and inhibitory responses of the cell.

Adenosine is also classically described as neuroprotective in the brain. Mimicking adenosine transients in mouse models of Parkinson's or in animal stroke models would provide insight into how adenosine rapidly responds during disease or acute injury. A slow build up of adenosine during brain injuries and non-physiological conditions such as hypoxia have been demonstrated, but studies with electrochemical sensors have shown that there are also rapid adenosine events during injury and hypoxia. Adenosine can be released immediately following hypoxia³¹, ischemia³² and during defense reactions³³; however, the function of rapid adenosine signaling and downstream effects have not been

fully characterized. Future studies to measure receptor activation will provide information about the functional consequences of rapid adenosine signaling.

Only a few disease models have been studied to examine the effects on rapid adenosine release.³⁴ Because adenosine is ubiquitous throughout the brain³⁵, real-time sensing of adenosine could potentially reveal adenosine signaling during behaviors or diseases. Understanding the mechanism of adenosine release during diseases or acute injury, such as Parkinson's disease³⁶ or stroke³⁷, may lead to development of novel drugs to manipulate adenosine regulation for therapeutic uses. The field of real-time monitoring of adenosine is still relatively young but it is growing as understanding of the role of adenosine signaling in many brain functions increases. The use of sensors to understand basic adenosine neurobiology could assist in therapeutic development in the future.

7.3 Final Conclusions

In conclusion, optimized electrochemical methods were developed to study transient adenosine changes in brain slices. Over the next few years, as optimized electrode modifications and new electrode materials become available, more sensitive and selective adenosine measurements will be made. Electrochemical monitoring of adenosine will be able to provide more information of adenosine rapid signaling in the brain, which will help piece together its intricate role in the brain. As our understanding of adenosine signaling in the brain becomes more fine-tuned, new therapeutics could be developed which target specific adenosine signaling pathways.

7.4 References

1. Brazell, M. P.; Kasser, R. J.; Renner, K. J.; Feng, J.; Moghaddam, B.; Adams, R. N. *J. Neurosci. Methods* **1987**, *22* (2), 167-172.
2. Peairs, M. J.; Ross, A. E.; Venton, B. J. *Anal. Methods* **2011**, *3*, 2379-2386.
3. Pihel, K.; Walker, Q. D.; Wightman, R. M. *Analytical Chemistry* **1996**, *68* (13), 2084-2089.
4. Hashemi, P.; Dankoski, E. C.; Petrovic, J.; Keithley, R. B.; Wightman, R. M. *Anal. Chem.* **2009**, *81* (22), 9462-9471.
5. Hocevar, S. R.; Wang, J.; Deo, R. P.; Musameh, M.; Ogorevc, B. *Electroanalysis* **2005**, *17* (5-6), 417-422.
6. Davis, V. A.; Parra-Vasquez, A. N.; Green, M. J.; Rai, P. K.; Behabtu, N.; Prieto, V.; Booker, R. D.; Schmidt, J.; Kesselman, E.; Zhou, W.; Fan, H.; Adams, W. W.; Hauge, R. H.; Fischer, J. E.; Cohen, Y.; Talmon, Y.; Smalley, R. E.; Pasquali, M. *Nat. Nanotechnol.* **2009**, *4* (12), 830-834.
7. Rossell, M.; Kuebel, C.; Ilari, G.; Rechberger, F.; Heiligtag, F.; Niederberger, M.; Koziej, D.; Erni, R. *Carbon* **2013**, *61*, 404-411.
8. Schmidt, A. C.; Wang, X.; Zhu, Y.; Sombers, L. A. *ACS Nano* **2013**.
9. Wang, J.; Deo, R. P.; Poulin, P.; Mangey, M. *J. Am. Chem. Soc.* **2003**, *125* (48), 14706-14707.
10. Hashemi, P.; Dankoski, E. C.; Wood, K. M.; Ambrose, R. E.; Wightman, R. M. *J. Neurochem.* **2011**, *118* (5), 749-759.
11. Glanowska, K. M.; Venton, B. J.; Moenter, S. M. *J. Neurosci.* **2012**, *32* (42), 14664-14669.
12. Klyuch, B. P.; Dale, N.; Wall, M. J. *Neuropharmacology* **2012**, *62* (2), 815-824.
13. Pajski, M. L.; Venton, B. J. *ACS Chem. Neurosci.* **2010**, *1* (12), 775-787.
14. Pajski, M. L.; Venton, B. J. *Purinergic Signal.* **2013**, *9* (2), 167-174.
15. Xia, J. S.; Lim, J. C.; Lu, W. N.; Beckel, J. M.; Macarak, E. J.; Laties, A. M.; Mitchell, C. H. *J. Physiol* **2012**, *590* (10), 2285-2304.
16. Schmitt, L. I.; Sims, R. E.; Dale, N.; Haydon, P. G. *J. Neurosci.* **2012**, *32* (13), 4417-4425.
17. Calker, D.; Biber, K. *Neurochemical Research* **2005**, *30* (10), 1205-1217.
18. Wall, M. J.; Dale, N. *J. Physiol.* **2013**, *591* (Pt 16), 3853-3871.

19. Lovatt, D.; Xu, Q.; Liu, W.; Takano, T.; Smith, N. A.; Schnermann, J.; Tieu, K.; Nedergaard, M. *Proc. Natl. Acad. Sci. U. S A* **2012**, *109* (16), 6265-6270.
20. Bezzi, P.; Carmignoto, G.; Pasti, L.; Vesce, S.; Rossi, D.; Rizzini, B. L.; Pozzan, T.; Volterra, A. *Nature* **1998**, *391* (6664), 281-285.
21. Casper, K. B.; Jones, K.; McCarthy, K. D. *Genesis*. **2007**, *45* (5), 292-299.
22. Olsen, S. M.; Stover, J. D.; Nagatomi, J. *Ann. Biomed. Eng.* **2011**, *39* (2), 688-697.
23. Wan, J. D.; Ristenpart, W. D.; Stone, H. A. *Proceedings of the National Academy of Sciences of the United States of America* **2008**, *105* (43), 16432-16437.
24. Nguyen, M. D.; Lee, S. T.; Ross, A. E.; Ryals, M.; Choudhry, V. I.; Venton, B. J. *Plos One* **2014**, *9* (1), e87165.
25. Okada, M.; Nutt, D. J.; Murakami, T.; Zhu, G.; Kamata, A.; Kawata, Y.; Kaneko, S. *J. Neurosci.* **2001**, *21* (2), 628-640.
26. Okada, Y.; Sakurai, T.; Mori, M. *Neurosci. Lett.* **1992**, *142* (2), 233-236.
27. Sperlagh, B.; Vizi, E. S. *Current Topics in Medicinal Chemistry* **2011**, *11* (8), 1034-1046.
28. Lugo-Morales, L. Z.; Loziuk, P. L.; Corder, A. K.; Toups, J. V.; Roberts, J. G.; McCaffrey, K. A.; Sombers, L. A. *Anal. Chem.* **2013**, *85* (18), 8780-8786.
29. Guyenet, S. J.; Matsen, M. E.; Morton, G. J.; Kaiyala, K. J.; Schwartz, M. W. *Mol. Metab* **2013**, *2* (2), 116-122.
30. Tian, F.; Gourine, A. V.; Huckstepp, R. T.; Dale, N. *Anal. Chim. Acta* **2009**, *645* (1-2), 86-91.
31. Frenguelli, B. G.; Llaudet, E.; Dale, N. *J. Neurochem.* **2003**, *86* (6), 1506-1515.
32. Frenguelli, B. G.; Wigmore, G.; Llaudet, E.; Dale, N. *J. Neurochem.* **2007**, *101* (5), 1400-1413.
33. Dale, N.; Gourine, A. V.; Llaudet, E.; Bulmer, D.; Thomas, T.; Spyer, K. M. *J. Physiol.* **2002**, *544* (Pt 1), 149-160.
34. Dale, N.; Frenguelli, B. G. *Current Neuropharmacology* **2009**, *7* (3), 160-179.
35. Latini, S.; Pedata, F. *J. Neurochem.* **2001**, *79*, 463-484.
36. Pinna, A.; Volpini, R.; Cristalli, G.; Morelli, M. *Eur. J. Pharmacol.* **2005**, *512* (2-3), 157-164.
37. Von Lubitz, D. K. *Expert. Opin. Investig. Drugs* **2001**, *10* (4), 619-632.

Appendix: Brain Slice protocol

Protocol for Brain Slice Preparation

Artificial cerebral spinal fluid (aCSF) recipe is a modified Krebs buffer:

126 mM Sodium chloride (NaCl)—7.362 g

2.5 mM Potassium chloride (KCl)—0.186 g

1.2 mM Sodium phosphate monobasic monohydrate (NaH_2PO_4)—0.166 g

2.4 mM Calcium chloride dehydrate ($\text{CaCl}_2 \cdot 2\text{H}_2\text{O}$)—0.353 g

1.2 mM Magnesium chloride hexahydrate ($\text{MgCl}_2 \cdot 6\text{H}_2\text{O}$)—0.244 g

25 mM Sodium bicarbonate (NaHCO_3)—2.1 g

11 mM D-glucose—1.982 g

15 mM Tris—1.8171 g

Optional: 3.97 mM Ascorbic acid (0.7 g)—possibly acts as a preservative; used by the Jones lab at Wake Forest University

Optional dissecting aCSF recipe: Reduce the NaCl by half (3.681 g) and add 63 mM sucrose (21.565 g). This improves the likelihood of slice viability.

Stock aCSF recipe (10x concentrated): (keep in the refrigerator)

1.86 g KCl

1.66 g NaH_2PO_4

3.53 g $\text{CaCl}_2 \cdot 2\text{H}_2\text{O}$

2.44 g $\text{MgCl}_2 \cdot 6\text{H}_2\text{O}$

1. Prepare aCSF the day before to sit overnight at room temperature or in the refrigerator.

-Dissecting: Take 100mL of stock and add ddH₂O to about 800mL. Add 7.362g sodium chloride, 1.982g D-glucose, 2.1g sodium bicarbonate and 1.8171 Tris. pH to 7.4, place in a 1L volumetric flask and add ddH₂O to 1L, then refrigerate overnight.

-Normal: Prepare like with the dissecting aCSF, only do not add Tris, and do not bring to 1L in volume. Let sit in an air tight container at room temperature overnight. (If the Tris is added now, the solution will become permanently cloudy)

2. Prepare aCSF for use in the morning.

--Normal: Add 1.8171g Tris and pH to 7.4. Place in a 1L volumetric flask and add ddH₂O to 1L.

-Dissecting: Re-pH to 7.4.

Fill a chilling tray with ice and water

3. Rinse **2** 250mL beakers and **1** 600mL beaker with ddH₂O and dissecting aCSF. Place 1 of the 250mL beakers and the 600mL beaker in chilling tray and fill with dissecting aCSF to below the ice line (only about 400mL of dissecting aCSF will be needed). Place air-stone bubbler in the 600mL beaker and perfuse with 95% O₂/5% CO₂ (carbogen).

4. Place the other 250mL beaker and a petri dish bottom in freezer.

5. Place a plastic spoon, fine-hair brush, 2 spatulas, one scalpel and thermometer in non-aerated beaker. Thread the slicing razor onto silver thread or a paperclip and suspend in non-aerated aCSF. **Optional:** Fill a syringe with dissecting aCSF and place in the non-aerated beaker to keep cool. This can be used later to start cooling the brain as soon as the cranial (skull) plates are removed.

6. Rinse and fill a 250mL beaker with normal aCSF and place net suspension device inside. Aerate with carbogen.

7. Get a liter beaker and fill with ice. Place the tub in the vibratome, with a folded paper towel inside of the tray. Make sure the tub is all the way down. Fill the area surrounding the tray with ice.

8. Get tissue slicer ready. Turn on slicer. Program slice thickness (400µm), speed (3, or 15mm/min), and frequency (9).

9. Let iced solutions chill to <3 °C.

10. Place guillotine at the edge of the sink and open a trash bag in the sink to place body and remains of head in.

11. Line a dissecting plate with paper towels. Place a pair of rongeurs (a pair of strong dissecting pliers), scissors, a razor blade and a timer in easy reach.

12. Get anesthetizing area ready. Place folded paper towel in the bottom of the dessicator and have the isoflurane ready.

13. Once the aCSFs have been aerated for 20-30 minutes, get rat from vivarium in biology. Don't forget the keys! Code is 100191. If there are dead rats in lab freezer, go to the

room at the middle right wall of the vivarium and place carcasses in floor box freezer. Then go to last room on the left (room 74K) and enter using longer key. Find a rat labeled "Venton." Pick rats up by tail to place in carrier. Sign rats out on form behind door. If you empty a cage while picking up rat, bring cage across the hall to the room next to the office and set on floor. Cover carrier with blanket and bring back to lab.

14. Weigh rat. Record date and weight in the rat surgery notebook. Measure 1mL of isoflurane per 100g of rat weight and pour onto paper towels in the bottom of the dessicator (located in hood). Place perforated bottom in the dessicator and close the dessicator.
15. Give the isoflurane time to vaporize. Remove the 250mL beaker from the freezer, place in ice tray and pour some aerated dissecting aCSF into it. Pour the rest of the aerated aCSF into the vibratome tray. If you have any dissecting aCSF ice cubes, place one or two in the vibratome tray as well to help maintain temperature. Super glue a small piece of agar gel onto the tissue mount.
15. Place the rat in the dessicator. Anesthetization should only take a minute or two. Don't wait too long or the rat will die. You should have time to clean out the carrier and weighting bowl if desired.
16. When the rat doesn't respond to tail pinch by tweezers, or starts gasping for breath, behead him **right** behind the ears and start timer. If he revives before beheading, return to desiccator and try again. Place body in trash bag.

Note: It is possible to behead the rat in such a way that the back of the skull is removed during beheading, making brain removal much faster and easier. However, if you slip and behead too far forward, you will risk not killing the rat (because enough hind brain is left behind for animation), or destroying useful areas of the brain.
17. Remove the brain: With a scalpel or razor blade, cut the scalp from between the eyes to the base of the skull and pull skin away from skull. Hold the head firmly by the sides. Using a sharp pair of scissors, carefully cut along the sagittal suture (between the cranial plates) to just behind the eyes. Insert the rogeures into the hole at the base of the skull and remove the cranial plates carefully, but quickly. Slide the flat edge of a spatula under the brain to sever eye and nose nerves. The mouse's jaw may twitch. Pour chilled aCSF onto the brain. Use the spatula to remove the brain from the skull and place in small beaker of aCSF. If you want, you may hemisect the brain (cut in half along the central division). This entire step should take less than 2 minutes.
18. Let brain sit in chilled aCSF for 2-3 minutes. This is enough time to rinse blood off the dissection tray and guillotine with cold water, and place the rat body in the freezer.
19. Remove Petri dish bottom from freezer and place a kimwipe saturated with dissecting aCSF on top.
20. Using the spoon, place brain on Petri dish and remove any remaining spinal chord, forebrain, and a good portion of the back.

21. Place some glue on tissue mount. Use a kimwipe to dab brain dry and place on glue, ventral side down (“eyes” upward). The medial edge (inside, cut) of the brain should be touching the agar.
22. Slice brain, holding agar in place with brush if necessary. Remove good slices with fine-bristled brush and place in room temperature, aerated normal aCSF. Alternatively, slices may be transferred using a disposable pipette whose tip has been cut off for a larger opening.
23. Allow slices to recover for at least an hour at room temperature. This is a good time to calibrate electrodes.
24. About 15 minutes before the slices are done equilibrating, start the slice system running. Take the slice chamber to the voltammetry system and hook up to the pump and heater (if desired). Fill with normal room temperature aCSF and start pumping aerated normal room temperature aCSF through the system at 1mL per minute (or 42.5 rpm). If desired, may use the heater to warm the aCSF to 30 or 34°C.
25. Start the waveforms running, and start cleaning the carbon electrodes in isopropanol. File the stimulating electrode prongs for a shiny surface.
26. When the slices are done recovering, or shortly before, transfer a slice to the slice chamber. Position the slice as desired so that it may be seen clearly under the microscope lens, then lower the reference electrode so that it is right next to (preferably touching) the slice. Lower and position the stimulating electrode somewhere in the dorsal (top) region of the slice. The stimulating electrode should barely touch the surface of the slice.
27. Take a carbon electrode, fill with 1M KCl and place in headstage. Position it between the prongs of the stimulating electrode to form a shallow triangle and lower 75µm into the slice. Allow the electrode to sit for at least 20 minutes in the tissue (longer is better) before taking measurements.

Basic Stimulation Parameters (these can change depending on your experiment):

-Input stimulation frequency = 1-100 Hz

-1-10 Hz = approximate dopamine neuron basal firing frequency;

-50 or 60 Hz = dopamine neuron burst firing frequency;

-Most Wightman dopamine experiments are done with 1 pulse

-Input number of pulses = 5-10

-150 pulses has been known to kill a slice

-Polarity = usually biphasic

-Width of pulses = 2-4 ms

-Amplitude:

-We usually use 6 Amp;

-Wightman often uses 6.5 Amp

-Multiplier = 1

-Stim-to-scan delay = default = 90.50 ms (i.e., data collected 90.50 ms after stimulation)

-Update Rate = default = 5×10^3 Hz

Always click “Update Stim,” even if you haven’t changed anything! Otherwise, the program won’t turn on the stimulation and you’ll get an error in your next data collection file.

Notes:

-For serious experiments, the carbon electrodes should be pre-calibrated. I prefer to do this on the same day as the experiment, using the same normal aCSF as will be used to perfuse the slices. Since usually only one to three slices can be tested in a day, if you start cleaning the electrodes before preparing the aCSFs, this can usually be done by the time the slices are recovered from surgery. If electrodes are calibrated on days before the actual experiment, they must be kept moist and clean in isopropanol until the experiment.

-The same electrode may be used for multiple slices (as long as experimental conditions for all slices are identical), but the potentials read by the electrode will shift over time. I recommend using a different electrode per slice.

-If you want to heat the slices, do it slowly. They respond just fine at room temperature, and many other labs test at room temperature. Even though room temperature is not technically physiological, there are added problems associated with heating (shock, lower signals, greater electrical noise, heater problems that can kill slices).

Trouble-shooting:

-Slices are very hard to kill. Signals may be low, signal amplitude might decrease over time, but for the most part no matter what you do, you will get a signal.

If you are getting no signal:

-Make sure the stimulator is turned on, and that the stimulation electrode is touching the slice. If they are:

-Your slices are probably dead or soon will be. The important part is to find out what is hurting them.

1. Check aCSF pH. An acidic aCSF will hurt the slices. Signs of pH shock are unusually pale coloration and curling of the tissue.

2. Check nearby equipment and unplug anything that is unnecessary, especially equipment that has been recently moved or changed. Your signal may be low and nearby electrical noise is drowning it out.
3. Variations in aCSF recipe, type of buffer, and incubation temperature (between 21° and 35°C) will not hurt the slices. If at any point during incubation there is a sudden increase in oxygenation rate, this will probably kill the slices.

If you are getting a dopamine signal, but not an adenosine signal:

-The reason for this may be very hard to determine. Things that I have found in the past to help:

1. Check electrode positioning. Do the stimulation prongs and the working electrode form a shallow triangle? Try increasing the distance between the working electrode and the stimulating electrode slightly. You can also try re-trimming the stimulating electrode to create a new surface, or widening the stimulating prongs slightly.
2. Make sure the working electrode isn't too deep into the slice.
3. When you make aCSF, make sure you are only adding 2.1 g of sodium bicarbonate. Too much may reduce your adenosine signal (evidence of this is purely circumstantial, so take it with a grain of salt).
4. Try as much as possible to position electrodes on or near a blood vessel. This greatly increases your chances of detecting adenosine.
5. Decrease oxygenation slightly.
6. Check nearby equipment for electrical interference.

If you are getting a signal, but it decays quickly over repeated stimulations:

-Then your slices are dying. See that section for suggestions. Also, try to increase oxygenation slightly.

If you are getting an adenosine signal in an area that you don't expect to see one, and it is a large signal:

-Then the carbogen tank is running low, leaving your slices low on oxygen (and possibly high on carbon dioxide). Replace it.

If your stimulation electrode is forming bubbles and "cooking" your slice:

-The stimulating electrode is oxidizing water. This is more likely to happen on humid days, and is hard to stop once it starts. You may have to scrap the experiment completely, but can try re-filing the stimulating electrode, trimming it so that the insulation surrounding the tip is intact, or wiping it off and trying again.